General Disclaimer

One or more of the Following Statements may affect this Document

- This document has been reproduced from the best copy furnished by the organizational source. It is being released in the interest of making available as much information as possible.

- This document may contain data, which exceeds the sheet parameters. It was furnished in this condition by the organizational source and is the best copy available.

- This document may contain tone-on-tone or color graphs, charts and/or pictures, which have been reproduced in black and white.

- This document is paginated as submitted by the original source.

- Portions of this document are not fully legible due to the historical nature of some of the material. However, it is the best reproduction available from the original submission.

Produced by the NASA Center for Aerospace Information (CASI)

PERFORMED UNDER
NASA CONTRACT NAS9-14776

FLEXIBLE RADIATOR SYSTEM

REPORT NO. 2-19200/3R-1195B

30 OCTOBER 1982

Submitted by:

Vought Corporation
P.O. Box 225907
Dallas, Texas 75265

To:

NASA Johnson Space Center
Houston, Texas 77058

PREPARED BY:

J. A. Oren

APPROVED BY:

R. L. Cox

TABLE OF CONTENTS

		PAGE
1.0	INTRODUCTION AND SUMMARY	1
2.0	REQUIREMENTS AND APPLICATION	2
3.0	DESIGN	4
	3.1 General Description	4
	3.2 Panel Design	7
	3.3 Performance	13
	3.3.1 Heat Rejection Performance	13
	3.3.2 Weight	13
	3.3.3 Panel Hydraulic Characteristics	19
	3.4 Deployment Methods	22
	3.4.1 Pneumatic Deployment	22
	3.4.2 Extendable Boom Deployment/Retraction	25
	3.4.3 Extendible Mast Deployment/Retraction	33
	3.5 Fluid System Considerations	33
	3.5.1 Working Fluid Selections	33
	3.5.2 Heat Load Control	40
	3.5.3 Fluid Circulation System	48
	3.6 Micrometeoroid Damage	48
4.0	PANEL MANUFACTURING METHODS	60
5.0	CONCLUSIONS AND RECOMMENDATIONS	68
6.0	REFERENCES	69
	APPENDIX A	70

LIST OF FIGURES

		PAGE
1	Prototype Flexible Radiator Panel	5
2	Prototype Flexible Radiator Panel	6
3	Flexible Radiator Fin Material	8
4	Flexible Radiator Panel Layup	9
5	System Weight for RS-89a	11
6	System Weight for Coolanol 15	12
7	Bending Moment Requirements	14
8	Soft Tube Flexible Radiator Rejection Heat Flux for $0^{o}F$ Sink Temperature	15
9	Soft Tube Flexible Radiator Rejection Heat Flux for $-40^{o}F$ Sink Temperature	16
10	Soft Tube Flexible Radiator Rejection Heat Flux for $-180^{o}F$ Sink Temperature	17
11	Soft Tube Radiator Pressure Drop Test Summary	21
12	Flexible Radiator Panel with Pneumatic Deployment	23
13	Soft Tube Radiator Deployment/Retraction Control	24
14	Flexible Radiator Pneumatic Deployment Package	26
15	Flexible Radiator Pneumatic Deployment in Stowed Position	27
16	Flexible Radiator, Dual Boom Deploy, Spool At Base	29
17	Flexible Radiator, Dual Doom Deploy, Spool Outboard	30
18	Coiled Flex Hose	31
19	Retraction Springs	32
20	Soft Tube Radiator Deployment/Retraction Control	34
21	Flexible Radiator - Boom Deployment Package	35
22	Flexible Radiator Boom Deployment in Stowed Position	36
23	Permeability Test - FEP (Teflon) Tubing & Freon Fluid	38
24	Approximate Stability Curves for Candidate Flexible Radiator Fluids	41
25	Approximate Stability Curve	42
26	Flow System for Flexible Radiator	49
27	Sundstrand Pump Model 145656	50
28	Representative Coolanol 20 Pump for Flexible Radiator	51
29	Representative Thermal Control Valve	53

LIST OF FIGURES

		PAGE
30	Vought Freon Swivel - Right Angle Design	54
31	Comparison of Penetration Equations	56
32	Effective Wall Thickness for Meteoroid Penetration of Flexible Radiator Tubing	57
33	Mold for Laminating Flexible Radiator Panel	61
34	Assembly for Fusion Bonding Radiator	62
35	Peak Temperature Distribution in Fusion Bond Process	64
36	Transient Temperature of Oven Atmosphere During Fusion Bonding Cycle	65

LIST OF TABLES

I	Applicable Requirements Range	3
II	Comparison of Flexible Radiator Designs	10
III	Thermophysical Properties of Fluids	20
IV	4 kW Flexible Radiator Module Pneumatic Deployment	28
V	4 kW Flexible Radiator Boom Deployment	37
VI	Comparison of Radiator System Design for Candidate Fluids	39
VII	Coolanol 20 Kit Accumulator	52

1.0 INTRODUCTION AND SUMMARY

The technology development for the flexible radiator system was initiated by the Vought Corporation in 1973 under Contract NAS9-13346 with NASA-JSC. Under that contract, two concepts for flexible fin radiator panels were evolved and feasibility test articles of both were built and tested.[(1)(2)*] The feasibility articles tested were a soft tube article measuring 3.3 feet by 6 feet and a hard tube article measuring 2.4 feet in diameter by 3.8 feet long. Following this effort, two prototype panels were built and tested. The contract for this effort, NAS9-14776, was initiated in 1976 and the thermal vacuum testing of the prototype panels (one soft tube and one hard tube panel) was conducted in October 1980.[(3)(4)(5)]

The soft tube flexible radiator prototype testing successfully demonstrated the panel in the simulated environment. This technology is considered ready for engineering design and development for application in space. While the hard tube approach has potential advantages of longer life and compatibility with better heat transport fluids, it has not been developed to the same readiness level. The prototype test for the hard tube was moderately successful but problems were revealed in the fabrication techniques and in the deployment system. More technology development is necessary to achieve the desired technology readiness.

This report describes the soft tube radiator subsystem. Discussed are the applicable system requirements, the design and limitations of the subsystem components and panel manufacturing method. The soft tube radiator subsystem is applicable to payloads requiring 1 to 12 kW of heat rejection for orbital lifetimes per mission of 30 days or less. The flexible radiator stowage volume required is about 60% and the system weight is about 40% of an equivalent heat rejection rigid panel. The cost should also be considerably less.

As a result of the studies and development work to date, it is recommended that the soft tube flexible radiator be utilized for thermal control of future payloads for which its capabilities fit the requirements. A significant savings in weight, stowage volume and cost should result. It is further recommended that the hard tube flexible technology advancement effort

---

*References listed in Section 6.0

be continued to take advantage of the lightweight fin approaches on future long life mission, such as space stations. The combining of this light weight fin technology with heat pipes to provide low weight heat pipe panels should be investigated.

The applicable requirements are discussed in Section 2.0, the design is discussed in Section 3.0 and manufacturing methods are discussed in Section 4.0. Conclusions and recommendations are discussed in Section 5.0.

2.0 REQUIREMENTS AND APPLICATION

The soft tube flexible radiator concept is a modular approach to spacecraft heat rejection. It is intended to meet the heat rejection needs of spacecraft and payloads with 1 to 12 kW of heat rejection and an operating temperature of 0° to $300^{o}F$. The applicable lifetime is 30 days maximum per mission with up to 80 missions in its useful lifetime. The applicable requirement ranges for the flexible radiator are summarized in Table I. The stowage volume of 17 ft^3/kW is about 60% of that required for equal heat rejection with a rigid panel, while the weight is about 40% of the equivalent rigid panel weight. Cost should be lower also, although good cost comparison numbers are not readily available.

The flexible radiator is particularly suited to Shuttle Orbiter Sortie payloads. The mission length and heat load capabilities fit well with the requirements of most Sortie payloads.

The flexible radiator is also applicable to free-flying payloads whose mission lengths do not exceed the 30 day design life.

TABLE I

APPLICABLE REQUIREMENTS RANGE

Item	Applicable Range
Heat Rejection	o 1 to 12 kw
Operating Fluid Temperatures	o 0 to 300°F
Control Temperature	o Set Point Temp ± 2°F
Fluid System Interface	o Heat Exchanger with Disconnect of Payload Side
	o Direct Connection to Payload System
Life	o 30 day mission length
	o 80 missions over 10 year period
	o 10 year service life
	o 5 full deployments + 50 half deployment/ retraction cycles per mission
Deployment/Retraction	o 5 minutes for full deployment or retraction
	o Must be compatible with outlet temperature control system
Stowage Volume	o 14 to 17 ft^3/kw
System Weight Including Fluid System	o 60 lbs/kw
Modularity	o Provide 1 to 12 kw of heat rejection with modular subsystem ranging from 1 to 4 kw each in size
Maintenance	o Between missions only
Environment	o Space orbital environment
	o All attitude pointing
Heat Load Ratio (high-to-low)	o 10 to 1 with proper thermal design
	o Requires active area control

3.0 DESIGN

3.1 General Description

The flexible radiator panel is an advanced technology, high performance thermal radiator panel concept which has the potential of significantly reducing heat rejection subsystem weight, stowage volume and cost for future space vehicles and payloads. This technology has been developed to a high readiness level during the past 9 years by the Vought Corporation under the direction of NASA Johnson Space Center. A full scale prototype panel has been designed, built and successfully tested in the thermal-vacuum environment. The technology is considered developed to the point of being ready for design and development for specific applications.

The flexible radiators were conceived to satisfy the needs of spacecraft and payloads which require deployed radiator area for heat rejection. They have performance and weight advantages over conventional rigid panels and radiators structurally integral with the vehicle skin. Flexible radiators are easily adapted to an existing vehicle since they can be stowed in compact units which are not susceptible to damage by dynamic loads during launch. The lightweight flexible panel can be integrated into a self contained fluid system which includes the equipment necessary to circulate the fluid, exchange the heat load to the fluid, and control the fluid temperatures to provide a Flexible Radiator Subsystem Module.

The full scale prototype panel which was tested is shown in Figures 1 and 2, has approximately 173 ft^2 of radiating area (3.2 ft. wide by 27 ft. long, 2 sided) and is designed to reject 1.33 kW of heat to a 0^oF sink with a 100^oF fluid inlet. The panel is constructed from a flexible Teflon/silver mesh fin surrounding 1/8 inch Teflon tubes. The prototype panel is stowed on a 10 inch diameter by 4 foot wide drum. (It rolls up to a diameter of 17 inches when fully stowed.) Deployment of the soft tube prototype is via two four inch diameter Kevlar/Mylar inflation tubes with flat springs incorporated in each tube. Nitrogen is normally used for the deployment with approximately 1 psi required. The springs retract the panels when the inflation tubes are deflated. Another method of deployment available for the soft tube flexible is a motor driven deployable boom. This eliminates the need for expendables when the panel area is varied during the mission for heat load control. The soft tube panel is designed for a 90% probability of no punctured tube in a 30

ORIGINAL PAGE IS
OF POOR QUALITY

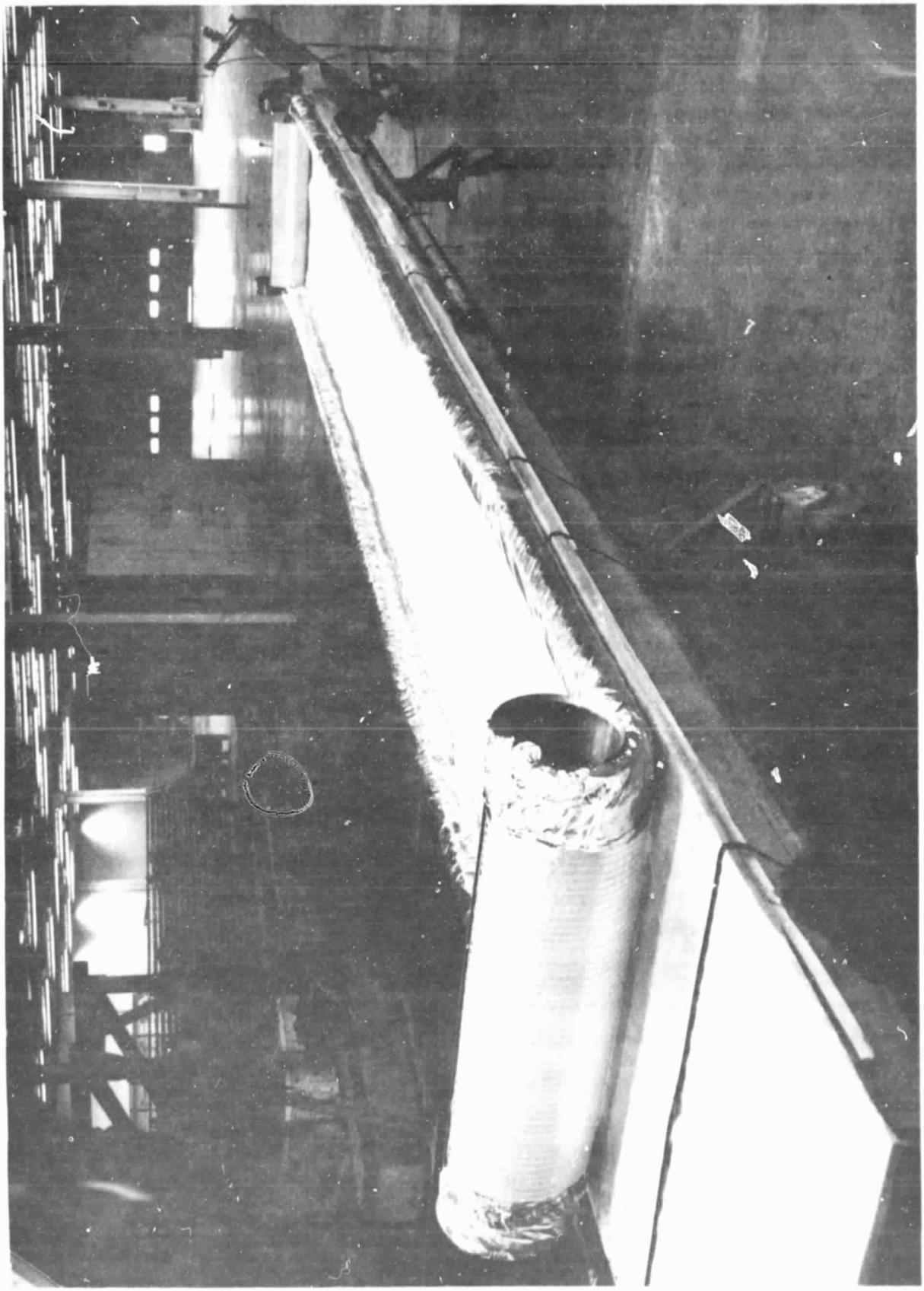

Figure 1 Prototype Flexible Radiator Panel

ORIGINAL PAGE IS
OF POOR QUALITY

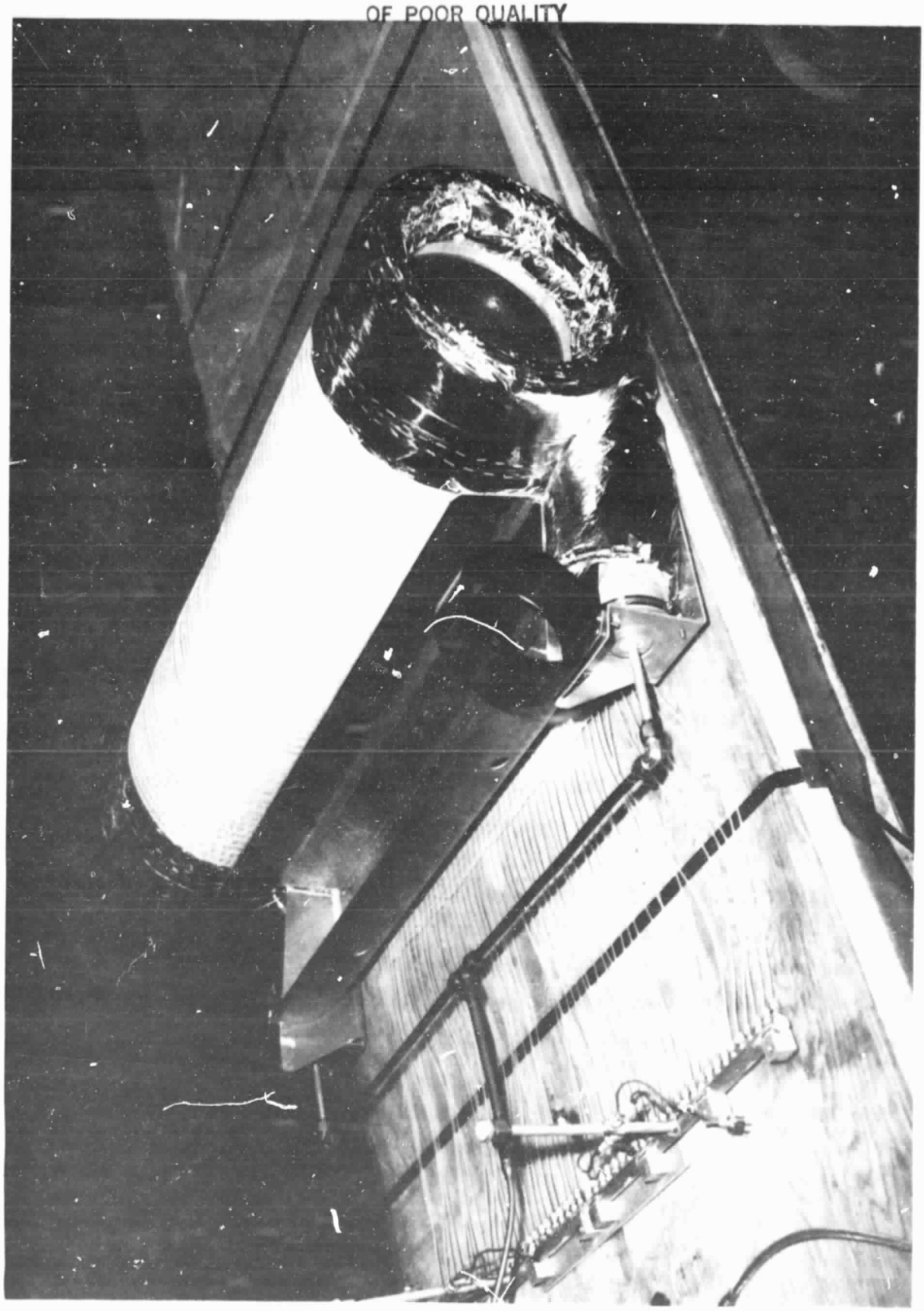

Figure 2 Prototype Flexible Radiator Panel

day mission. The acceptable working fluids for this soft tube flexible radiator are Coolanol 15, Coolanol 20 and Glycol/water (an eutectic mixture).

3.2 Panel Design

The flexible radiator panel is constructed from four basic components: (1) the flexible fin, (2) panel flow tubes, (3) fluid manifolds, and (4) the stowage drum. Principal to the capability of the panel to reject heat is the fin material. The fin material is fabricated by hot rolling a 40 x 67 silver wire mesh into 3 Mil FEP Teflon film. Figure 3 shows a cross section of the fin laminate. Two of the three mil laminates are fusion bonded together with the flow tubes sandwiched in between as shown in Figure 4. The flow tubes are PFA Teflon (typically 1/8" O.D. x 1/16" I.D.) and are normally spaced 0.75" apart on the panel. Solar absorptance value of the mesh/film laminate is 0.16. The emissivity of the fusion bonded laminate is 0.70.

The PFA Teflon flow tubes distribute the heat from the transport fluid over the panel area. These flow tubes run parallel to the long dimension of the radiator panel and connect to aluminum manifolds. The tube-to-manifold connections are made with standard Swagelok fittings, an adhesive (3M EC2216) and tube inserts which allowed the fittings to capture the soft tube without collapsing the tube wall. These connections have been tested for extended periods and have been shown to be leak free.

The fluid manifolds distribute the flow to the panel such that half the flow tubes receive inlet flow. At the deployed end of the radiator, a second manifold collects the flow and directs it into the other half of the flow tubes on the return leg back along the panel into the outlet manifold. The outlet manifold collects the transport fluid from the radiator and directs it back into the environmental control system.

The radiator panels were optimized using existing Vought radiator optimization computer routines for two working fluids identified as the best candidates in the fluid trade study: Ethylene-Glycol/water (60%/40%) and Coolanol 15. A comparison of radiator designs for Glycol/water and Coolanol 15 as working fluids is shown in Table II. While the optimum tube inside diameter was determined to be 0.075 inches for Glycol/water and 0.080 for Coolanol 15 (see Figures 5 and 6), a value of 0.0625 inches was selected for the prototype design. This selection was made because of the availability of standard fitting sizes which limit the tube inside diameter to 0.0625 or 0.125. The larger value would cause a four fold increase in bending moment

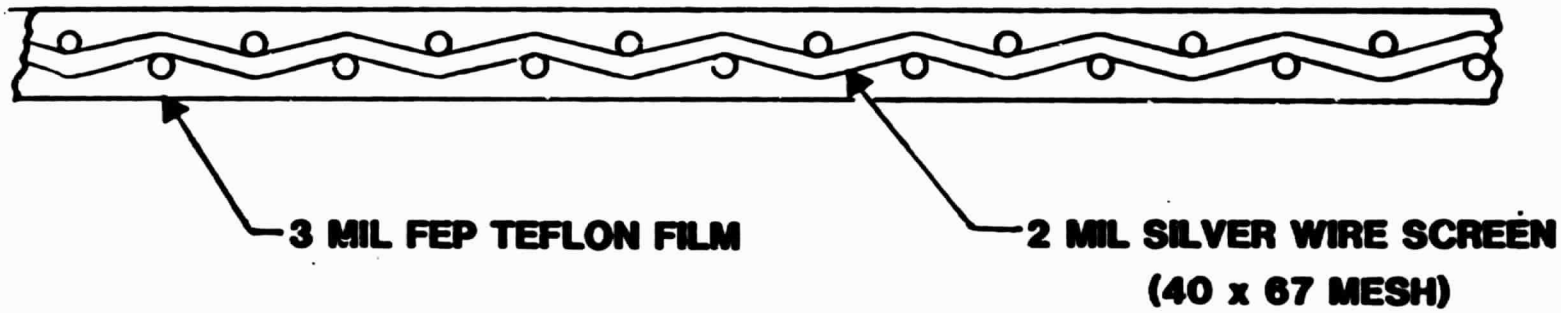

NOTE: ONE LAYER OF TWO-LAYER LAMINATE SHOWN

FIGURE 3 FLEXIBLE RADIATOR FIN MATERIAL

ORIGINAL PAGE IS
OF POOR QUALITY

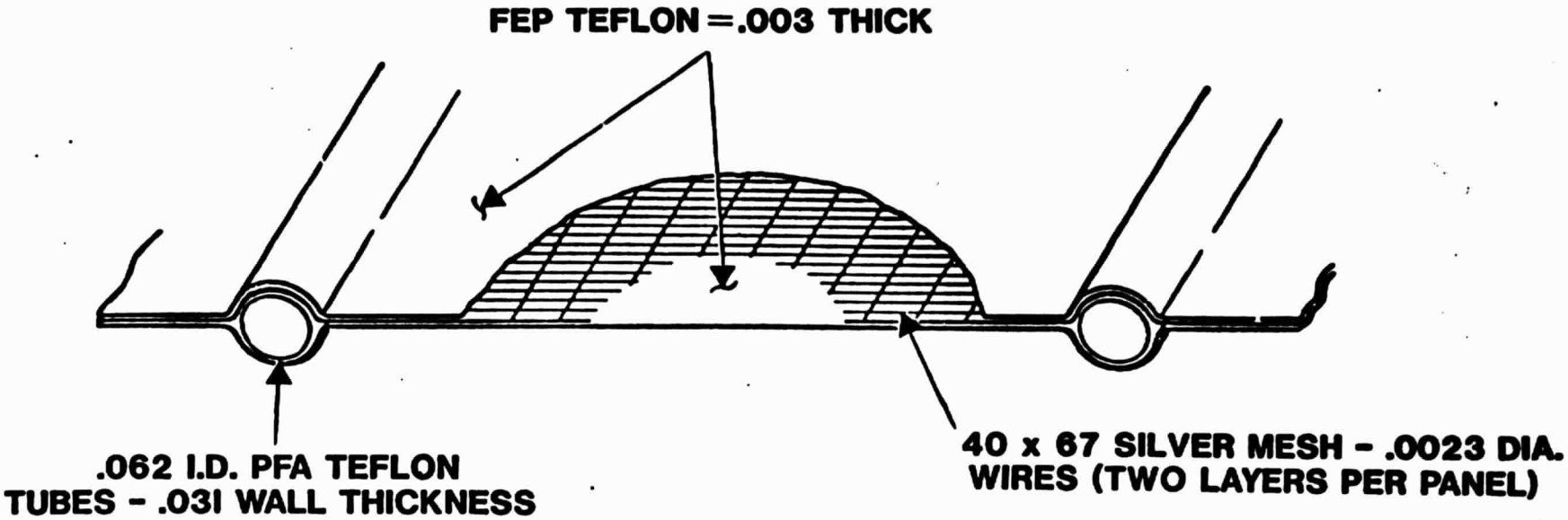

TWO-SIDED RADIATOR DESIGN

- TRANSPORT FLUID : GLYCOL/WATER, COOLANOL 15 OR COLLANOL 20
- RADIATOR PANEL AREA : 173 FT^2
- TUBE SPACING : 0.75 IN.
- PROJECTED TUBING AREA : 16.6%
- SILVER WIRE MESH : 5% FIN CONDUCTION AREA
  23% PROJECTED RADIATION AREA
- WEIGHTS : PANEL + FLUID - 47.3
  POWER PENALTY - 3.3
  50.6 lb.

ORIGINAL PAGE IS OF POOR QUALITY

FIGURE 4 FLEXIBLE RADIATOR PANEL LAYUP

TABLE II
COMPARISON OF FLEXIBLE RADIATOR DESIGNS

DESIGN VARIABLE	RS-89A *	COOLANOL 15
Radiator Panel Length	24.1'	25.7'
Radiator Panel Area	76.9 Ft^2	82.0 Ft^2
Radiator Panel Width	38"	38"
Number of Tubes	50	50
Tube Spacing	0.75"	0.75"
Tube Outside Diameter	0.125"	0.125"
Tube Inside Diameter	0.0625"	0.0625"
Relative Weight**	51.3 lb	58.3 lb
Pressure Drop	33.0 psi	25.5 psi
Bending Moment for 10" Dia Drum	14 in-lb	14 in-lb
Minimum Outlet Temp (100°F)	-20°F	-70°F
Radiator Fin Emissivity	0.71	0.71
Radiator Fin Efficiency	0.943	0.943
Spring Dimensions (5" Dia Mandrel)	.0167"x3"x29'	.0167"x3"x31'

* 60/40% mixture of ethylene-glycol/water.

**The relative weight includes manifolds, the deployment drum, retraction springs, transport tubing and fittings, transport fluid, radiator fins, and the weight penalty for fluid pressure drop.

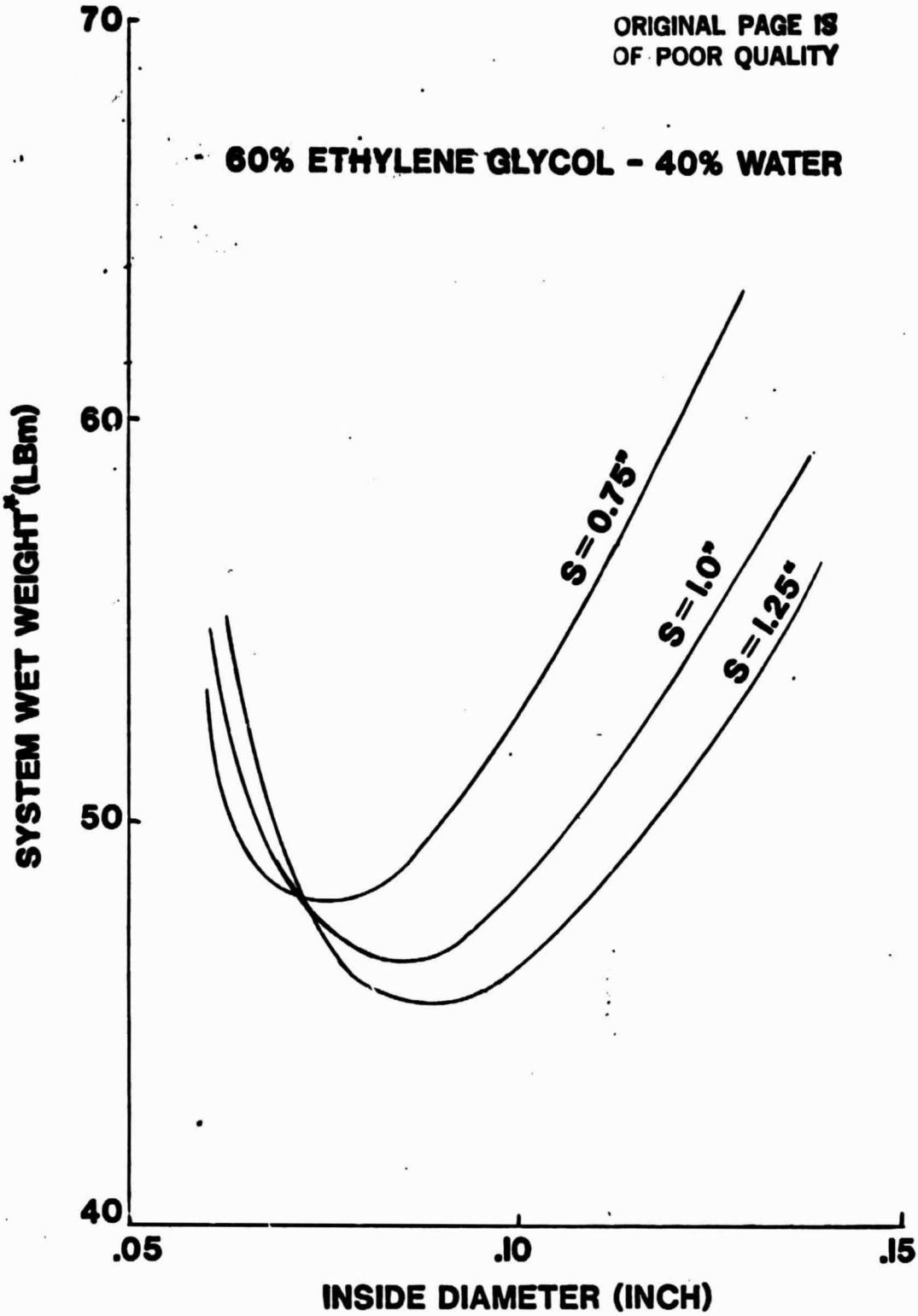

FIGURE 5 SYSTEM WEIGHT FOR RS-89a

*Weight includes manifolds, drum, retraction springs, transport tubing and fittings, fluid, radiator fins and pumping penalty

ORIGINAL PAGE IS
OF POOR QUALITY

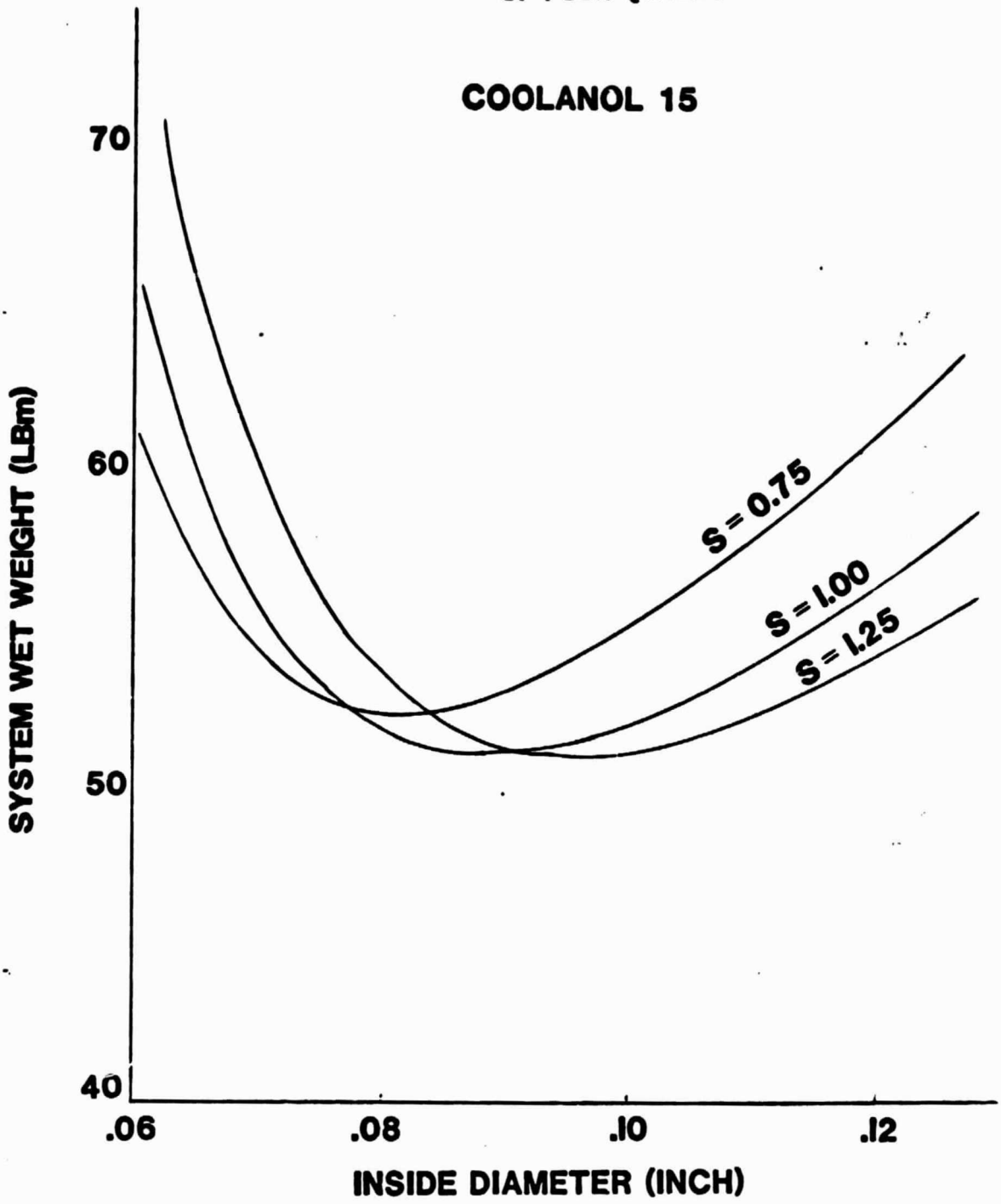

FIGURE 6 SYSTEM WEIGHT FOR COOLANOL 15

* Weight includes manifolds, drum, retraction springs, transport tubing and fittings, fluid, radiator fins and pumping penalty

around the 10 inch drum, as shown in Figure 7.

3.3 Performance

3.3.1 Heat Rejection Performance

The heat rejection performance of the soft tube radiator is a function of the fluid temperatures (inlet and outlet), the radiation sink temperature and the physical panel configuration (tube spacing, tube diameter, and composite fin design). The heat rejection performance is shown parametrically in Figures 8 through 10 for the prototype panel configuration. The performance is shown in terms of heat rejected per unit radiation area vs inlet, outlet and sink temperatures. The performance is approximately the same for each of the three acceptable fluids (Coolanol 15, Coolanol 20 or Glycol/water). Thus, the curves can be used to determine the panel area required, regardless of the fluid used.

Flow stability restricts the panel outlet temperature for low sink temperature conditions the minimum allowable outlet temperature for a given fluid is a function of the inlet temperature, as discussed in Section 3.5. The minimum allowable outlet temperatures for Glycol/water, Coolanol 20 and Coolanol 15 are shown on Figures 8 through 10. The heat load turn down ratio (high load to low load ratio) can be estimated from the curves if inlet temperatures and maximum and minimum sink temperatures are known. If, for instance, the high load fluid temperatures are 140°F in and 40°F out, and a sink temperature of -40°F, the maximum Q/A is 45 BTU/hr-ft^2. If the minimum inlet temperature is 60°F, and the minimum sink temperature is -180 F, the minimum Q/A is 41 BTU/hr-ft^2 for Glycol/water. Thus, the turn down ratio is 1.1 to 1. Area modulation is necessary for heat load control because of this low turn down ratio. Methods for doing this are discussed in Section 3.4.

3.3.2 Weight

The dry panel weight in pounds can be estimated as follows:

$$W_p = W_{manifold + fittings} + W_{tubes} + W_{fins}$$

$$W_p = .0674\ W + 8.86\ \frac{A}{S}\ (d_o^2 - d_i^2) + [\ .1397 + .080\ \frac{do}{S}]A$$

where:
- W = the width of the radiator panel in inches
- A = the panel projected area in ft^2
- S = tube spacing in inches
- d_o = outside tube diameter in inches
- d_i = inside tube diameter in inches

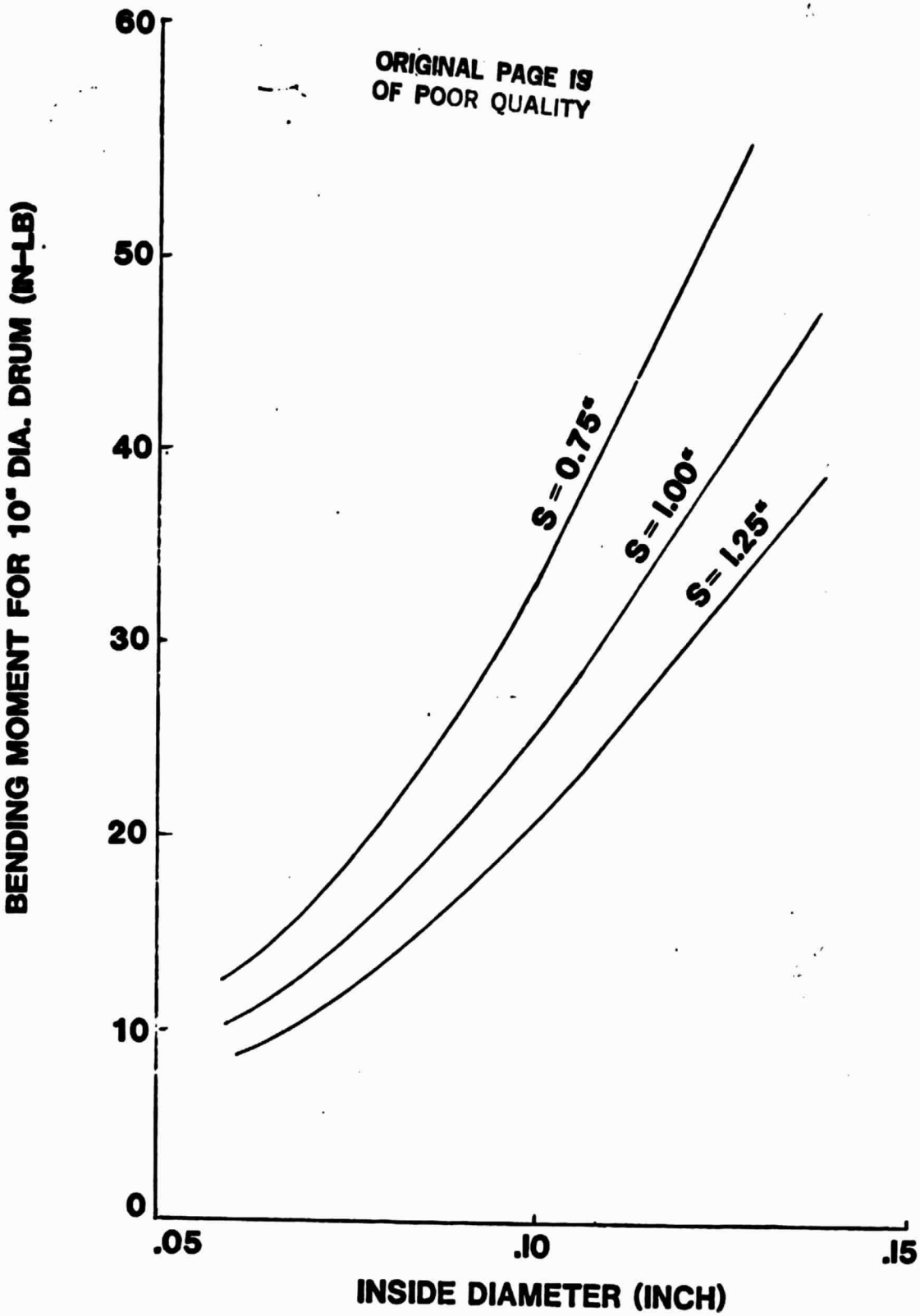

FIGURE 7 BENDING MOMENT REQUIREMENTS

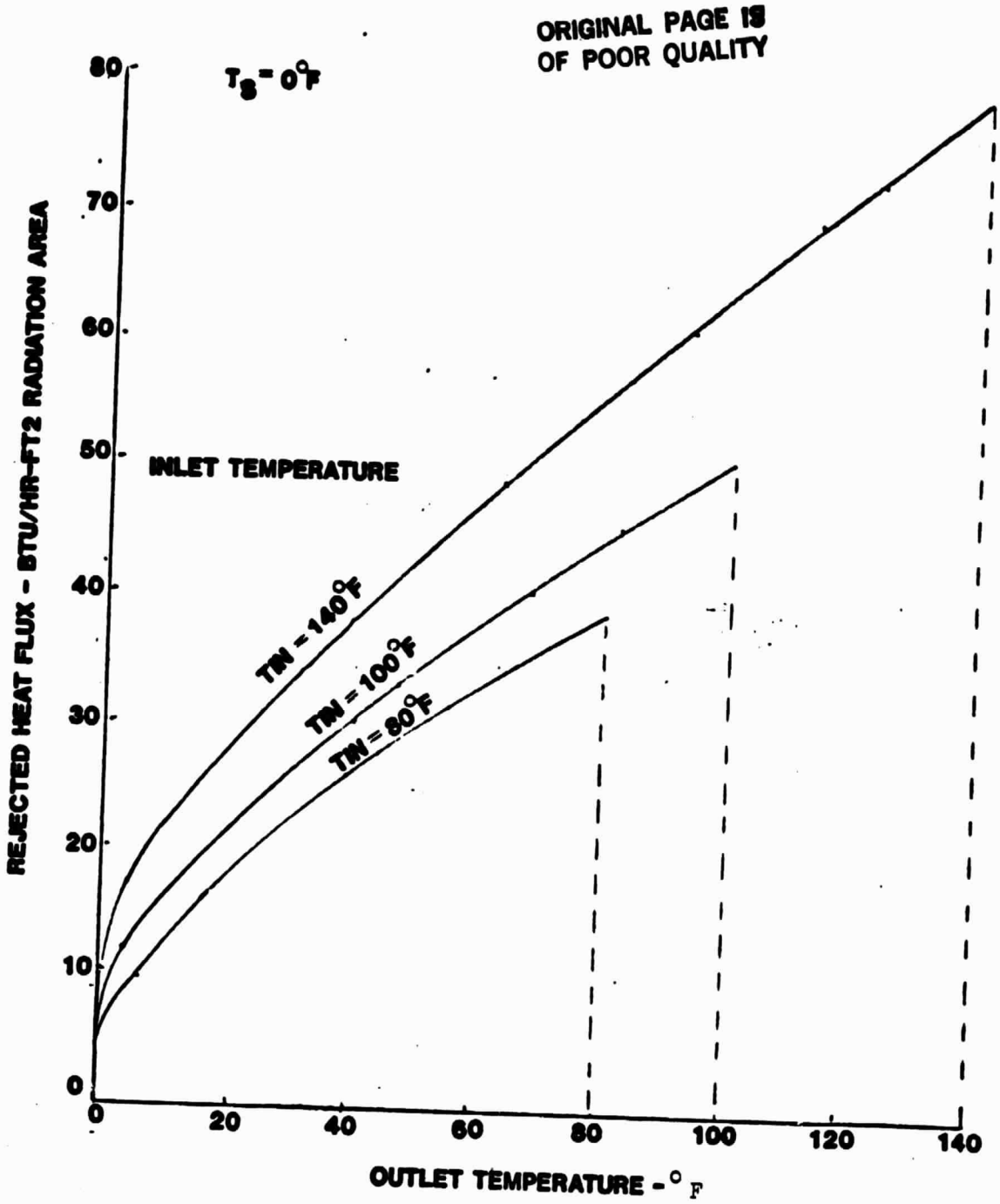

FIGURE 8 SOFT TUBE FLEXIBLE RADIATOR REJECTION HEAT FLUX FOR 0°F SINK TEMPERATURE

ORIGINAL PAGE IS
OF POOR QUALITY

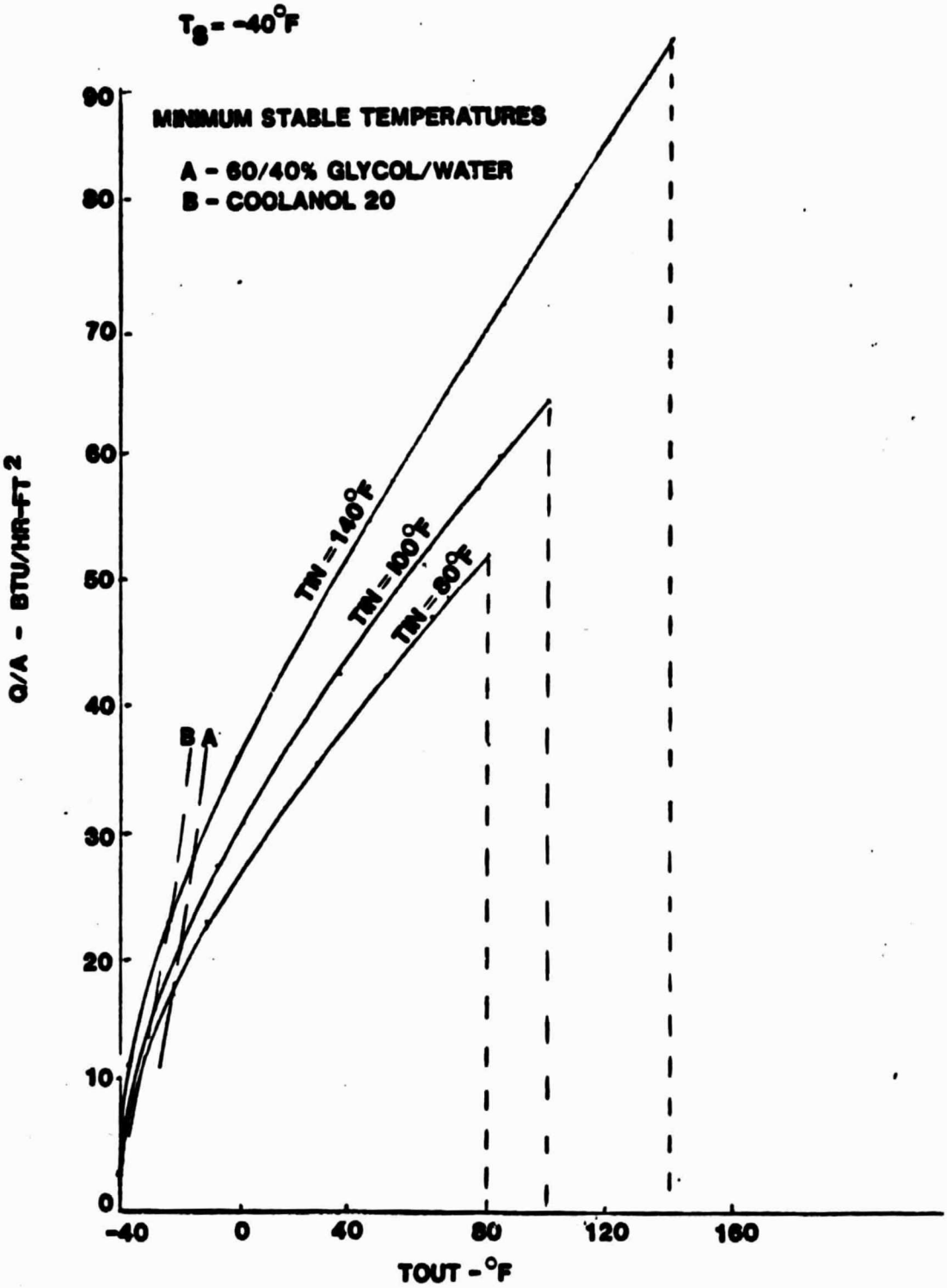

FIGURE 9 SOFT TUBE FLEXIBLE RADIATOR REJECTION HEAT FLUX FOR -40°F SINK TEMPERATURE

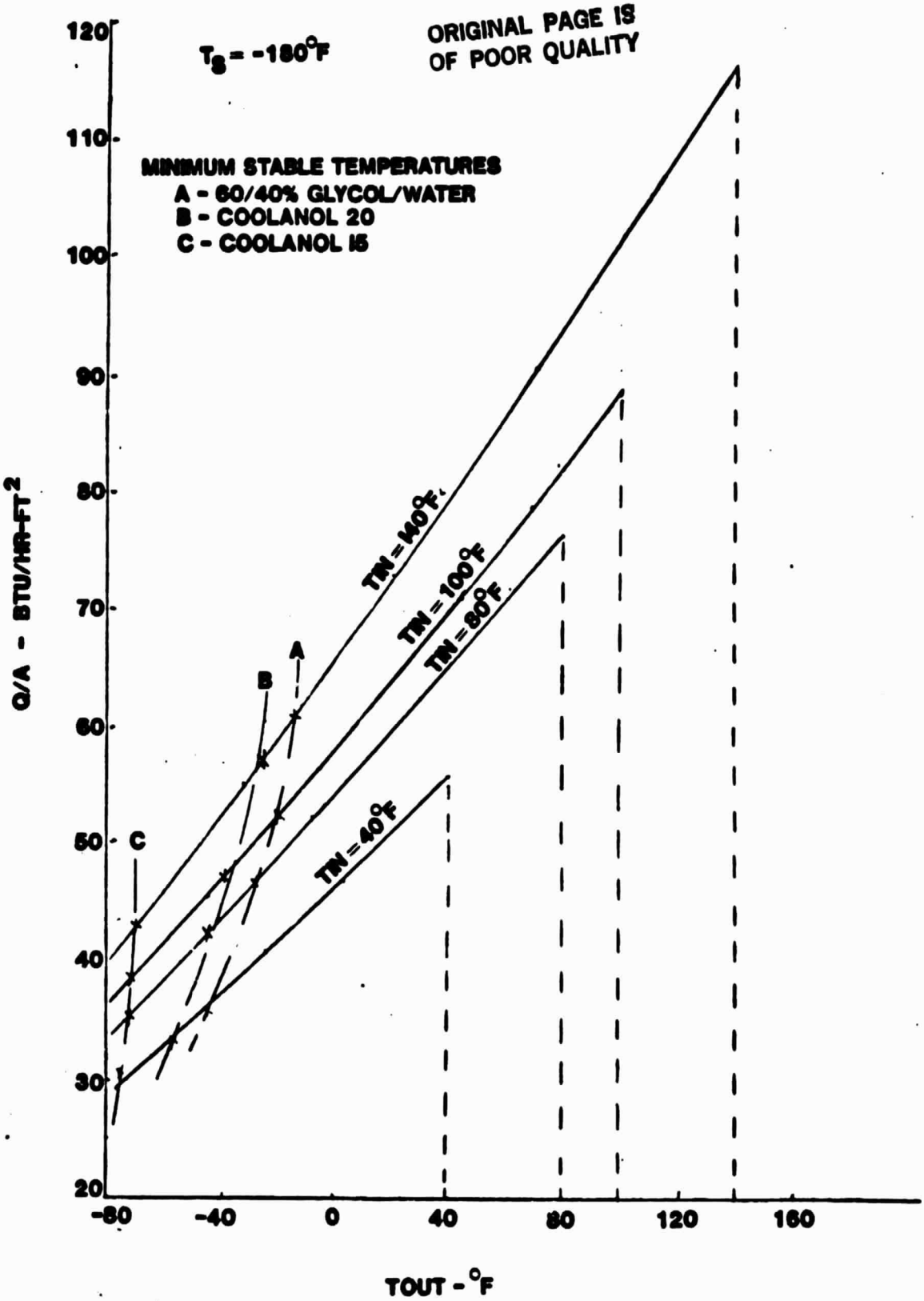

FIGURE 10 SOFT TUBE FLEXIBLE RADIATOR REJECTION HEAT FLUX FOR -180°F SINK TEMPERATURE

For the baseline design, S = .75 inches, d_o = .125 inches, d_i = 0.62 inches, W = 38 inches, and the length is 27 ft (A = 85.5 ft^2).

This gives, for the baseline design

$$W_p = 2.56 + .139A + .153A$$

or

$$\frac{W_p}{A} = .32 \text{ lb/ft}^2 \text{ dry panel weight}$$

The fluid weight can be estimated by

$$W_f = [\, 4.08 \ \frac{A}{S} \ d_i^{\,2} + .01 \ W] \ \rho/\rho_{H_2O}$$

For S = .75, d_i = .062, ρ = 67 (Glycol/water) and W = 38 inches,

$$\frac{W_f}{A} = .028 \text{ lb/ft}^2$$

The inflation tube deployment system weight can be estimated by

$$W_D = .0195 \ DW + 23 \ tL$$

where:
- D = diameter of deployment drum in inches
- W = panel width in inches
- t = thickness of retraction springs in inches
- L = length of panel in feet

For the baseline panel, D = 10 inches, W = 38 inches, t = .0167 inches, and L = 27 ft.

$$W_D = 17.8 \text{ lb}$$

or

$$\frac{W_D}{A} = .208 \text{ lb/ft}^2$$

The pumping power weight can be estimated by

ORIGINAL PAGE IS
OF POOR QUALITY

$$W_{pp} = 9.87 \times 10^{-17} \frac{S \cdot L}{W d_i^4} \dot{m}^2 \cdot \frac{PP}{N}$$

For the baseline panel, S = .75 inches, L = 27 feet, W = 38 inches and d_i = .062 inches. Also, if we assume $\dot{m}$ = 100 lb/hr, the pump power penalty, PP_1 = 350 lb/kW, and a pump efficiency, N, of 0.3:

$$W_{pp} = 3.33 \text{ lbs.}$$

or

$$\frac{W_{pp}}{A} \quad 0.039 \text{ lb/ft}^2$$

The total weight can be summarized as

$$\frac{W_t}{A} = \frac{W_p}{A} + \frac{W_f}{A} + \frac{W_D}{A} + \frac{W_{pp}}{A}$$

$$= (.32 + .028 + .208 + .039) \text{ lb/ft}^2$$
$$= .595 \text{ lb/ft}^2 \text{ of projected area}$$
$$= .298 \text{ lb/ft}^2 \text{ of radiating area}$$

If the pumping power weight is ignored (i.e., hardware weight only), the total wet hardware weight of the baseline system is

$$\frac{W_t}{A} = \frac{W_p}{A} + \frac{W_f}{A} + \frac{W_D}{A}$$

$$= (.32 + .028 + .208) \text{ lb/ft}^2$$
$$= .554 \text{ lb/ft}^2 \text{ of projected panel area}$$
$$= .277 \text{ lb/ft}^2 \text{ of radiating area}$$

3.3.3 Panel Hydraulic Characteristics

The pressure drop of the flexible radiator is a function of the panel flow geometry (number of tubes, tube I.D., and tube length) and the fluid thermophysical properties (which are a function of temperature distribution). The pressure drop can be calculated by the equation

$$\Delta P = 6.795 \times 10^{-10} \left(\frac{\mu}{\rho}\right)\left(\frac{LS}{W d_i^4}\right) \dot{m} + 3.4 \times 10^{-7} \left(\frac{1}{\rho}\right)\left(\frac{S}{W d_i^2}\right) \dot{m}^2$$

ORIGINAL PAGE IS
OF POOR QUALITY

where ΔP = panel pressure drop, psi

m = mass flowrate, lbm/hr

L = length of flow path, ft.

w = panel width in flow direction, inches

S = tube spacing, inches

d_i = internal diameter, feet

μ = fluid viscosity, lb/ft-hr

ρ = fluid density, lb/ft^3

Figure 11 summarizes the pressure drop estimates for the baselined (prototype) panel design. The geometric values used are:

L = 58.5 feet

W = 18.75 inches

S = .75 inches

d_i = .005208 feet

The thermophysical property values for Glycol/water used in the predictions are summarized in Table III, along with those for the Coolanol fluids.

TABLE III
THERMOPHYSICAL PROPERTIES OF FLUIDS

TEMP, °F	VISCOSITY, LB/HR-FT			DENSITY, LB/FT3		
	GLY/WATER	COOLANOL 15	COOLANOL 20	GLY/WATER	COOLANOL 15	COOLANOL 20
-50	700	28.6	58.1	69.4	59.0	59.9
0	76.0	10.5	15.7	69.6	57.4	58.0
50	18.0	5.42	6.97	67.6	56.0	56.2
70	12.0	4.19	5.46	67.2	55.4	55.2
100	7.25	3.21	4.06	66.6	54.5	54.3
150	3.65	2.26	2.57	65.4	53.0	52.4

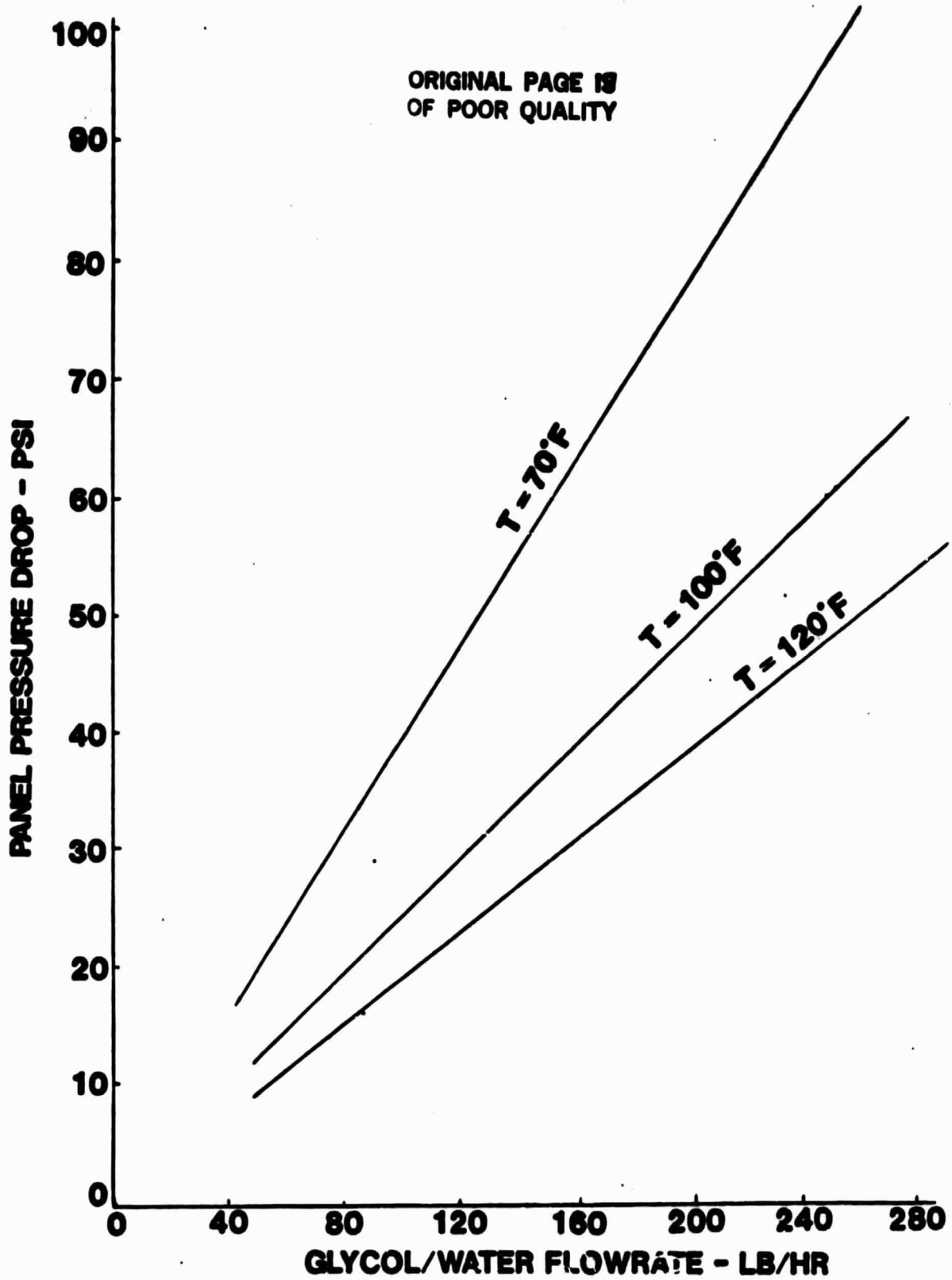

FIGURE 11 SOFT TUBE RADIATOR PRESSURE DROP TEST SUMMARY

ORIGINAL PAGE IS
OF POOR QUALITY

3.4 Deployment Methods

Two basic approaches are candidates for deployment of the soft tube flexible radiator. These are the inflation tube/retraction spring deployment or pneumatic method and an extendable boom deployment method. These approaches are discussed below.

3.4.1 Pneumatic Deployment

With the pneumatic inflation tube deployment/spring retraction concept, the flexible radiator panel, which is stored (wrapped) onto a cylindrical drum, is deployed into a near planar panel by inflating tubes on each side of the panel with nitrogen gas. The pressurizing of the tubes causes them to straighten against the retraction springs contained inside the tubes. Retraction is accomplished by deflating the deployment tubes, allowing the retraction spring to roll the flexible panel up around the drum.

Figures 12 through 15 illustrate the pneumatic deployment approach. Figures 1 and 2 show the prototype panel configuration which uses this method. In its design, a 4 inch diameter inflation tube is attached to each edge of the radiator panel. The tube is fabricated from .030" thickness of Kevlar/Mylar and a pocket is fabricated onto the inflation tube (on the drum side of the tube) into which the 3 inch wide by 0.016 inch thick flat steel spring is attached. The panel is stowed in approximately eight wraps on a 10 inch diameter by 30 inches wide stowage drum. The drum is deployed on the end of the panel as illustrated in Figure 12. The deployment is accomplished by supplying low pressure nitrogen ($\approx$ 1 psig) to the inflation tube. The magnitude of the force exerted by the two retraction springs must be closely matched to effect a straight roll-up of the radiator panel onto the drum. A spring adjustment capability is designed into the spring hold-down to permit fine tuning of the panel retraction force.

Figure 13 shows a schematic of the nitrogen pressurization system interfaces with the inflation tube deployment approach. This nitrogen pressurization system is configured to permit active control of deployment length for heat load control. Deployment is accomplished by increasing nitrogen pressure in the inflation tubes. Retraction is accomplished by venting the tubes to reduce pressure. This method of deployed area control requires a sufficient supply of nitrogen gas to replace that expended. Also shown in Figure 13 is the deployment action as a function of radiator outlet temperature. The area control system attempts to maintain the radiator outlet

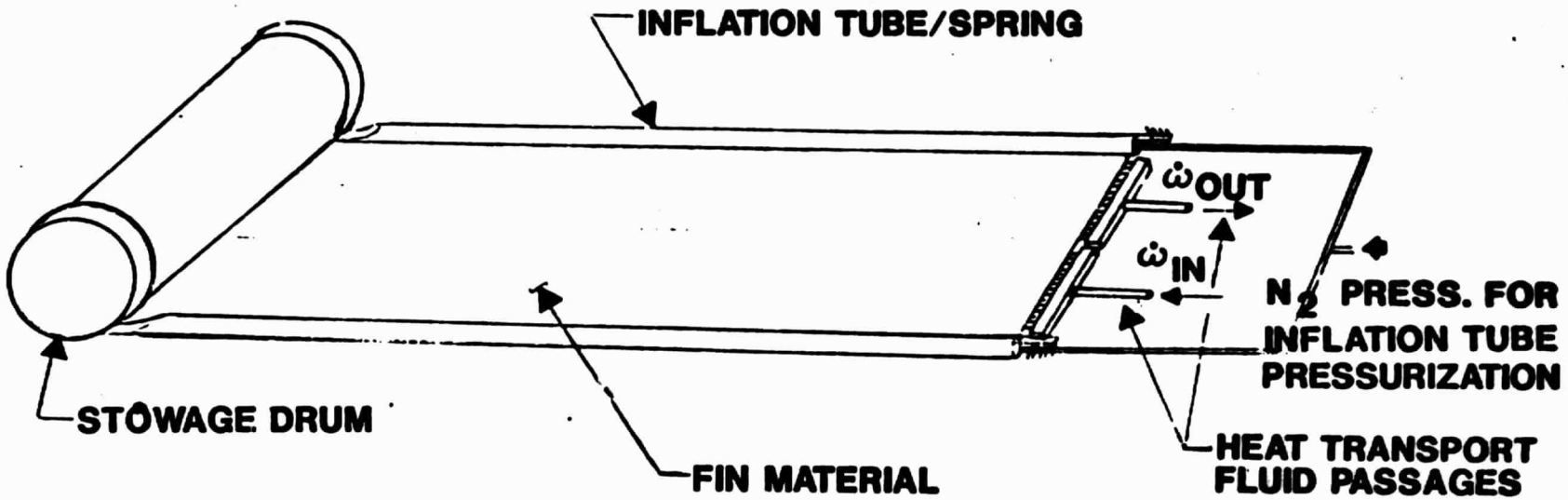

Figure 12 Flexible Radiator Panel with Pneumatic Deployment

ORIGINAL PAGE IS OF POOR QUALITY

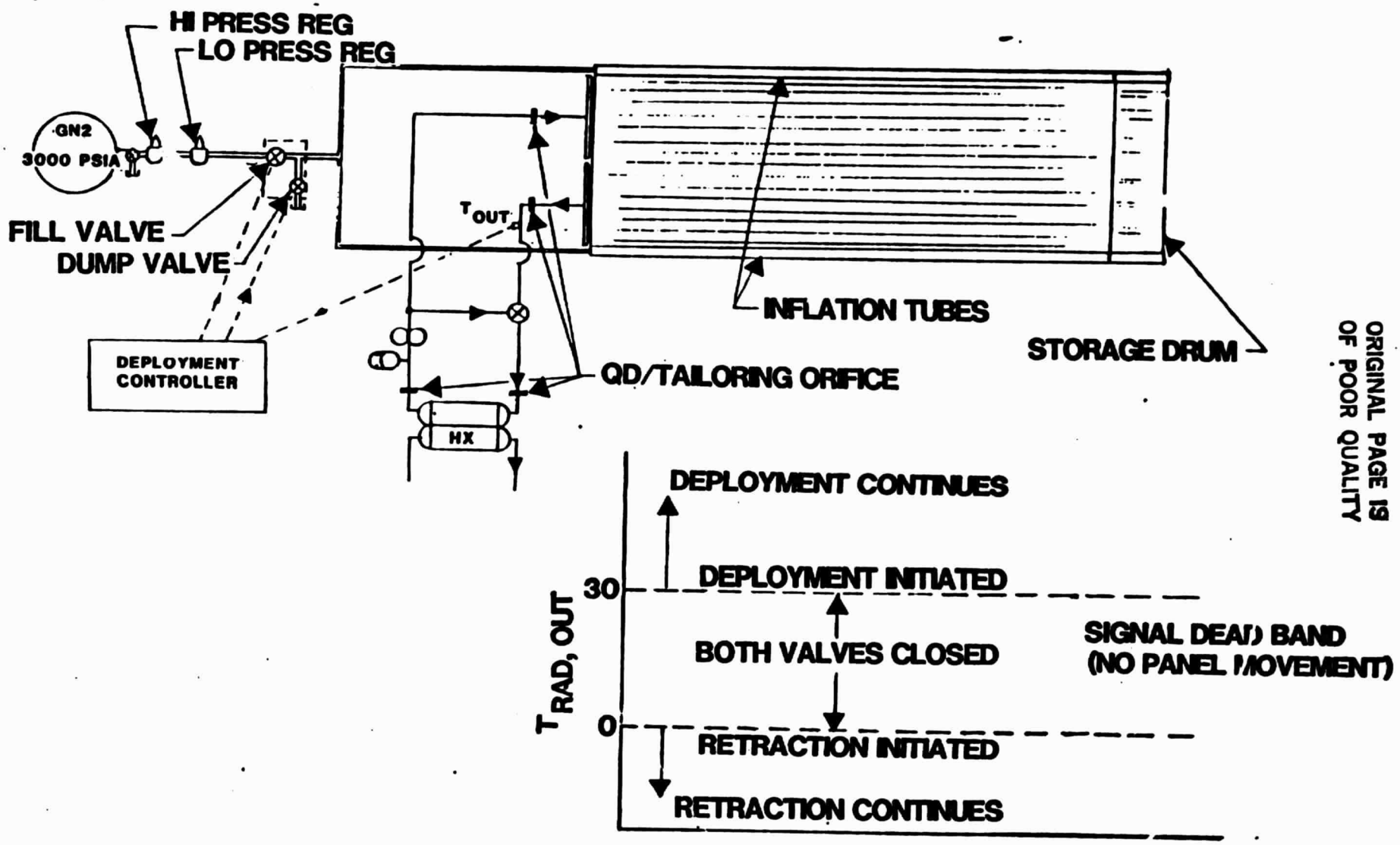

ORIGINAL PAGE IS
OF POOR QUALITY

FIGURE 13 SOFT TUBE RADIATOR DEPLOYMENT/RETRACTION CONTROL

temperature between $0^{o}F$ and $30^{o}F$.

Figure 14 shows a drawing of a 4 kW heat rejection subsystem (3.4 kW with $0^{o}F$ sink temperature; 5.1 kW with a $-40^{o}F$ sink temperature) with $110^{o}F$ inlet temperature and $40^{o}F$ outlet temperature.

Figure 15 shows two 4 kW wings stowed in the cargo bay of the Shuttle Orbiter. Weight estimates for the 4 kW subsystem using the pneumatic deployment are shown in Table IV. The total system weight is approximately 368 pounds.

3.4.2 Extendible Boom Deployment/Retraction

The mechanically driven extendible boom is an attractive alternate to the pneumatic deployment system described in the previous section. As with the pneumatic deployment, the flexible panel is stowed on a cylindrical drum. The panel is deployed into a planar configuration by extending the extendible boom, thus unrolling the panel from the drum. The stowage drum can be either located at the outboard end of the panel, as shown in Figure 17, or at the panel base, as shown in Figure 16. When the drum is located outboard, no fluid swivels are required. However, the concentrated outboard mass (of the drum) adversely impacts the extendible boom design. When the drum is located inboard, fluid swivels or a flexible hose transfer device is required. Figure 18 illustrates the coiled flexible hose transfer device which has been built and tested at Vought.

The flex hose transfer device which was built will allow 5.8 revolutions and 250 cycles. Fluid swivels will do the same job with much lower weight, less volume, less pressure drop, and less complexity. The baselined approach for the extendible boom deployment method is with drum at the base of the radiator with fluid swivels for fluid transfer across the rotating joints (see Figure 16). Using this method, two extendible booms (one on each side) push on the end of the panel to deploy it, pushing against the retraction springs in the drum (see Figure 19). As the radiator panel is deployed, retraction springs (Figure 19) are extended by a 1/16 inch stainless steel cable which winds up on a cable spool attached to the storage drum axle. Panel retraction torque is a constant torque applied by a set of springs through the cable to the storage drum axle. This torque remains constant throughout panel deployment and retraction. Since the storage drum always has a restoring torque applied, panel retraction is initiated by retracting the deployable boom. This retraction mechanism was successfully used in the hard tube flexible radiator design.

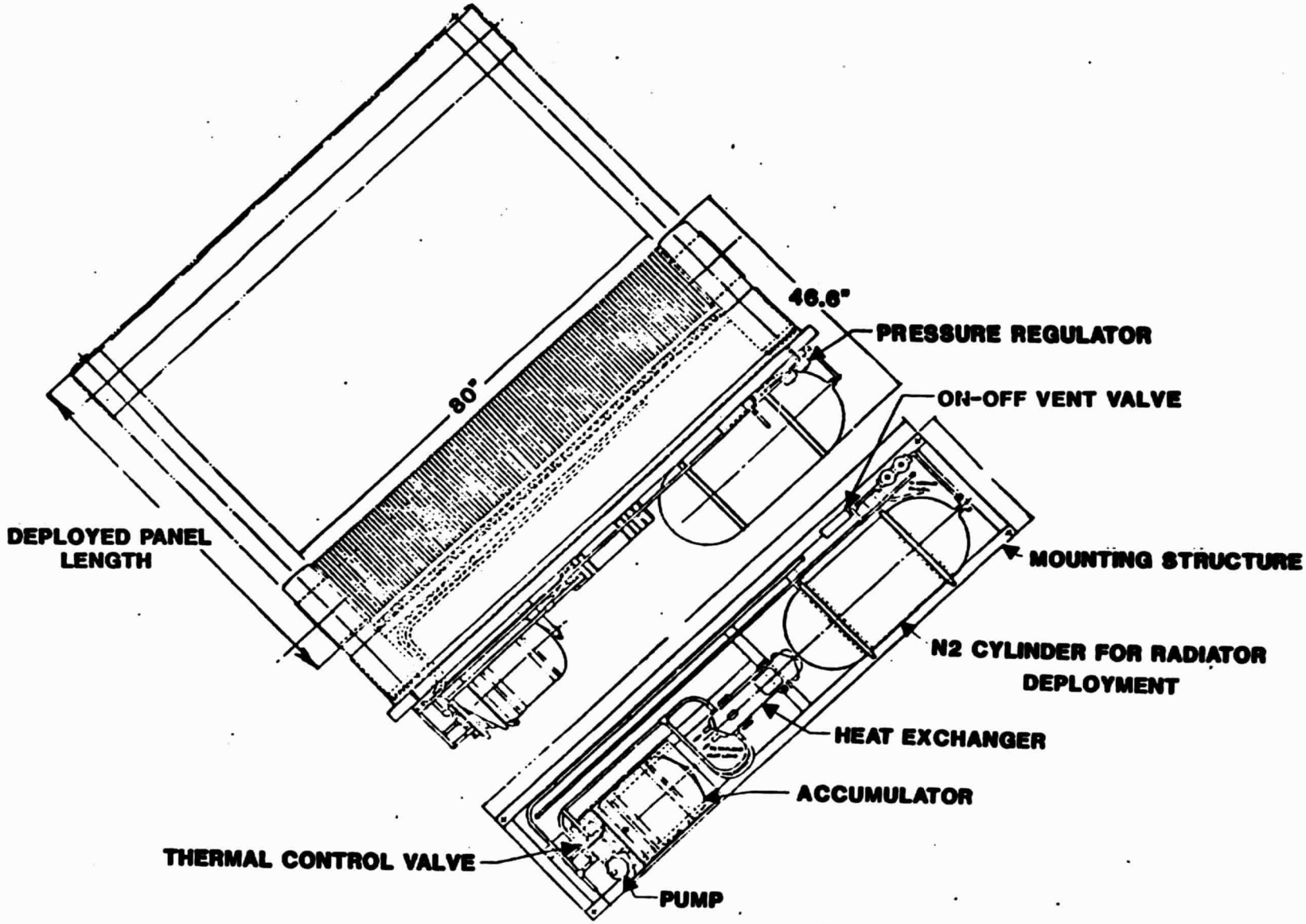

FIGURE 14 FLEXIBLE RADIATOR PNEUMATIC DEPLOYMENT PACKAGE

ORIGINAL PAGE IS OF POOR QUALITY

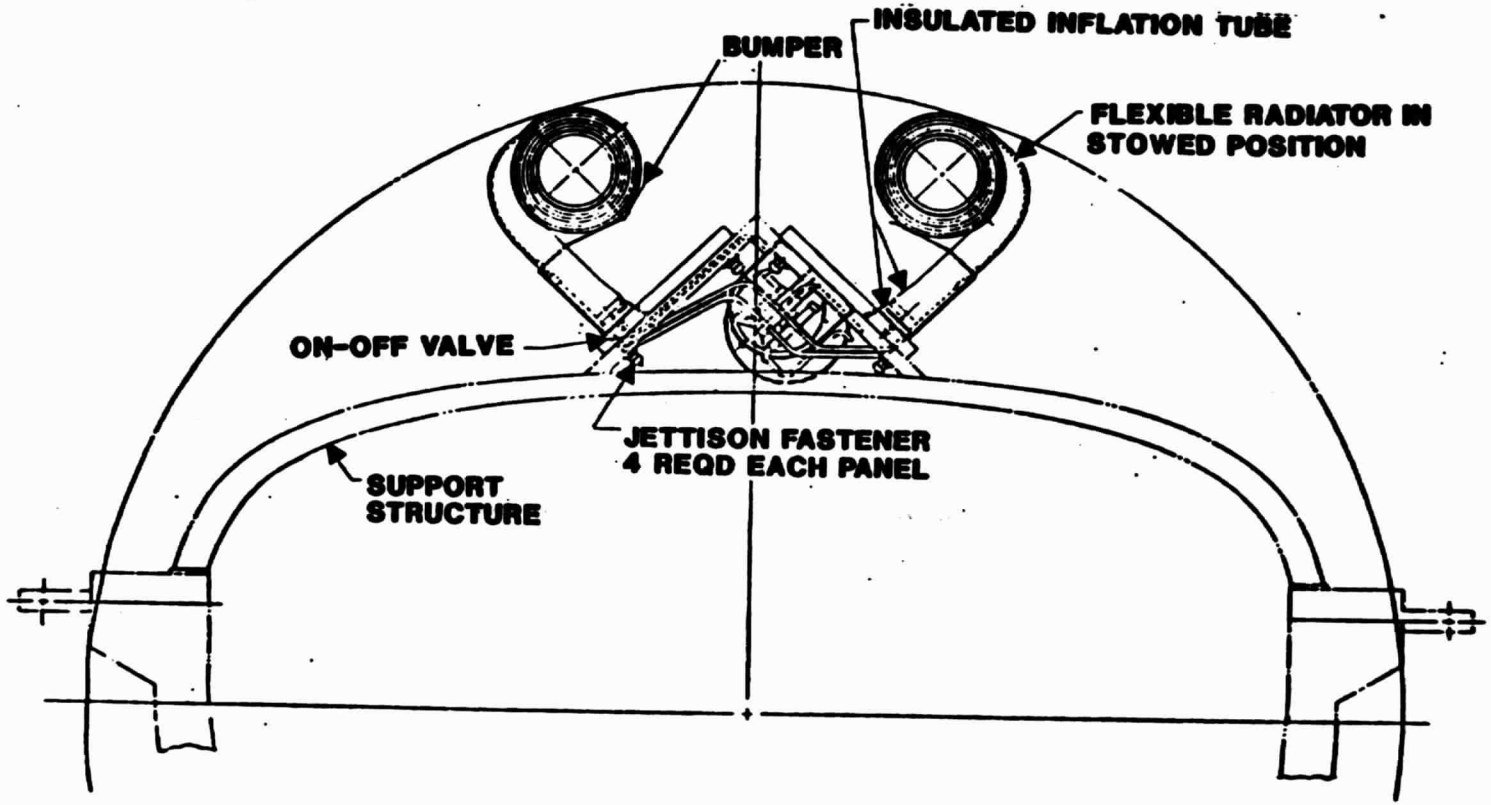

ORIGINAL PAGE IS OF POOR QUALITY

FIGURE 15

FLEXIBLE RADIATOR PNEUMATIC DEPLOYMENT IN STOWED POSITION

TABLE IV
4 kW FLEXIBLE RADIATOR MODULE
PNEUMATIC DEPLOYMENT

Panel (80" wide by 27' long)		33.5
Panel Clamp		4.0
Panel Manifold and Fittings		6.0
Drum and Plumbing		15.6
Inflation Tube & Spring Support, Clamps, and Hardware		54.5
Accumulator Package		20.5
Heat Exchanger		16.4
Coolant Plumbing, Clamps and Hardware		5.4
N_2 Cylinder		88.5
Cylinder Mtg. Clamps		2.8
N_2 On-Off-Vent Valve (2)		3.0
N_2 Plumbing, Clamps and Hardware		2.5
N_2 Regulator		1.0
N_2 Elect. Control Box		2.0
Mounting Frame		32.5
Jettison Fasteners		2.0
	DRY WEIGHT	290.2
Coolanol 20		27.0
N_2 Gas		23.4
	WET WEIGHT	340.6
Production Growth (8%)		27.2
	PRODUCTION WEIGHT	368

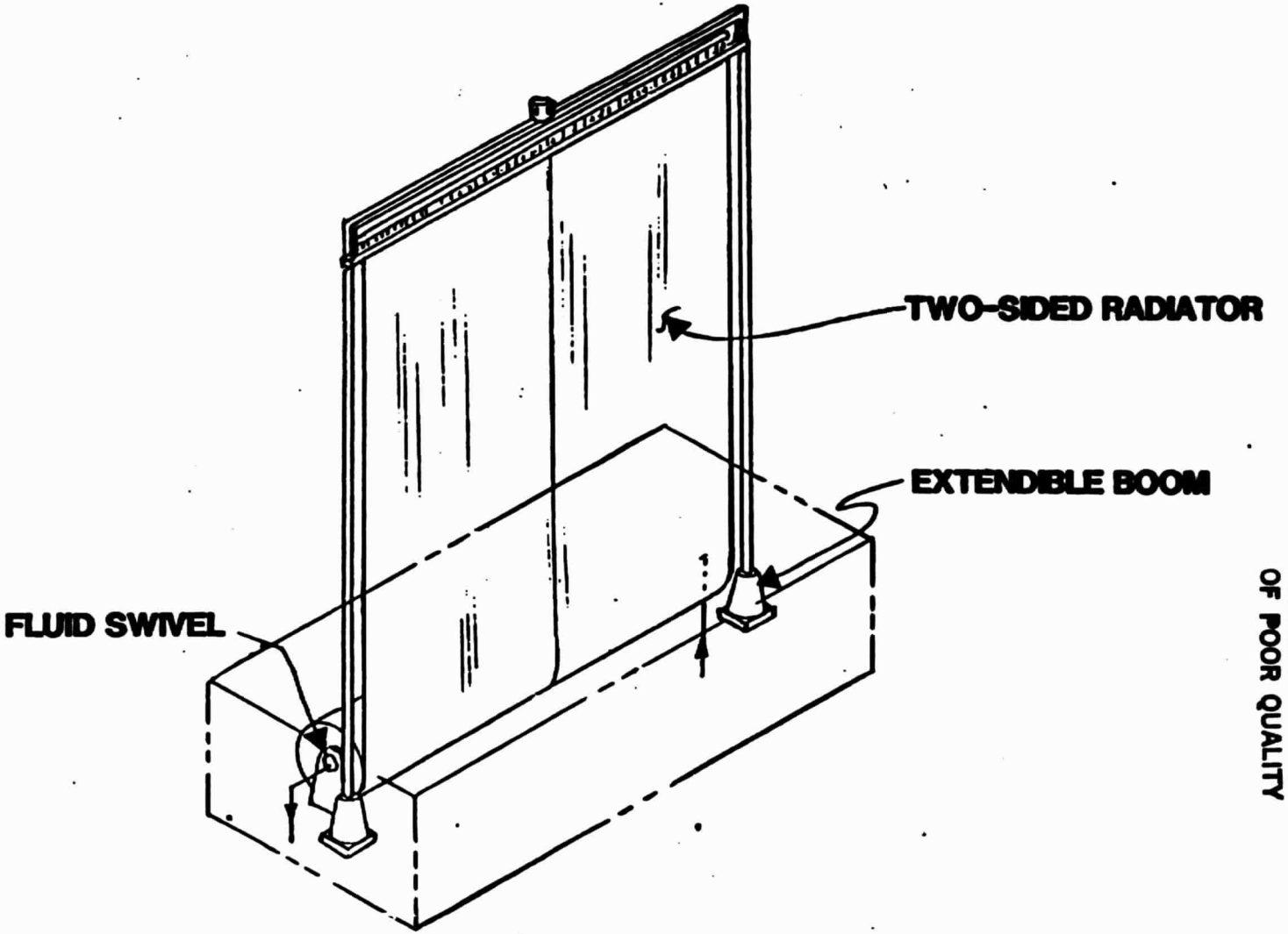

FIGURE 16 FLEXIBLE RADIATOR, DUAL BOOM DEPLOY, SPOOL AT BASE

ORIGINAL PAGE IS
OF POOR QUALITY

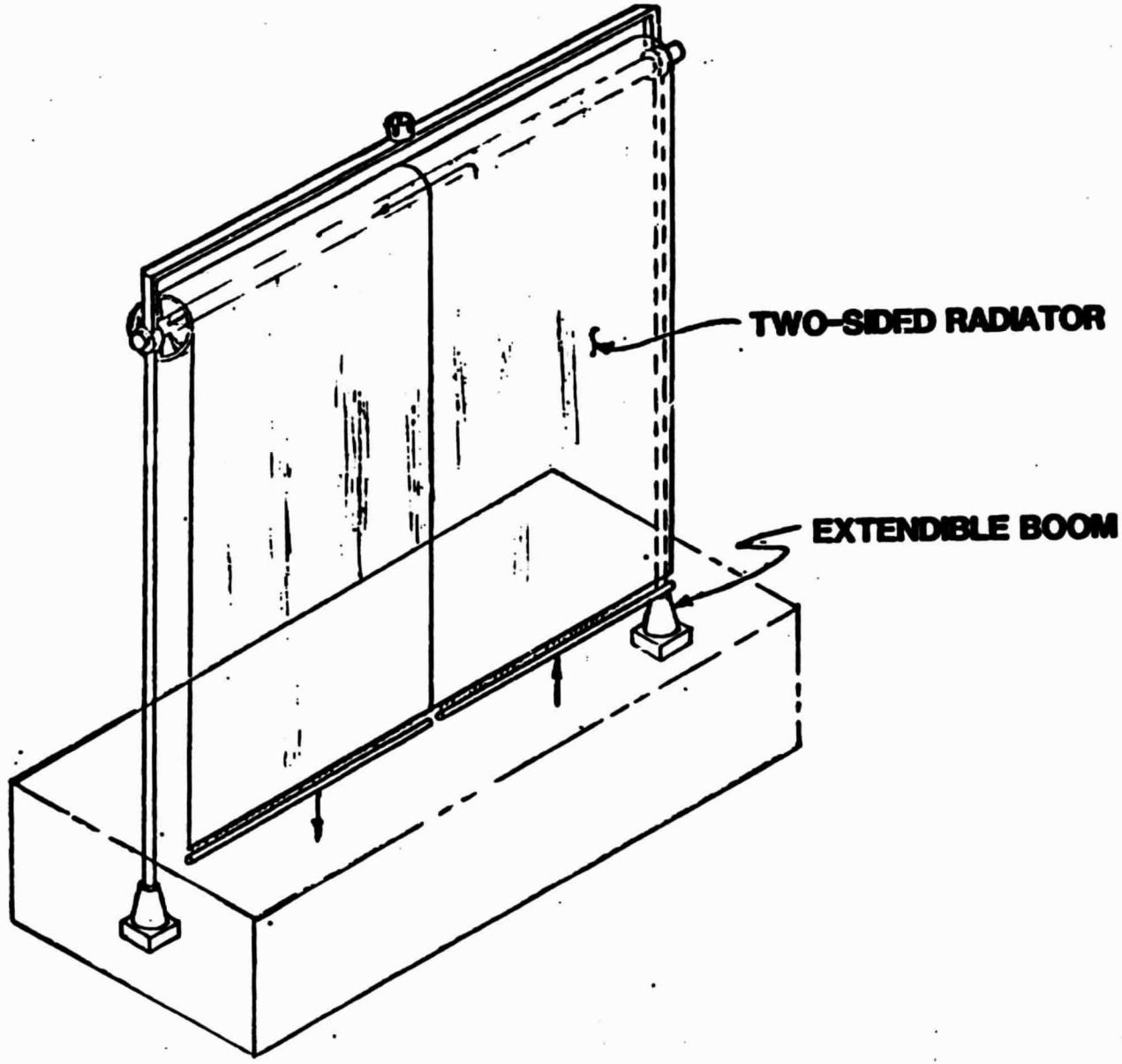

FIGURE 17 FLEXIBLE RADIATOR, DUAL BOOM DEPLOY, SPOOL OUTBOARD

ORIGINAL PAGE IS
OF POOR QUALITY

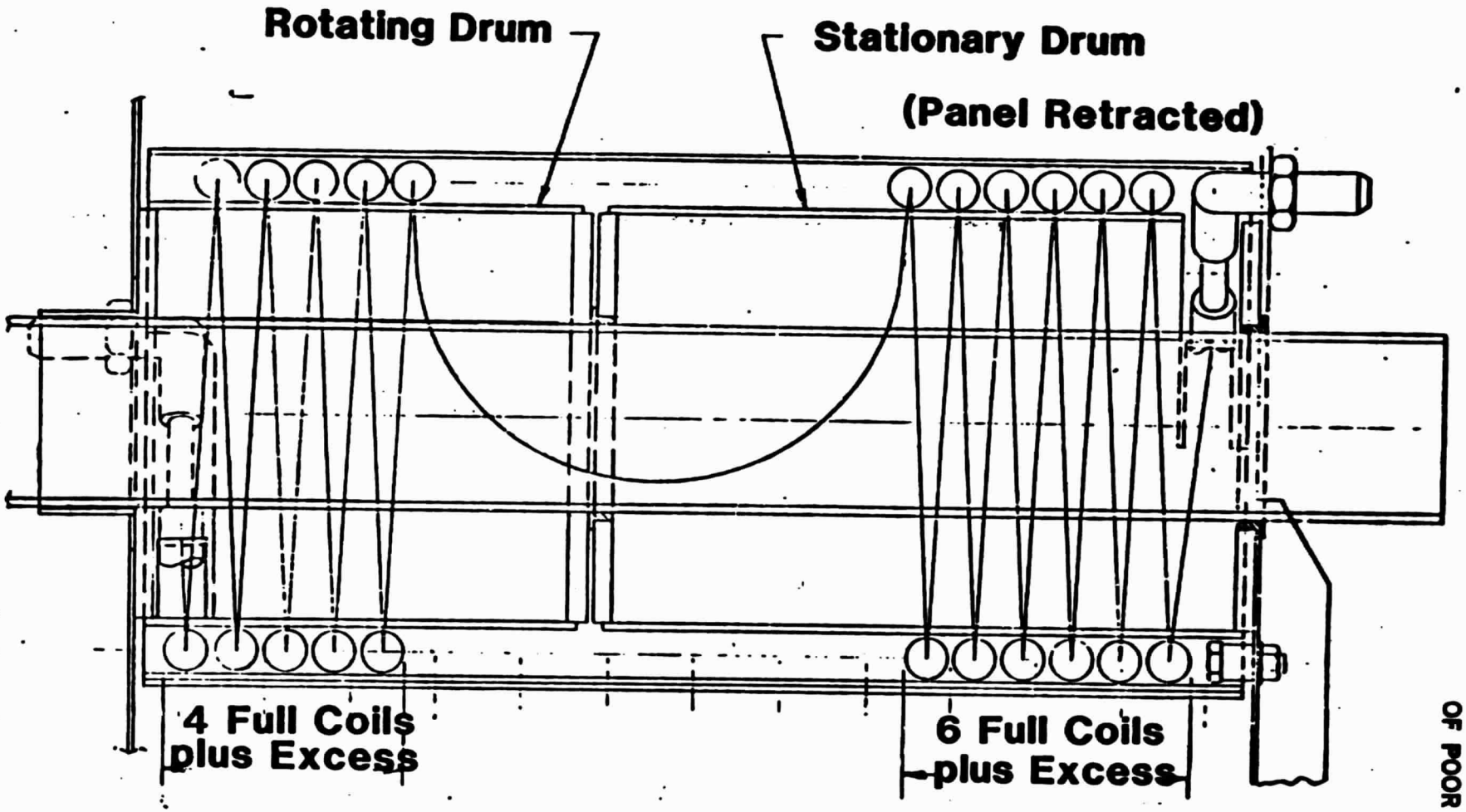

Figure 18 Coiled Flex Hose transports the fluid across the rotating joint

ORIGINAL PAGE IS
OF POOR QUALITY

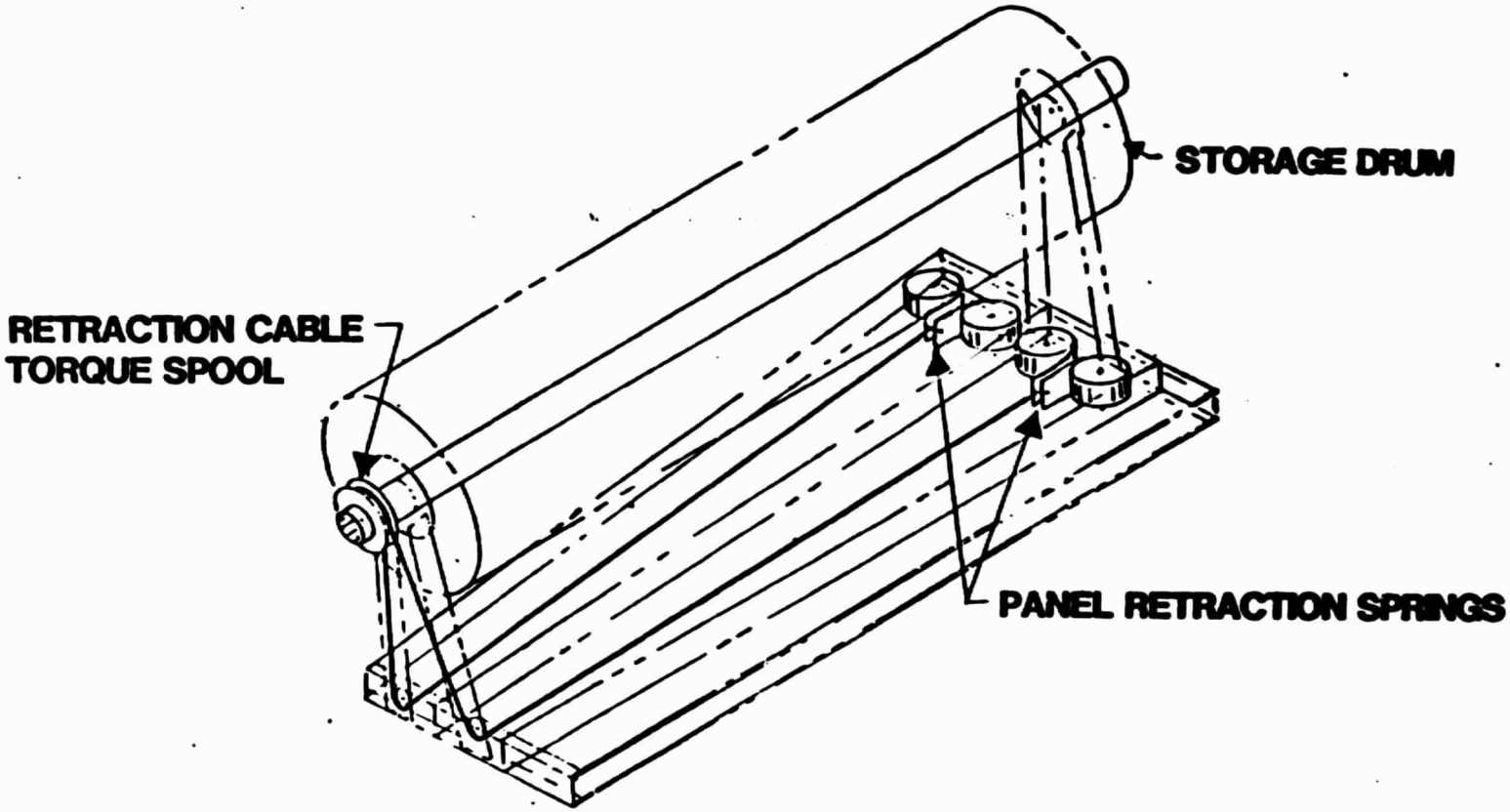

FIGURE 19 RETRACTION SPRINGS apply a panel retracting torque to the storage drum

ORIGINAL PAGE IS
OF POOR QUALITY

One advantage the extendible boom deployment method has over the pneumatic deployment method is the ability to actively control the panel area without the use of expendables. Since the booms are electric motor driven, electric power is used for active area control. Figure 20 illustrates system interfaces required for this. The boom deployment rate is controlled electronically based upon the sensed radiator outlet temperature.

Figure 21 shows a 4 kW boom deployed flexible radiator subsystem module (3.4 kW to a $0^{\circ}F$ sink temperature; 5.1 kW to a $-40^{\circ}F$ sink temperature). It also shows the fluid circulation components required for a subsystem module. Figure 22 shows two 4 kW modules stowed in the Space Shuttle Orbiter cargo bay. Weight estimates for the boom deployed 4 kW system are shown in Table V. The total system weight is approximately 228 pounds compared to 368 pounds for the pneumatic deployment method.

3.4.3 Extendible Mast Deployment/Retraction

An alternate mechanically driven deployment system would utilize a mast triangular truss structure. Masts are much more rigid than the previously-discussed booms and are, likewise, space proven. The Solar Electric Propulsion (SEP) deployable solar array will soon demonstrate the feasibility for using a mast on a large 12.5 kW wing, as a Shuttle pallet mounted flight experiment.

Because of its stiffness, only a single mast would be required for flexible radiator deployment/retraction. It would be centrally mounted on one side of the panel, and interface the outboard end of the radiator through a yoke. To support this concept a specification was prepared and submitted to potential suppliers for informational proposals. An example is provided in Appendix A.

3.5 Fluid System Considerations

The selection of the working fluid involves a number of system considerations which include materials compatibility, flow stability and low load performance. The fluid selection is discussed below.

3.5.1 Working Fluid Selections

Early fluid studies for the soft tube flexible radiator revealed that some of the commonly used Freon type fluids were not acceptable for the Teflon tube because of excessive permeability. Literature data for Freon 22 and 12 indicate high leakage rates due to permeability of the tubing. Tests were made for Freon 11 and 21 by Vought (Figure 23) which showed the permeability at $80^{\circ}F$ for Freon 21 to be 1.42×10^{-8} lb/day-in-psi and for Freon 11 to be 0.36×10^{-8} lb/day-in-psi. These rates result in a leakage, for a 30 day mission for one panel at 100 psi, of 17 lb of Freon 21 and 4 lb

ORIGINAL PAGE IS
OF POOR QUALITY

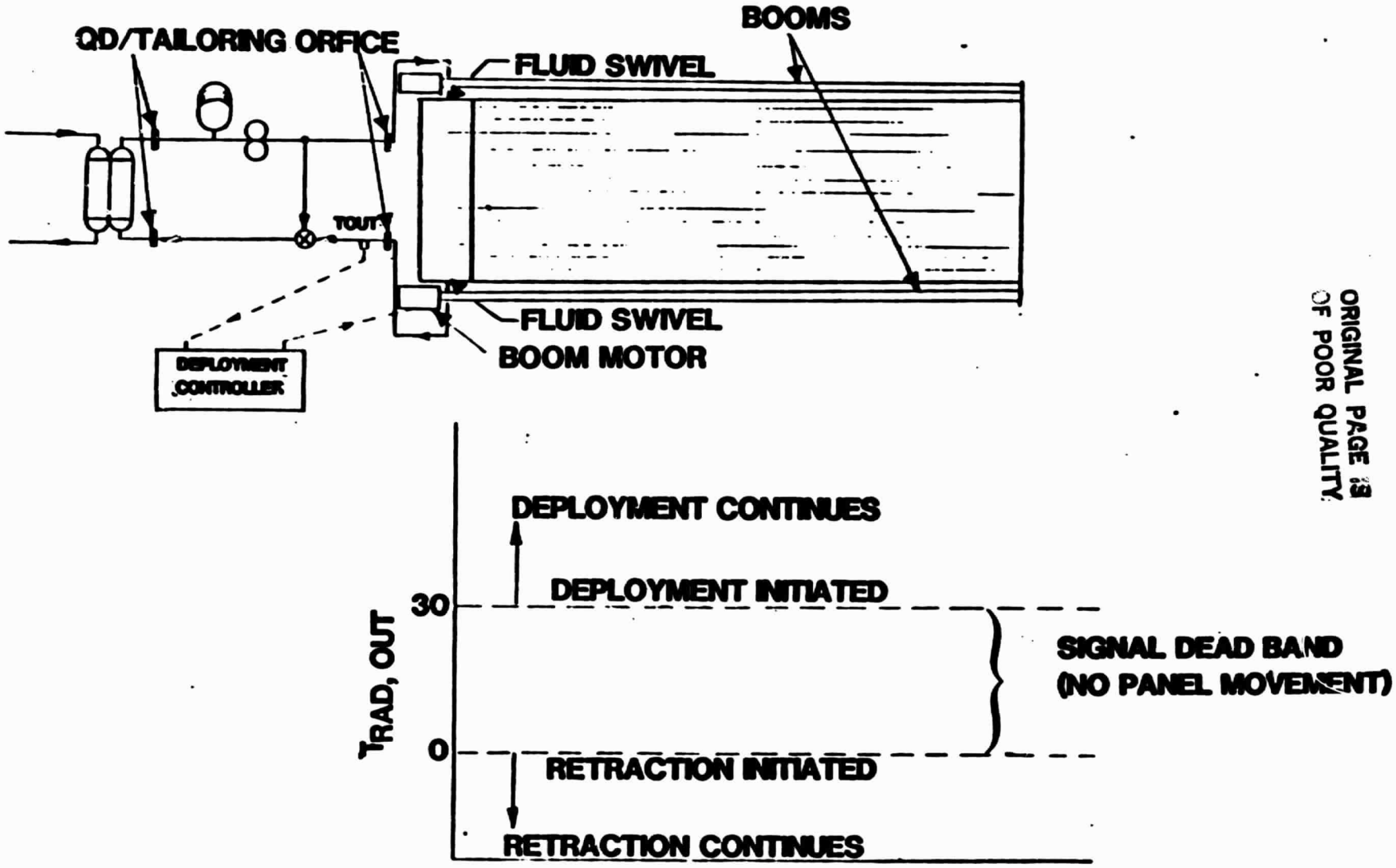

ORIGINAL PAGE IS
OF POOR QUALITY

FIGURE 20 SOFT TUBE RADIATOR DEPLOYMENT/RETRACTION CONTROL

BOOM DEPLOYMENT - DRUM NOT DEPLOYED

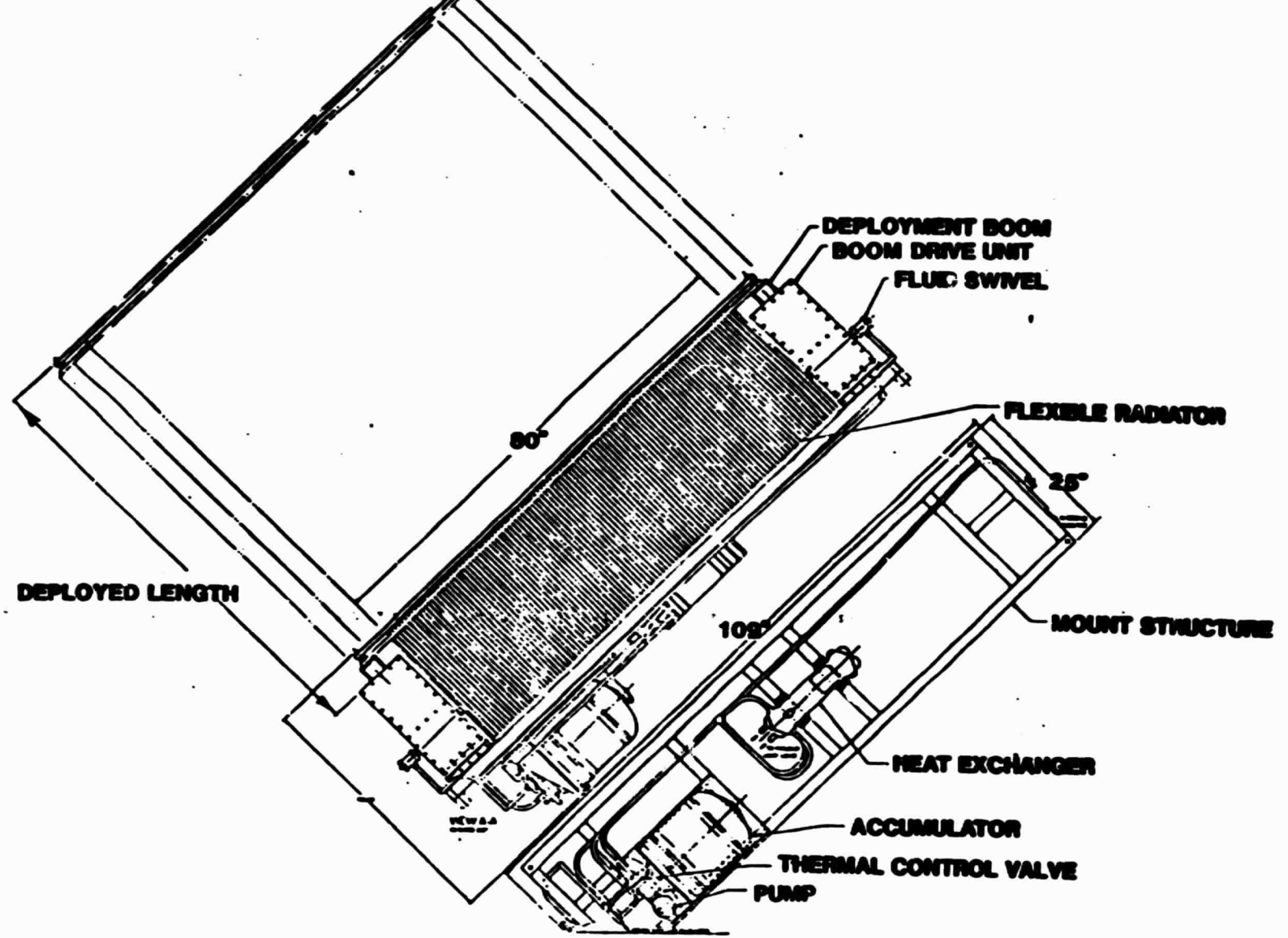

FIGURE 21 FLEXIBLE RADIATOR - BOOM DEPLOYMENT PACKAGE

ORIGINAL PAGE IS
OF POOR QUALITY

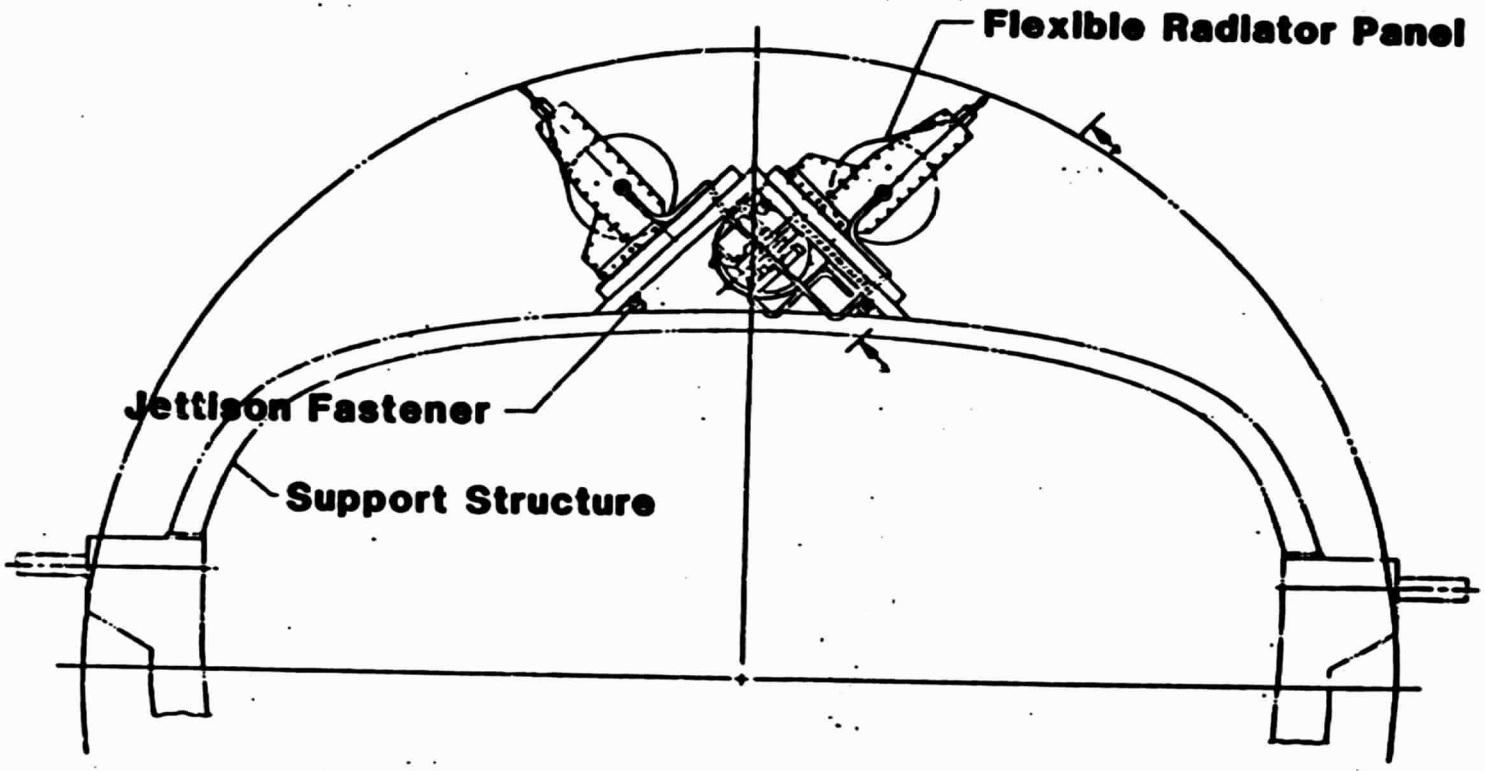

Figure 22 Flexible Radiator Boom Deployment in Stowed Position

ORIGINAL PAGE IS
OF POOR QUALITY

TABLE V
4 kW FLEXIBLE PANEL RADIATOR
BOOM DEPLOYMENT

Panel (80" wide by 27' long)		33.5
Boom Drive Unit		26.0
Manifold and Fittings		6.0
Clamp		4.0
Swivel		2.5
Drum with Plumbing and Shaft to Swivel		31.0
Accumulator Package		20.5
Heat Exchanger		16.4
Coolant Plumbing, Clamps and Hardware		5.4
Mounting Frame		36.4
Jettison Fasteners		2.0
	DRY WEIGHT	183.7
Coolanol 20		27.0
	WET WEIGHT	210.7
Production Growth (8%)		16.9
	PRODUCTION WEIGHT	228

ORIGINAL PAGE IS
OF POOR QUALITY

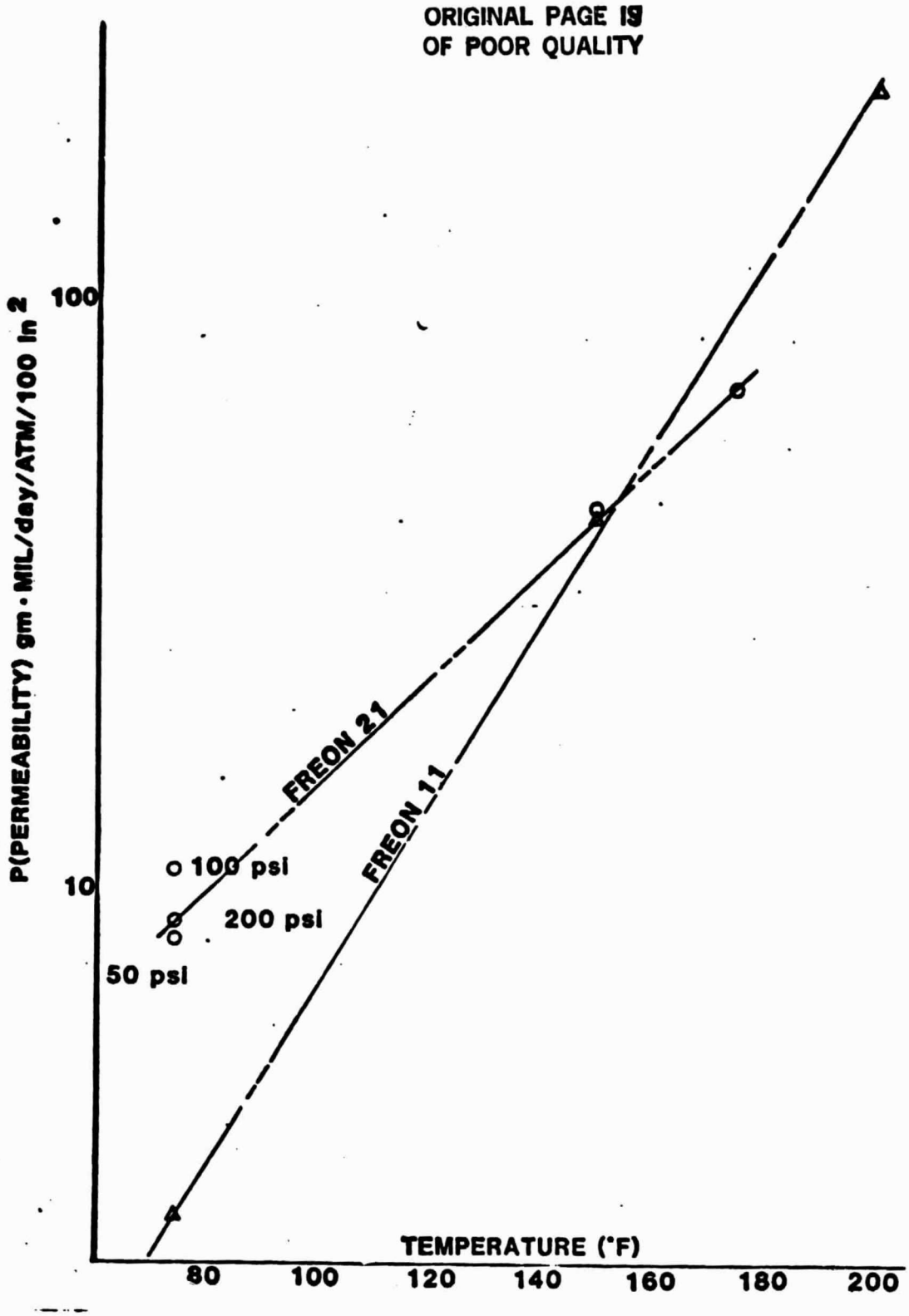

Figure 23 Permeability Test - FEP (Teflon) Tubing & Freon Fluid

TABLE VI
COMPARISON OF RADIATOR DESIGN FOR CANDIDATE FLUIDS

FLUID	OPT DIA (INCH)	OPT WT (LB)	A/Amin	ADJUSTED WT (LB)	WEIGHT R-21 WT (LB)	A / A(R-21)
Oronite FC-100	.100	24.5	1.151	28.2	3.4	1.090
Ethylene Glycol Water (RS-89a)	.085	22.7	1.069	24.3	-0.5	1.012
Freon 21	.085	23.5	1.056	24.8	0	1.000
Freon 11	.090	26.0	1.062	27.6	2.8	1.006
Freon E-1	.075	24.0	1.075	25.8	1.0	1.018
Freon E-2	.080	24.4	1.204	29.4	4.6	1.140
FC-88	.075	24.0	1.075	25.8	1.0	1.018
FC-75	.075	26.0	1.128	29.3	4.5	1.068
FC-77	.075	26.6	1.220	31.7	6.9	1.155
Coolanol 15	.095	23.6	1.143	27.0	2.2	1.082

of Freon 11. At temperatures above 100°F, the Freon 11 leakage is higher than Freon 21 (see Figure 23). Permeability tests were also conducted for the 3M Company FC fluids (FC 77 and 88). It was found that these fluids also permeate the Teflon tubing at unacceptable rates.

The leakage problem discussed above resulted in a fluid trade study to evaluate alternate candidate fluids. Table VI shows a comparison of the fluids considered in the study, along with a relative weight and area comparison. Glycol/water was determined to be the best all around fluid with Coolanol 15 a second choice. (Coolanol 20 was not included in the comparison.) All the other candidates considered have a problem with permeating the Teflon tube. Glycol/water is the lowest weight and area for the two fluids but requires a higher minimum outlet temperature. Figure 24 shows the allowable outlet temperatures as a function of inlet temperatures for stable fluid flow. At 100°F inlet temperature, Glycol/water can operate down to -20°F and Coolanol 15 can operate down to -70°F. Manufacture of Coolanol 15 has been discontinued since the fluid evaluation was performed. A similar fluid, Coolanol 20, is a candidate for its replacement, but it requires that the outlet temperature not go below -38°F for 100°F inlet as shown in Figure 25.

3.5.2 Heat Load Control

Because the low load heat rejection would be excessively high at the minimum outlet temperatures allowed for the acceptable fluids, a heat load control method other than a simple bypass of the radiator is required. One attractive method for heat load control on the flexible radiator is by varying the area by continuously deploying or retracting to provide the amount of heat rejection needed for the heat load. A control system rate analysis for the area control was performed for the prototype flexible radiator to determine the approximate rate of deployment and retraction required. The prototype system should move at a rate which requires approximately 7 or 8 minutes for full deployment or retraction. By using this method of heat load control, a very high maximum-to-minimum heat load can be achieved. By proper thermal design, the radiator can be surrounded with insulation in the retracted condition, reducing the minimum load heat rejection to a negligible amount. This would permit storage on orbit during quiescient periods with little or no heat load.

The deployment method has a significant impact on the ability to control the panel area. Two deployment methods are described in Section 4.0. The pneumatic method, which has been built and tested on the prototype unit, requires the use of expendable nitrogen gas for each retraction/deployment cycle. The deployable boom method requires no expendable gas but requires power. See Section 4.0 for more detail on the deployment methods.

ORIGINAL PAGE IS
OF POOR QUALITY

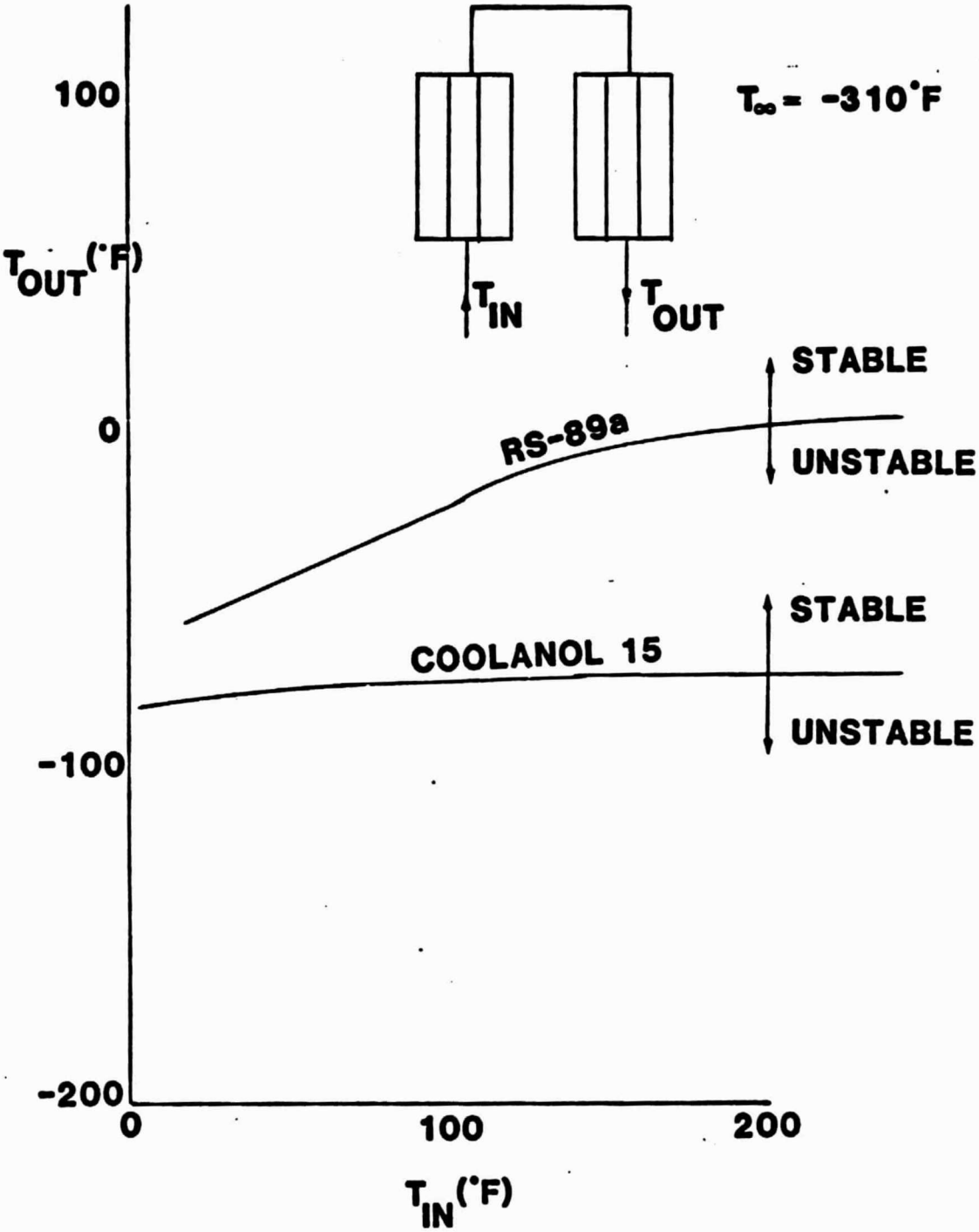

Figure 24 Approximate Stability Curves for Candidate Flexible Radiator Fluids

ORIGINAL PAGE IS
OF POOR QUALITY

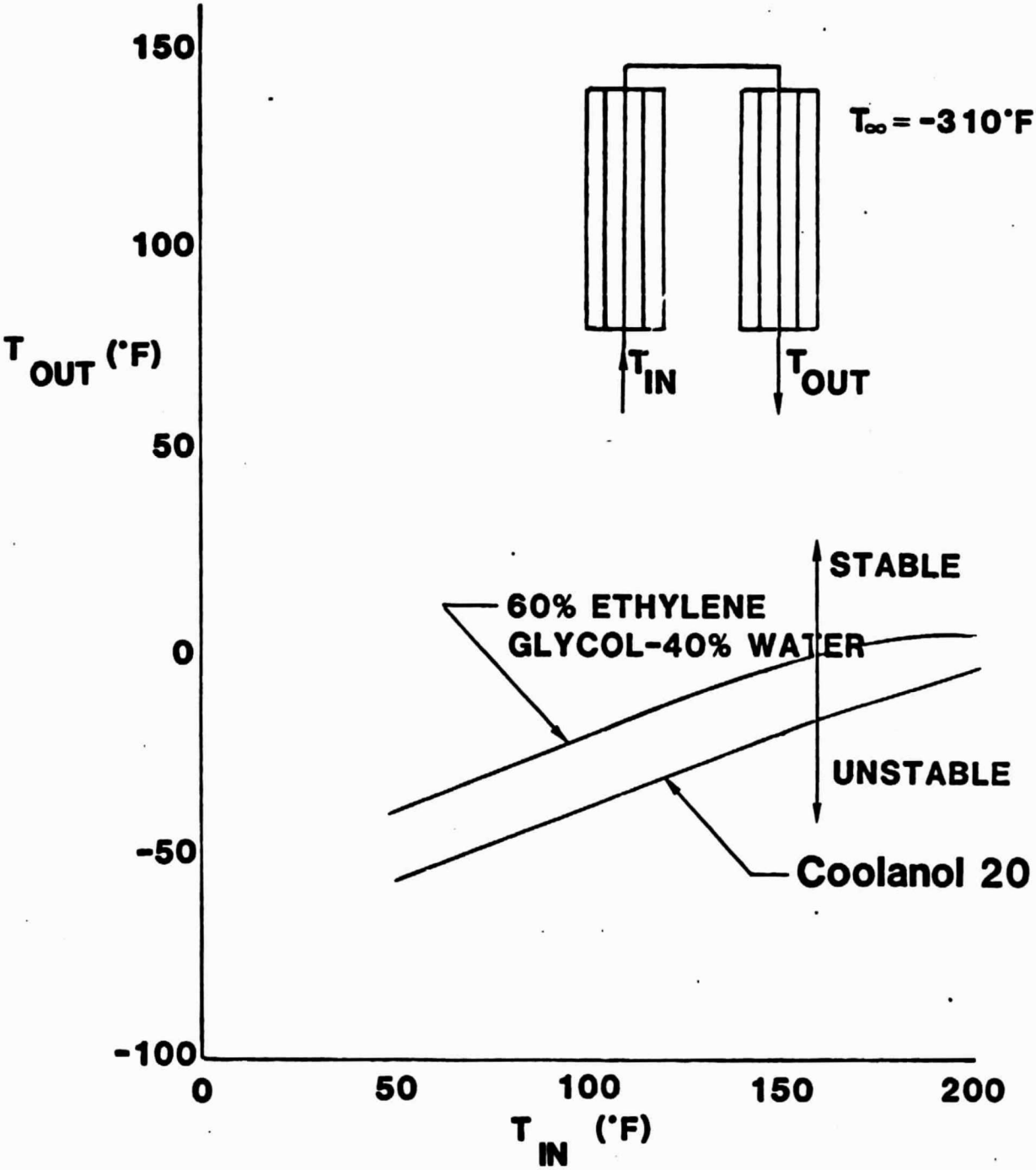

Figure 25 Approximate Stability Curve

ORIGINAL PAGE IS
OF POOR QUALITY

A stability analysis was performed for the area control system to determine the deployment/retraction velocity requirements for stable operation (i.e., no oscillation). Assume the following variable area radiator system:

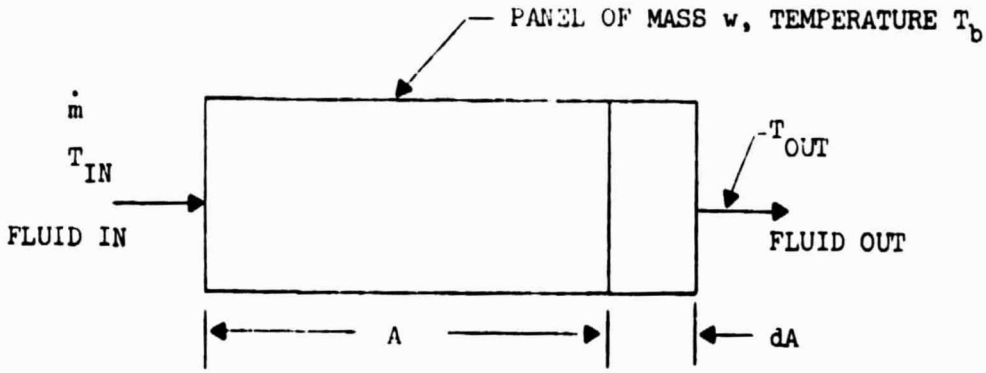

A differential equation can be derived which approximates the time dependency of the fluid outlet temperature. A heat balance for the panel gives:

$$\omega \; c \left(\frac{dT_b}{dt}\right) = \text{Heat in} - \text{Heat out}$$

$$= Q_{fluid} - Q_{radiated}$$

or

$$\omega \; c \left(\frac{dT_b}{dt}\right) = \dot{m}Cp\,(T_{in} - T_{out}) - h_r A_r (T_b - T_s) \qquad (1)$$

Let $T_b = \dfrac{T_{in} + T_{out}}{2}$

T_{in}, T_{out} = fluid inlet and outlet temperature

T_s = sink temperature

Then

$$\frac{\omega \; c}{2} \frac{d}{dt} (T_{in} + T_{out}) = \dot{m}\,Cp\,(T_{in} - T_{out}) - \frac{h_r A_r}{2} (T_{in} + T_{out} - 2Ts)$$

ORIGINAL PAGE IS
OF POOR QUALITY

where:

wc	=	the weight times specific heat of the panel
$\dot{m}$	=	mass of low rate of the coolant fluid
Cp	=	specific heat of the fluid
ηr	=	radiator heat transfer coefficient
Ar	=	panel radiation area
Tin	=	fluid inlet temperature
Tout	=	fluid outlet temperature
T_s	=	radiation sink temperature

Assume $\frac{dT_{in}}{dt} = 0$

$$\frac{\omega}{2} c \frac{dT_{out}}{dt} = -(\dot{m}\, Cp + \frac{h_r A_r}{2}) T_{out} - \frac{h_r A_r}{2} (T_{in} - 2Ts) + \dot{m}\, Cp\, T_{in} \qquad (2)$$

ORIGINAL PAGE IS
OF POOR QUALITY

Assume the panel movement is given by

$$\frac{dX}{dt} = R(T_{out} - T_{set}) \tag{3}$$

where X is the fraction fully deployed and R is a control constant.

$$T_{out} = \frac{1}{R}\frac{dX}{dt} + T_{set}$$

$$\frac{dT_{out}}{dt} = \frac{1}{R}\frac{d^2X}{dt^2} \tag{4}$$

Substituting equations (3) and (4) into equation (2) gives

$$\frac{d^2X}{dt^2} + \left(\frac{2\dot{m}Cp + h_r A_r}{\omega c}\right)\frac{dX}{dt} + \frac{h_r A_{max} R}{\omega c}(T_{in} + T_{set} - 2Ts)X$$

$$= \frac{2R\dot{m}Cp}{\omega c}(T_{in} - T_{set}) \tag{5}$$

Notice that the equation is non-linear since A_r in the coefficient of $\frac{dX}{dt}$ is equal to $X \cdot A_{max}$. However, we will assume the variation in X is small enough that it will not significantly affect the coefficient of $\frac{dX}{dt}$ thus making all coefficients constant.

Let

$$\alpha = \frac{2\dot{m}Cp + h_r A_r}{\omega c}$$

$$\beta = \frac{h_r A_{max} R}{\omega c}(T_{in} + T_{set} - 2T_s) \tag{6}$$

$$\gamma = \frac{2R\dot{m}Cp}{\omega c}(T_{in} - T_{set})$$

ORIGINAL PAGE IS
OF POOR QUALITY

Then the equation is given by

$$\frac{d^2X}{dt^2} + \alpha\frac{dX}{dt} + \beta X = \gamma \tag{7}$$

The characteristic equation of the homogenous part of equation (7) is given by

$$m^2 + \alpha m + \beta = 0$$

with solution for m given by

$$m = \frac{-\alpha \pm \sqrt{\alpha^2 - 4\beta}}{2} \tag{8}$$

The system is critically damped (i.e., exponentially damped to steady state) when

$$\alpha^2 > 4\beta \tag{9}$$

Substituting for values for α and β in equation (6) into equation (9) gives

$$R < \frac{(2\dot{m}Cp + h_r A)^2}{4h_r A_{max}\omega c(T_{in} + T_{set} - 2Ts)} \tag{10}$$

This is the value of R which results in critical damping.

Inserting the following typical values: m = 100 lb/hr, Cp = .72 BTU/lb-^{o}F, h_r = .57 BTU/hr-ft^2-^{o}F, A = 346 ft^2, A_{max} = 346 ft^2, ω = 40 lbs, c = .28 BTU/lb-^{o}F, T_{in} = 110°F, T_{set} = 0°F, Ts = -40°F; results in

$$R = .069 \text{ cycles/hr-}^oF$$

ORIGINAL PAGE IS
OF POOR QUALITY

This indicates that the movement must be very slow for critically damped operation.(It takes 1 hour to move from fully deployed to fully retracted with an error of $8^{o}F$).

This indicates the need to go to an underdamped condition in which

$$\alpha^2 < 4\beta$$

In this case, the roots of the characteristic equation are given by

$$m = -\frac{\alpha}{2} \pm \frac{1}{2}\sqrt{4\beta - \alpha^2}\ i$$

which gives a solution of

$$X = e^{-\frac{\alpha t}{2}}\left(A \cos\left(1/2\sqrt{4\beta - \alpha^2}\right) t + B \sin\left(1/2\sqrt{4\beta - \alpha^2}\right)\right)$$

This results in damped oscillation with the time constant of the damping effect being given by

$$\tau_c = 2/\alpha = .065 \text{ hrs} = 3.9 \text{ minutes}$$

Thus, the amplitude of the oscillation will be reduced to 10% of its original value after 8.9 minutes.

A separate analysis was performed to determine the maximum rate of change of outlet temperature expected due to the influences of the environment. It was estimated that the maximum rate of change in the outlet temperature is approximately $20^{o}F$/minute. If we relate the rate of change of outlet temperature to area change by

$$\frac{dT_{out}}{dt} = \frac{dT_{out}}{dQ} \cdot \frac{dQ}{dA} \cdot \frac{dA}{dt}$$

ORIGINAL PAGE IS
OF POOR QUALITY

- We can solve for the rate of change of the area to compensate for the outlet temperature change

$$\frac{dA}{dt} = \frac{\frac{dT_{out}}{dt}}{\frac{dT_{out}}{dQ} \cdot \frac{dQ}{dA}}$$

$$\frac{dT_{out}}{dt} \lesssim 20^{o}F$$

$$\frac{dQ}{dA} = \sigma\varepsilon\eta(T_b^4 - T_s^4) \approx \sigma\varepsilon\eta(535^4 - 460^4) \approx 43.55 \text{ BTU/hr-ft}^2$$

$$Q = h_r A\,(T_b - T_s)$$

$$= h_r A\left(\frac{T_{in} + T_{out}}{2} - T_s\right)$$

$$\frac{dQ}{dT_{out}} = \frac{h_r A}{2}$$

$$\frac{dT_{out}}{dQ} = \frac{2}{h_r A} \approx \frac{2}{(.5)(534)} = .0105\ \frac{^{o}F\text{-}HR}{BTU}$$

$$\frac{dA}{dt} = \frac{20}{(43.55)(.0105)} = 43.73\ FT^2/\text{Minute}$$

This is the panel deployment velocity which corresponds to 7.6 minutes for full panel deployment.

3.5.3 Fluid Circulation System

The flexible radiator deployable panel may be converted into a flexible radiator heat rejection subsystem by the addition of a fluid circulation system. This fluid system provides the interface between the heat rejection panels and source of the heat load on the vehicle.

Figure 26 is a schematic of the fluid circulation system. It includes the fluid pump, fluid accumulator, interface fluid line connections at both the panel and heat load side, temperature control valve, an optional heat exchanger, and the interconnecting plumbing. The system shown is designed for three panels, each of which could reject 4.0 kW of heat for a total of 12 kW rejection. Pumps which were developed for the Orbiter can be used in this system with little modification. A derivative of Sundstrand pump Model 145656, shown in Figure 27, would be used for the Glycol/water system. This pump was developed to circulate water in the Orbiter environmental control system. A derivative of a similar pump, Model 145660 (Figure 28) would be used for Coolanol 20. Table VII summarizes the fluid volume requirements for a 12 kW system (three 4 kW wings). The estimated volume change for the fluid over the maximum allowable temperature range is 500 to 550 in^3 for both Coolanol 20 and Glycol/water. Figure 29 shows a candidate temperature control valve. Figure 30 summarizes the fluid swivels that would be needed for the boom deployed system.

3.6 Micrometeoroid Damage

The limited data available in the literature on micrometeoroid penetration of plastic materials indicates that plastics are more effective for resisting micrometeoroid penetration than is predicted using data for metals. An equation given in reference (6) predicts depth of penetration conservatively for polyethylene. The equation is

$$t = 0.65 \left(\frac{1}{\varepsilon t}\right)^{1/8} \left(\frac{\rho m}{\rho t}\right)^{1/2} (Vm)^{7/8} (dm)^{19/18} \qquad (11)$$

where:

t = thickness of target material penetrated (cm)

ε_t = percentage elongation of sheet material

ρ_t = mass density of sheet material (gm/cm^3)

ρ_m = mass density of meteoroid (gm/cm^3)

V_m = normal impact velocity (km/sec)

d_m = meteoroid diameter (cm)

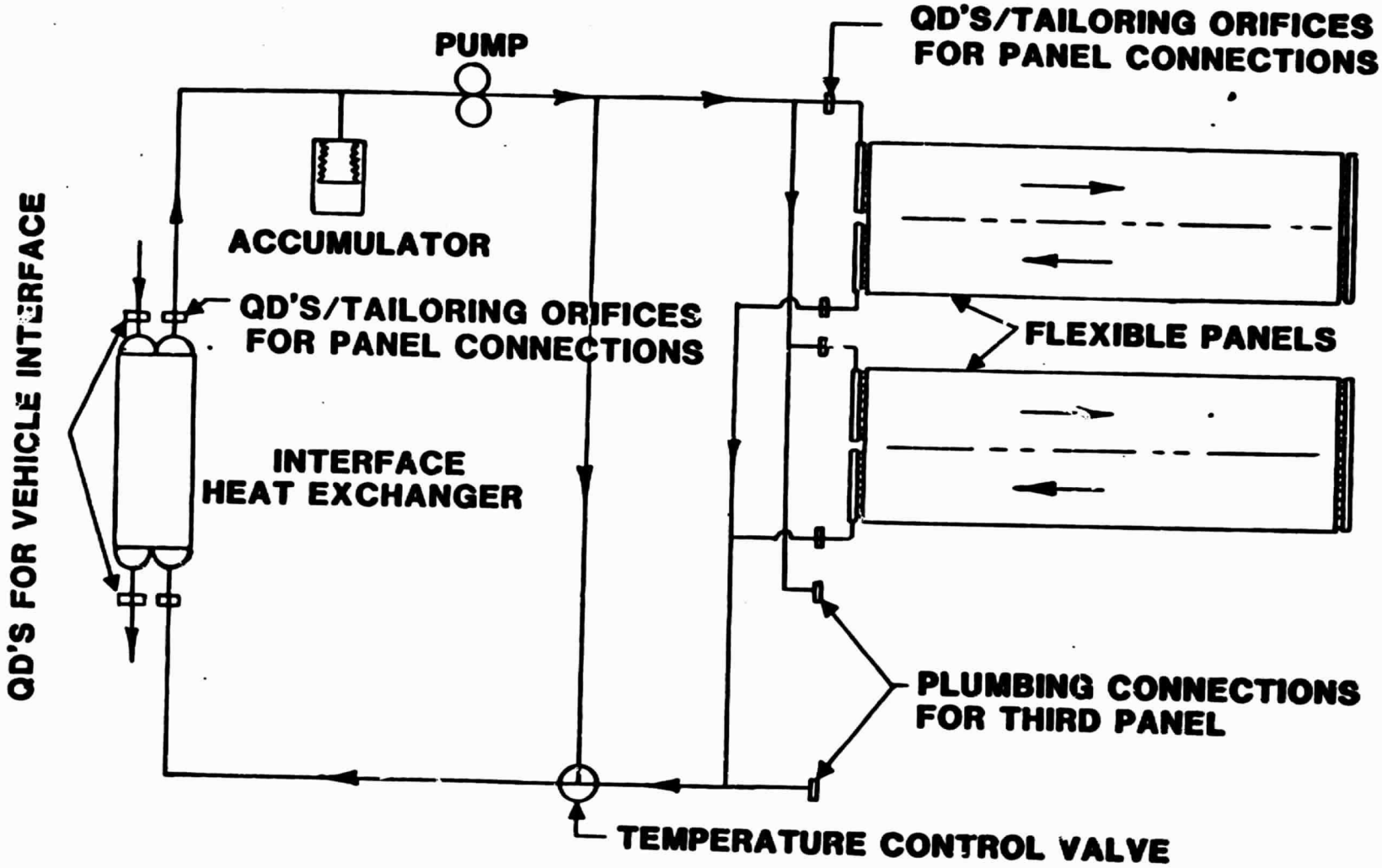

Figure 26 Flow System for Flexible Radiator

ORIGINAL PAGE IS
OF POOR QUALITY

PERFORMANCE

ORIGINAL PAGE IS
OF POOR QUALITY

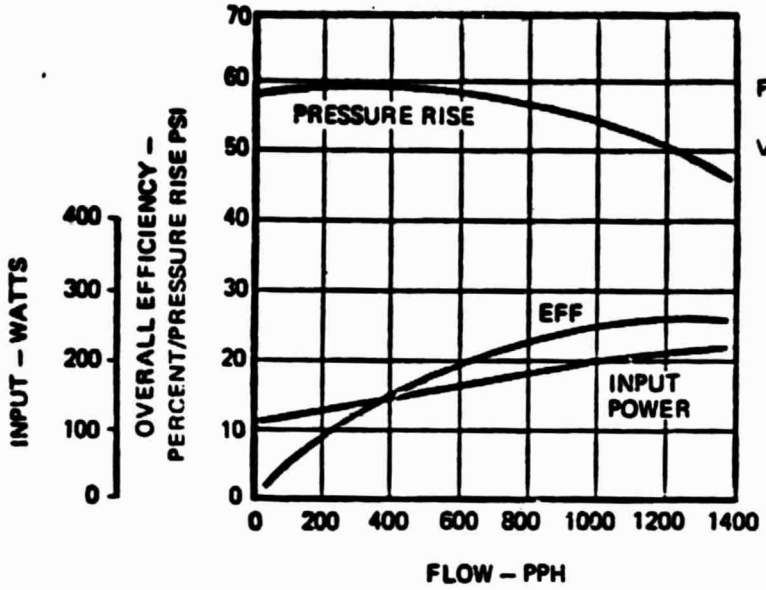

FLUID: DEIONIZED WATER AT 70°F
VOLTAGE: 115/200 VOLTS/ 400 Hz, 3 PHASE

Model 145656

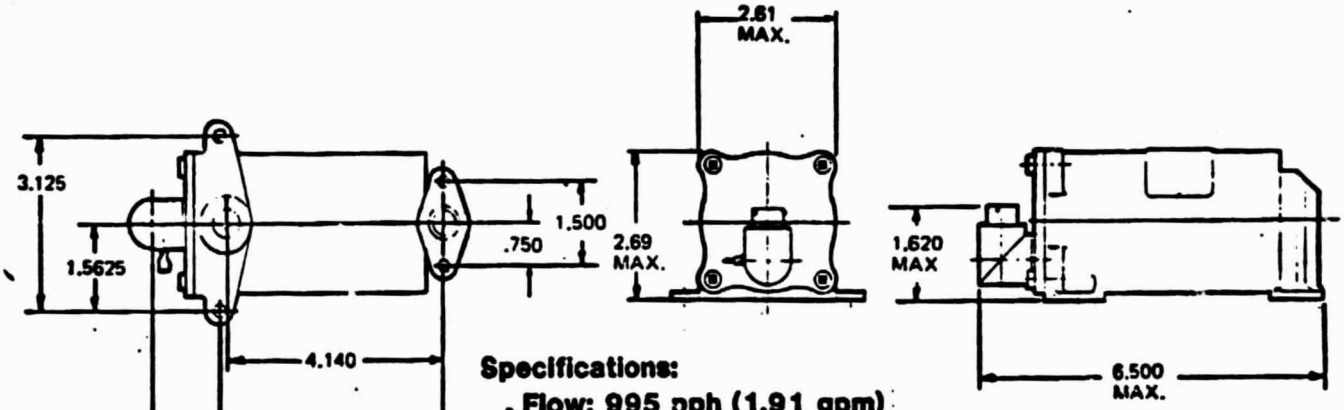

Specifications:

- Flow: 995 pph (1.91 gpm)
- Pressure Rise: 51-56 psi
- Fluid: De-ionized Water
- Input Power: 115/200 Volts, 400 Hz, 43 Phase
- Current: 1.06 Amps per Phase
- Weight: 4.0 lbs

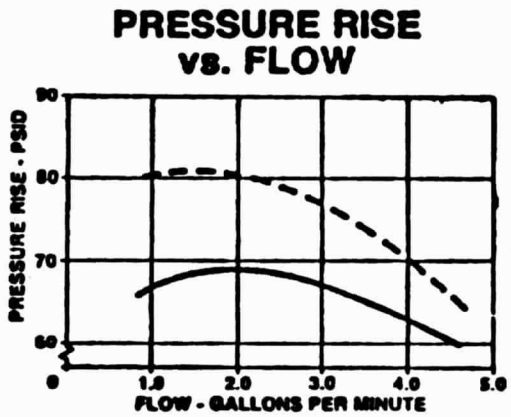

SHUTTLE MOTOR/PUMP AT 400 HZ, 115 VAC WITH FREON 21 FLUID

SIMILAR MOTOR/PUMP AT 450 HZ, 46.4 VAC WITH COOLANOL 20 FLUID

- ESTIMATED 1-3 GPM COOLANOL 20 REQUIRED FOR KIT RADIATOR CONFIGURATIONS
- ESTIMATED 35-50 PSI PRESSURE RISE REQD
- MODIFIED ORBITER FREON 21 PUMP MEETS THESE REQUIREMENTS - USE TAILORING ORIFICE TO ADJUST TO SPECIFIC KIT RADIATOR MISSION NEEDS
- SIMILAR ORBITER PUMP MODIFICATION FOR SIRE PROGRAM

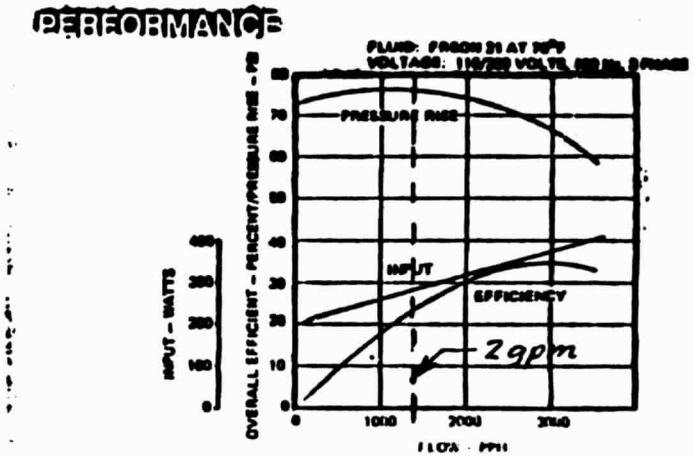

ORIGINAL PAGE IS OF POOR QUALITY

Model 145660

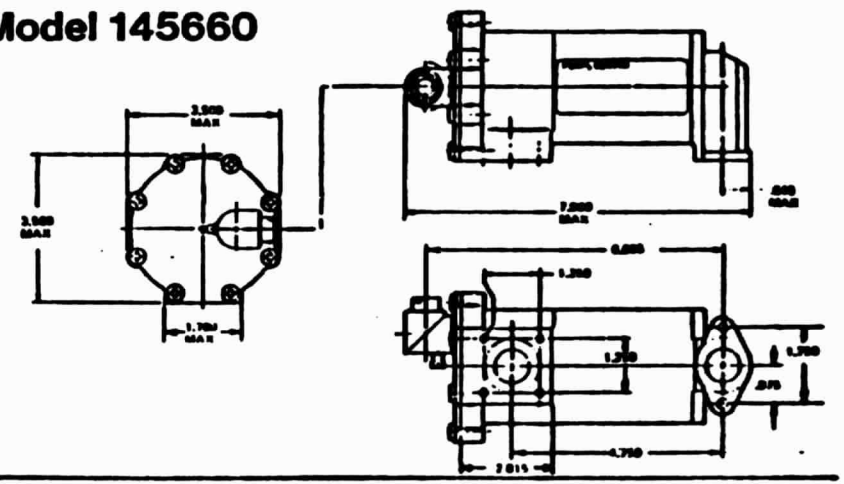

Sundstrand Aviation Mechanical

Figure 28 Representative Coolanol 20 Pump for Flexible Radiator

TABLE VII
COOLANOL 20 KIT ACCUMULATOR

COMPONENT DESCRIPTION	VOLUME, FT^3
Radiators (3 Wings, 1000 Ft^2)	0.550
Coldplates (20)	0.586
Payload Heat Exchanger (2 Loops)	0.071
Flex Hoses (Connecting C/P)	0.219
Hardlines	0.127
Interface Hose Assembly	0.253
Ullage	0.014
Miscellaneous	0.028
	1.848

Fluid Volume Temperature Range + 200°F to -50°F

Present Volume Change = 16.6%

Accumulator Volume = .31 Ft^3

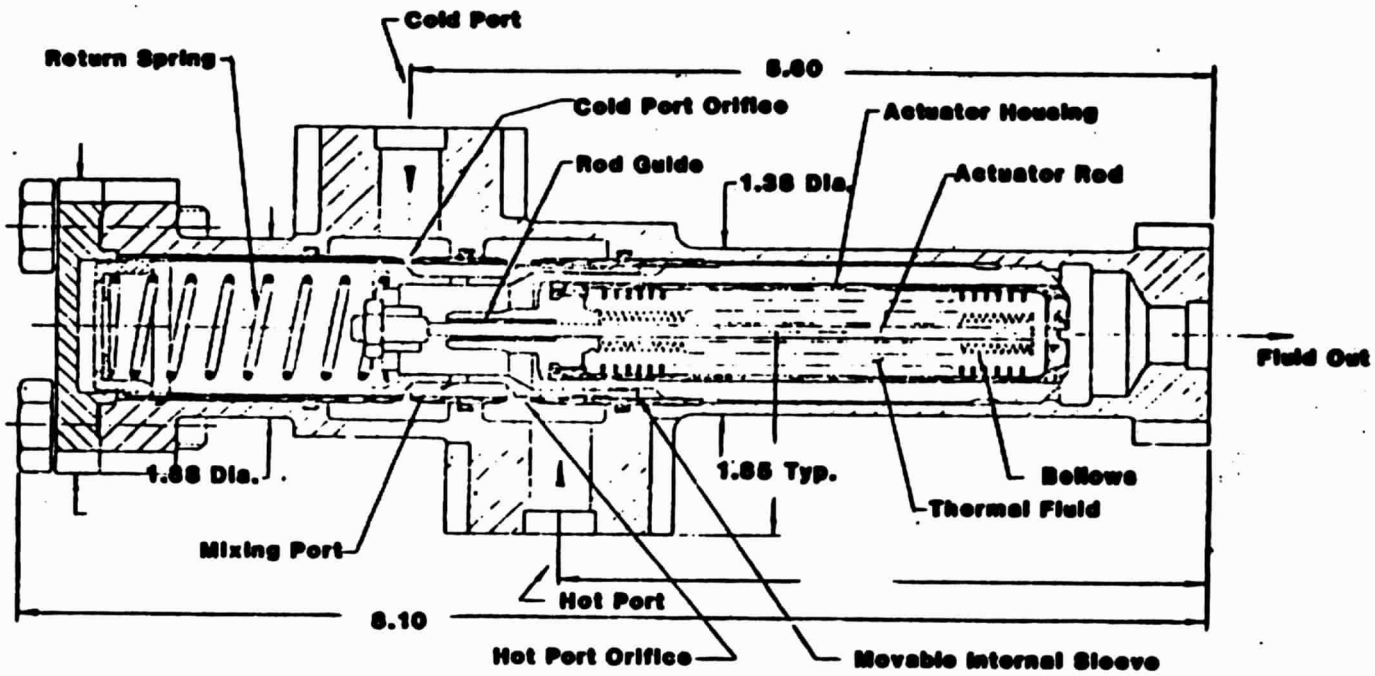

VALVE SCHEMATIC

- Prior use on Skylab
- Control mixed temperature to ± 2°F
- 2.5-5 psid Delta-P at 450 pph Coolanol
- Weight 3 lbs

Figure 29 Representative Thermal Control Valve (William Wahl Corp)

ORIGINAL PAGE IS OF POOR QUALITY

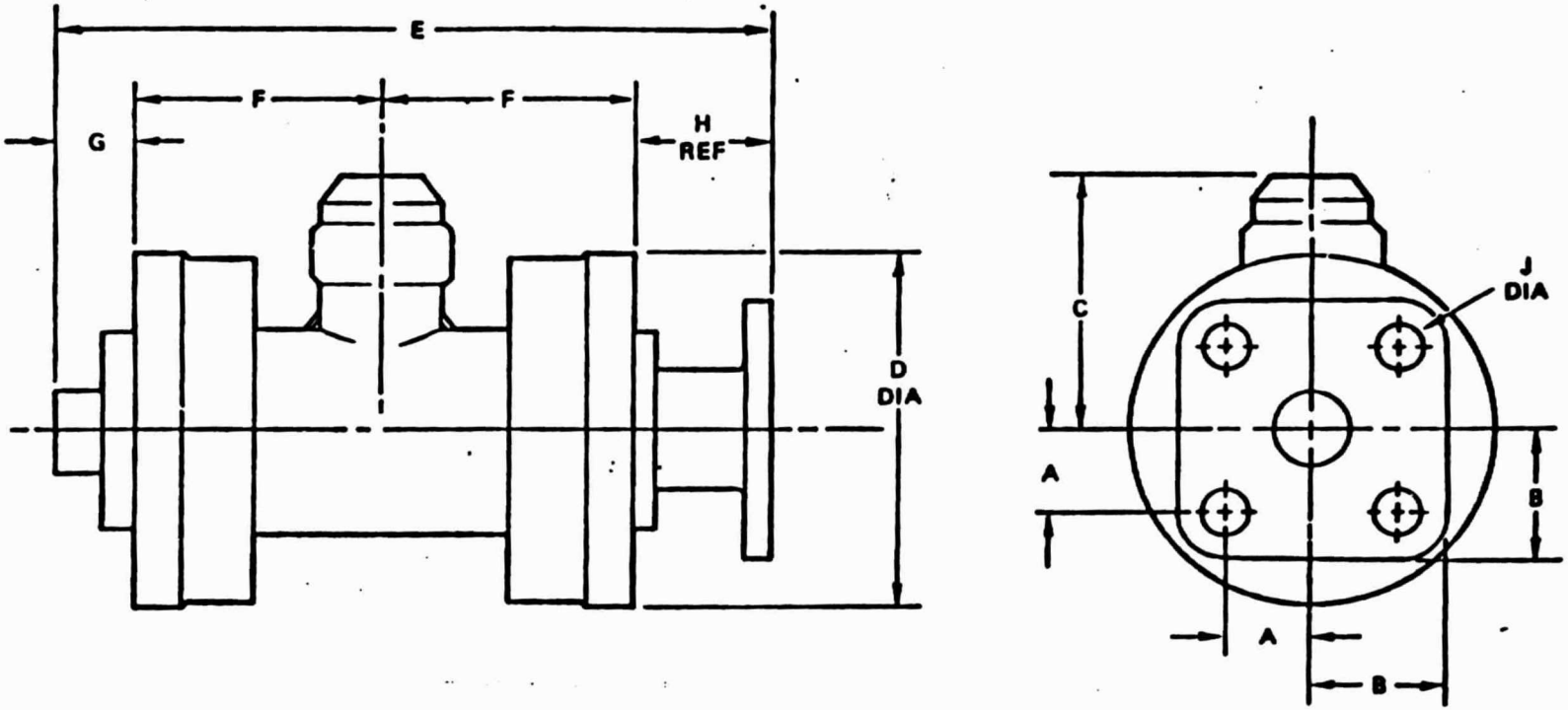

SWIVEL SIZE	WEIGHT *STEEL	WEIGHT AL	A	B	C	D DIA	E	F	G	H	J DIA
1/2	1.34	80	.44	.72	1.40	1.96	3.81	1.34	.38	.75	.25
5/8	1.42	.85	.48	.74	1.44	1.96	3.94	1.44	.40	.66	.25
3/4	2.04	1.22	.56	.80	1.78	2.22	4.35	1.61	.40	.73	.25
1.0	2.69	1.81	.62	.87	2.00	2.46	4.50	1.68	.40	.74	.25

SWIVEL SHOWN →

Figure 30 Vought Freon Swivel - Right Angle Design

ORIGINAL PAGE IS OF POOR QUALITY

Figure 31 compares the depth of penetration predictions for 2024-T6 aluminum with those of other equations developed for metal. It agrees relatively well with the other prediction methods, being somewhat conservative. It is the only equation which accounts for elongation, important to plastics.

The elongation term in the above equation is much larger for plastics (ε = 300) than for metals ($\varepsilon \approx 3$), and has a significant impact on the design of flexible radiators. For example, the wall thickness computed from Figure 31 for 30 days lifetime for polyurethane tubing is 0.032 inches. If the elongation term were assumed to be that of a metal, the required wall thickness is 0.058 inches.

Analyses were made to determine the average depth that a meteoroid must penetrate to puncture a tube. The average depth is greater than the tube wall thickness because most meteoroids do not strike the tubing from a direction which is normal to the surface. Figure 32 shows a typical trajectory of a meteoroid which is directed towards an element on the interior tube wall. The depth that the meteoroid must penetrate to reach the interior wall is

$$h = \frac{-ri + \sqrt{(ro^2 - ri^2)(1 + \cos^2\phi \tan^2\theta) + ri^2}}{\cos\theta \left[1 + \cos^2\phi \tan^2\theta\right]} \qquad (12)$$

The number of meteoroids which strike the surface from the θ , ϕ direction with velocity v and mass sufficient to penetrate the depth h is

$$d^2 n_{\theta,\phi} = \frac{N}{\pi} \sin\theta\cos\phi \, d\theta d\phi \qquad (13)$$

where N is the cumulative flux of meteoroids, per unit area per unit time given as a function of meteoroid mass in meteoroid environment models. For the meteoroids of interest in this work

$$\mathrm{Log}_{10}N = -14.37 - 1.213 \, \mathrm{Log}_{10}M \qquad (14)$$

ORIGINAL PAGE IS
OF POOR QUALITY

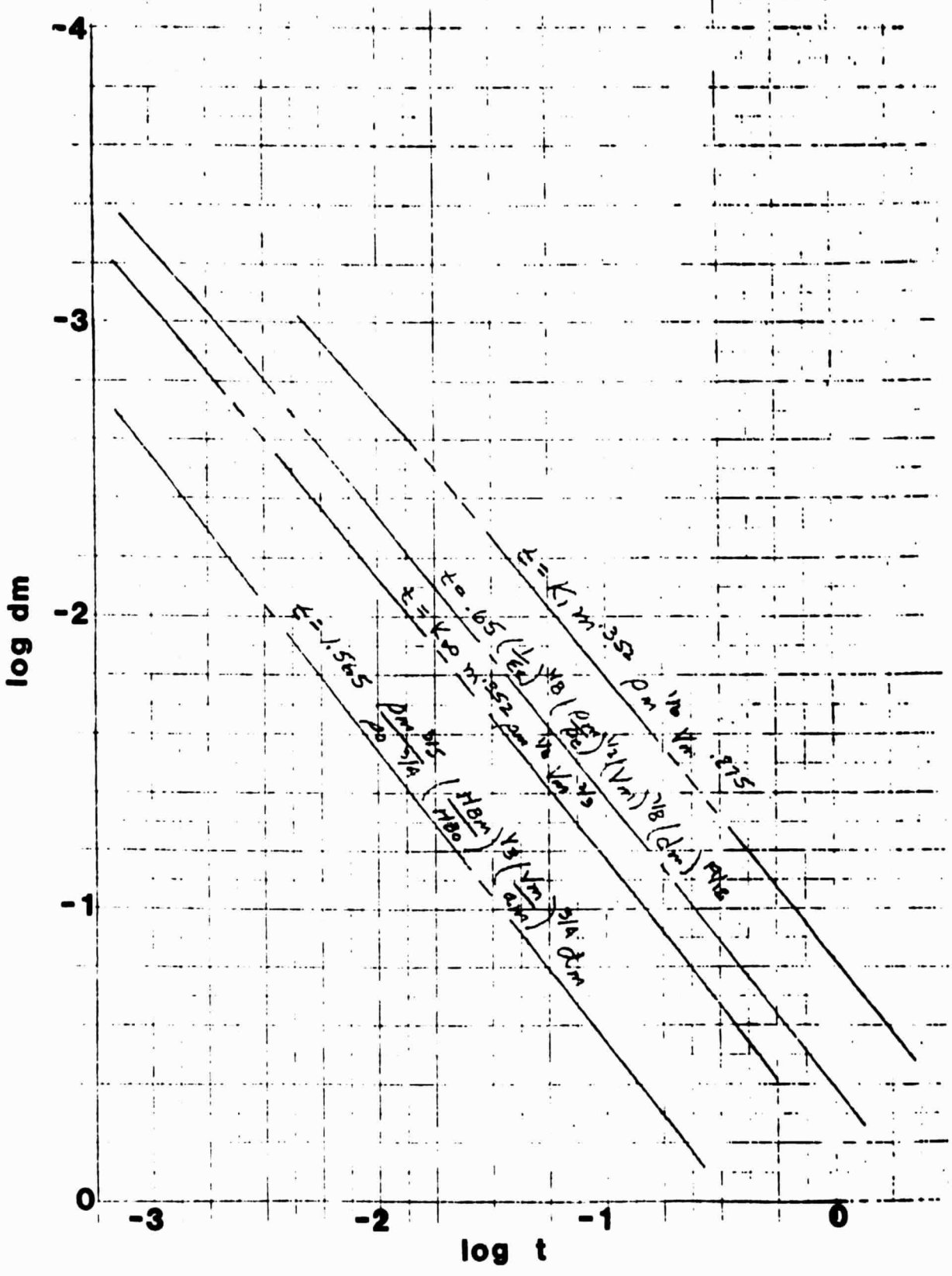

Figure 31 Comparison of Penetration Equations

ORIGINAL PAGE IS
OF POOR QUALITY

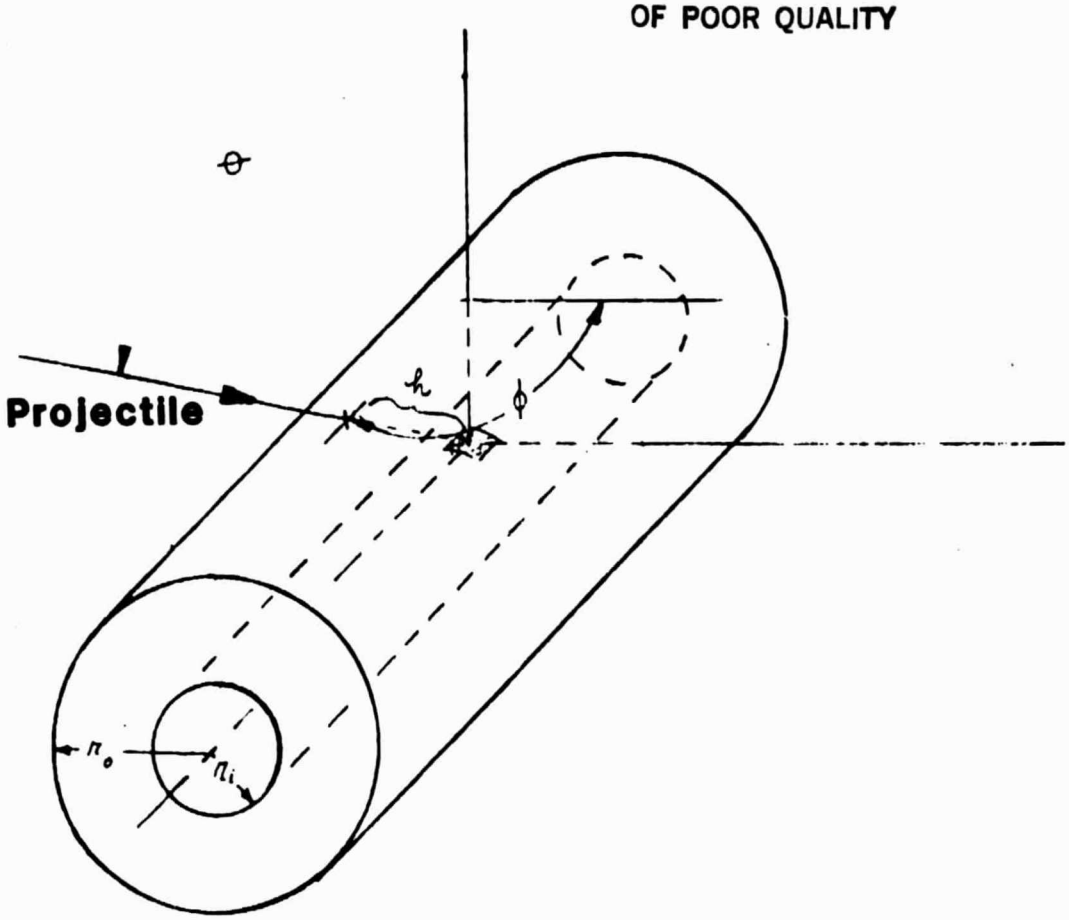

$$h = \frac{-r_i + \sqrt{(r_o^2 - r_i^2)(1 + \cos^2\phi \tan^2\theta) + r_i^2}}{\cos\theta\,[1 + \cos^2\phi \tan^2\theta]}$$

Figure 32

Effective Wall Thickness for Meteoroid Penetration of Flexible Radiator Tubing

The total number of meteoroids which strike the element which are capable of penetrating the tubing is obtained by integrating

$$\bar{N} = \frac{4}{\pi} \int_{\phi=0}^{\pi/2} \int_{\theta=0}^{\pi/2} N \, \mathrm{Sin}\theta \mathrm{Cos}\phi \, d\theta \, d\phi \qquad (15)$$

N is computed from equation (14) above for each angle after the mass required to penetrate the depth $h(\theta,\phi)$ is computed from equation (11). The integral in equation (15) is then evaluated numerically.

The probability of no penetration is given by

$$P_o = e^{-\zeta \bar{N} A t} \qquad (16)$$

where:

ζ is the shielding factor

A is the exposed area

t is the time of exposure

The shielding factor accounts for metecroid blockage by the earth, the orbiting payload, and by the radiator itself. In this analysis, only the earth shielding factor is taken into consideration. For a 200 n.m. orbit ζ = 0.685. Because of shielding by other factors, the actual shielding factor will be less, and the radiator will have a higher probability of success than is computed from equation (16).

Analyses were made to determine the additional wall thickness required to prevent leakage after a meteoroid has penetrated to the depth computed from equation (11). The tube wall thickness must be increased by this amount to prevent failure even though the meteoroid does not actually penetrate the tubing. Calculations showed that the additional wall thickness is approximately 0.002 inch for polyurethane tubing, and 0.004 inch for teflon tubing.

For the total radiator system to have a 90% survivability, the transport tubing and the inflation tubing must independently have higher

probabilities of success. Thus, the inflation tubing was designed for 96% survivability (wall thickness = 0.044 inch for 4" o.d. tubing). The polyurethane tubing was selected so that the outside diameter is a standard dimension (0.1875" for polyurethane tubing and 0.125" for teflon tubing). For the optimum inside wall diameters the wall thickness for polyurethane is 0.0488 inch and the wall thickness for teflon is 0.0325 inch. Subtracting the thickness required for pressure retention, the thickness left for meteoroid protection is 0.0468 inch for polyurethane and 0.0285 for teflon. Treating the tubing as a thin sheet (not accounting for variable has given by the second equation above) the probabilities for surviving 90 days are 0.965 for polyurethane and 0.940 for teflon. If the variable h is taken into account, the probabilities are 0.983 for polyurethane and 0.974 for teflon. The combined probabilities of survivability for the inflation tubing and the transport tubing exceeds 90%.

4.0 PANEL MANUFACTURING METHODS

Fusion bonding was chosen as the method of forming the laminate of the two fin layers sandwiching the flow tubes. PFA Teflon tube material was used to guard against the tubes collapsing during the bonding process. An assembly table (See Figure 1) on which the complete radiator panel can be laid out is used for fabrication. The table surface has a groove for each tube, at the correct spacing (Figure 33). To aid in assembly, holes drilled in the grooves were connected to a vacuum source which pulled one layer of fin material into the grooves. The flow tubes were then sandwiched between the fin material in the grooves and a second layer of fin material with Kapton vacuum bagging material holding the flexible fin assembly together. The flexible fin assembly on the assembly table is rolled into an autoclave (5.5' x 33') for the fusion bonding process. The autoclave is programmed to reach 570°F within ± 3°F over a three hour heat-up period. The fusion bond attained between the layers of fin material and between the flow tubes and the fin material was very strong mechanically.

When the assembly was allowed to cool under a pressure of 1 atm, a strong bond formed between the two layers of fin material. A weaker bond is obtained between the fin material and the PFA transport tubing, with the strength of the bond depending on the maximum temperature experienced in the bonding process. The strongest bonds are obtained for processing temperatures in excess of 600°F. However, the PFA tubing has very little strength at such temperatures, and tends to collapse, apparently because of gravity or surface tension forces. Element tests showed that an adequate bond is obtained without deformation of the transport tubing if the processing temperature is maintained at 570 ± 5°F.

The seal of the vacuum bag (Figure 34) is designed so that the ends of the transport tubes extended through the vacuum bag, and were open to the atmosphere. This equalizes the internal and external atmospheric pressure components, and prevents the vacuum bag from tending to flatten the transport tubing. The temperature variations across the panel are held within narrow limits by heating the oven slowly so that transient temperature gradients are minimized, and by covering the radiator panel with Beta cloth insulation to shield it from temperature variations in the heated atmosphere of the oven. The panel was heated on a large aluminum table which is insulated on the bottom side. The conductance of the table thus tended to reduce any remaining

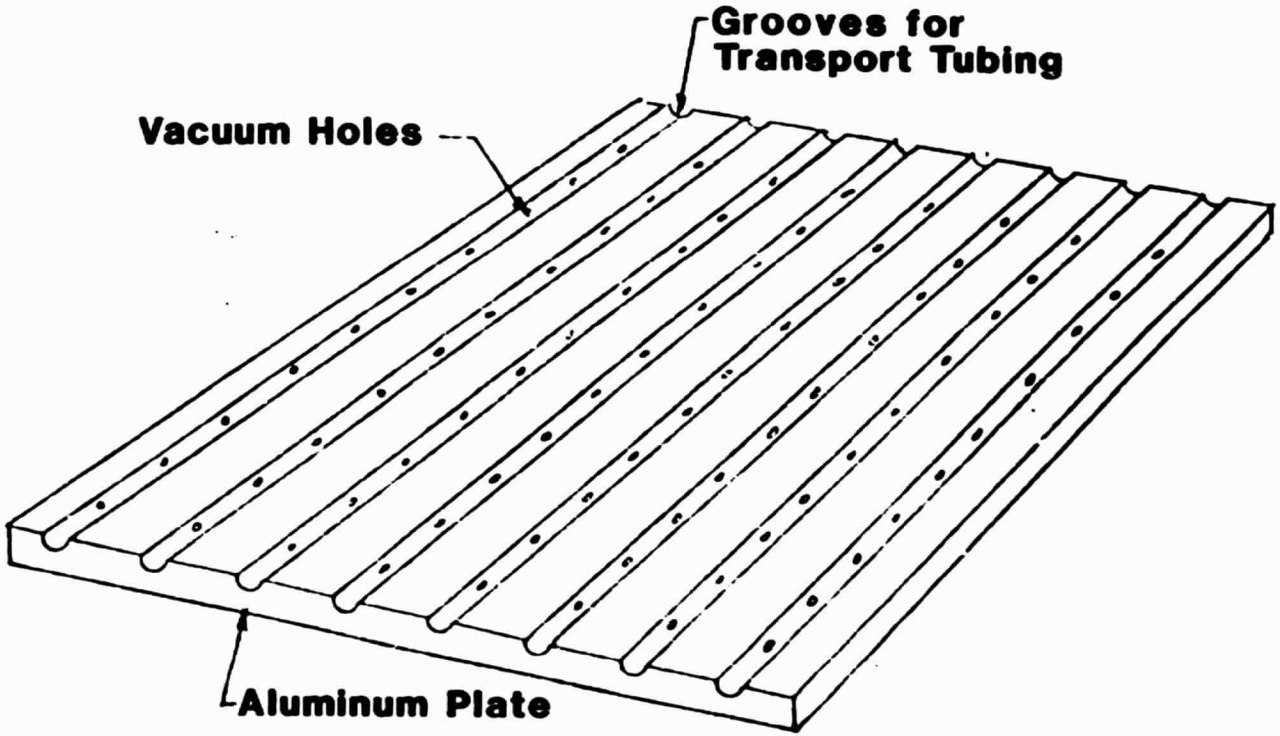

Figure 33 Mold for Laminating Flexible Radiator Panel

ORIGINAL PAGE IS
OF POOR QUALITY

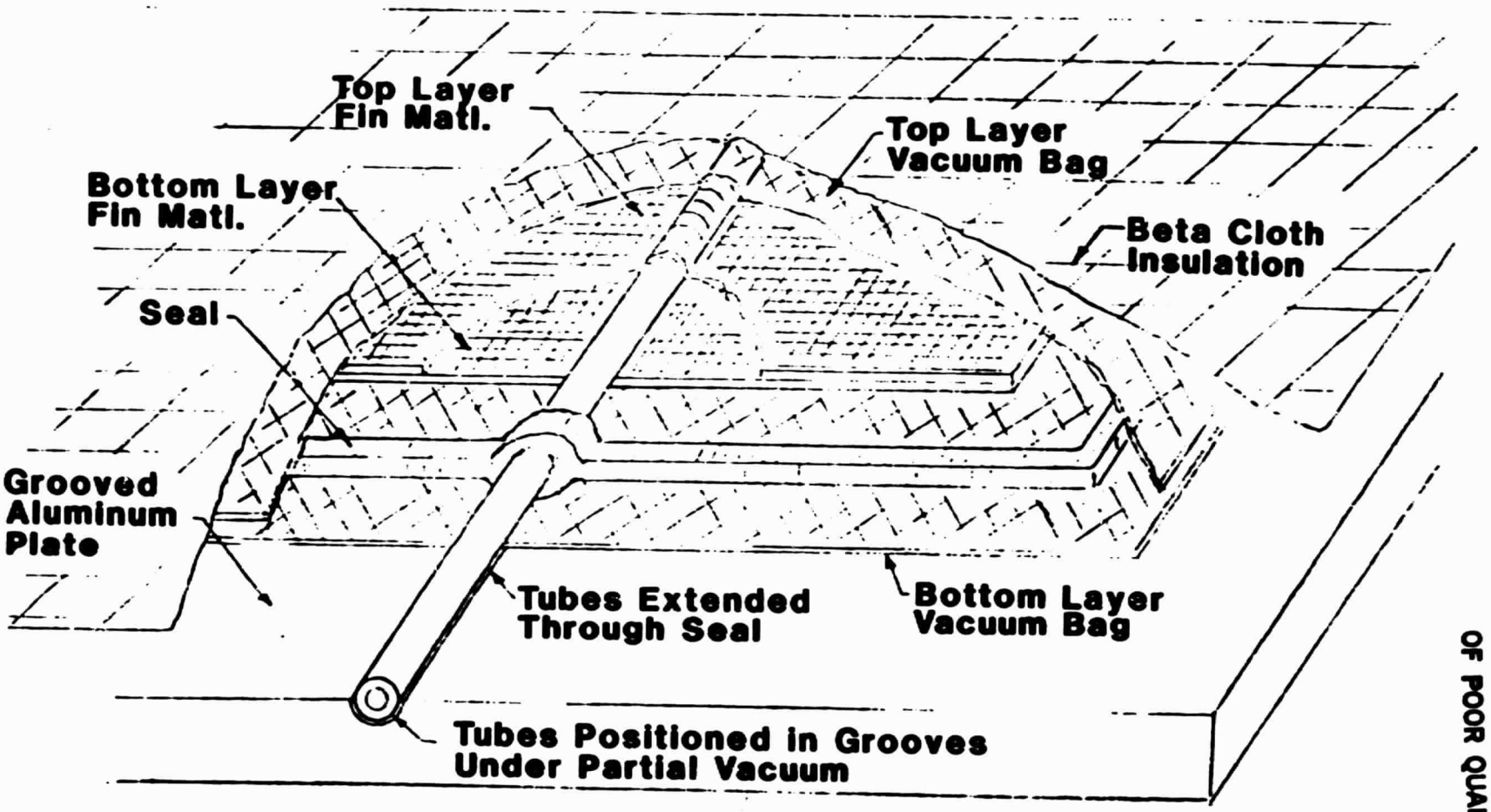

Figure 34 Assembly for Fusion Bonding Radiator

ORIGINAL PAGE IS
OF POOR QUALITY

temperature gradients.

The temperature distribution across the radiator panel measured at the hottest point of the bonding cycle for the prototype panel fabrication is shown in Figure 35. The temperatures were measured with Iron-constantan thermocouples placed inside the transport tubes. The transient temperature profile measured during this bonding process is shown in Figure 36. This profile was obtained by initially setting the thermostats of the oven heaters at 550°F, and observing the temperature distribution across the panel as it approached equilibrium. The thermostat settings of the individual oven heaters were then adjusted as required to achieve a uniform panel temperature of 570°F. The panel was bonded in Vought's oven No. 12, building 22. This is a 5.5' x 5.5' x 33' oven with 6 individually controlled heated zones. The equilibrium temperatures of the individual zones are automatically controlled within ± 3°F. However, the transient responses of the individual heaters are significantly different so that it is necessary to manually adjust the control settings as described above.

The radiator panel fabricated by this procedure is entirely satisfactory for testing purposes. Very little shrinkage or distortion of the transport tubing occurred, and a strong bond was obtained. The transport tubes are straight and evenly spaced, and the appearance of the panel is satisfactory. A few isolated wrinkles occurred where the Teflon film material had been locally stretched prior to assembly and could not be permanently removed by releasing the vacuum and straightening the material. The wrinkles recurred at approximately the same locations each time the vacuum was applied.

The stretching of the fin material probably occurred when the wire mesh was being embedded in the Teflon film. If additional panels are to be fabricated by this process, the screen mesh and Teflon film should be fusion bonded together at the same time that the fin material is bonded to the transport tubing. In this case the Teflon film will not have been deformed prior to assembly, and the cause of the wrinkles thus eliminated. Also, the screen mesh will serve as a bleeder cloth and assist in the removal of air pockets between the layers of fin material.

A second fabrication problem which affects the appearance of the radiator concerns the separation of the fin material from the vacuum bag subsequent to heating the assembly to bonding temperatures. Kapton was selected as the material for the vacuum bag because it has adequate strength

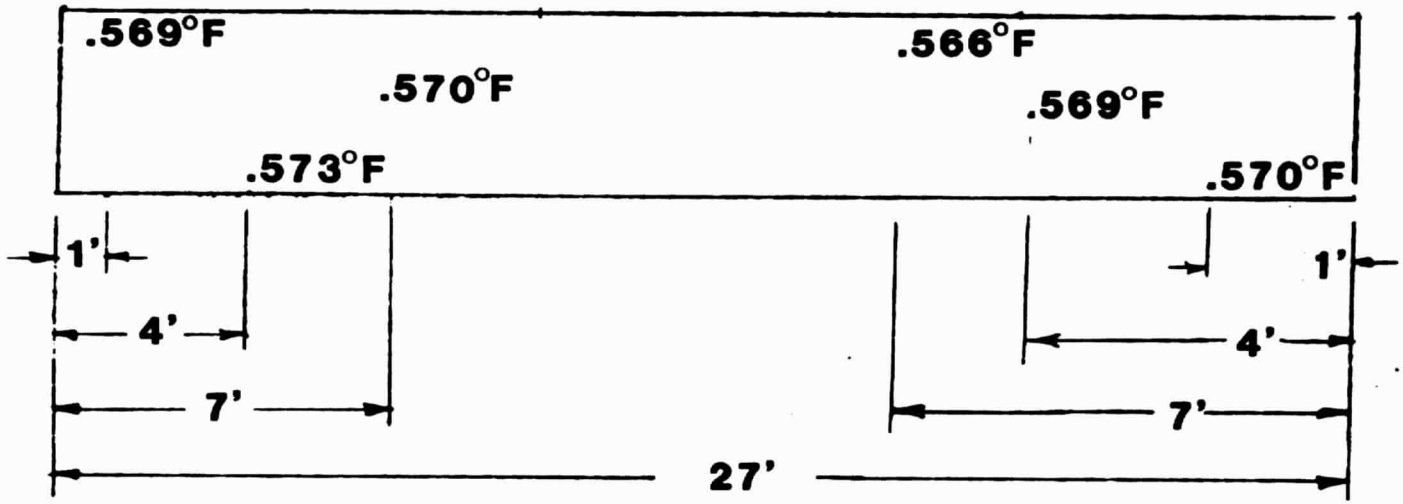

Figure 35 Peak Temperature Distribution in Fusion Bond Process

ORIGINAL PAGE IS
OF POOR QUALITY

ORIGINAL PAGE IS
OF POOR QUALITY

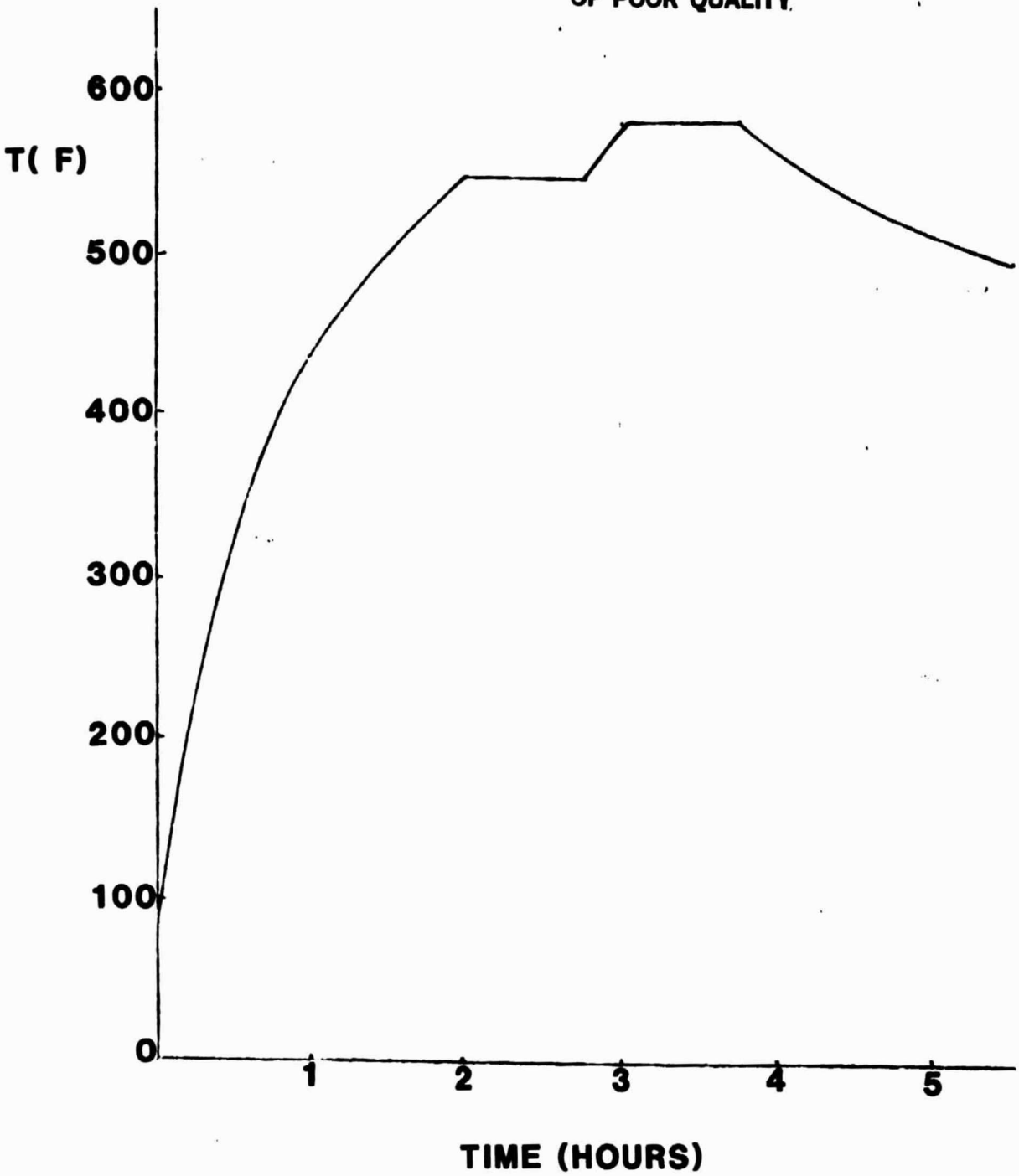

Figure 36
Transient Temperature of Oven Atmosphere During Fusion Bonding Cycle

and does not tend to bond to FEP Teflon at the temperatures required for this application. Element tests on small radiator sections indicated that Kapton is an acceptable vacuum bag material. However, when the prototype panel was fabricated, the bond between the radiator and vacuum bag was much stronger than had occurred in the element tests. Apparently the additional time required to heat the large prototype panel contributed to the strength of the bond. When the Kapton vacuum bag was removed from the prototype radiator panel the surface of the Teflon radiator fin was found to have a diffuse appearance. Also, in a few small areas, the bond between the radiator fin and Kapton was so strong that the fin material would tear away from the transport tubing before it would separate from the Kapton. Liquid nitrogen was poured over small sections of the radiator in areas where the bond was exceptionally strong so that differences in the thermal expansion coefficients of Kapton and Teflon would cause the two layers to separate. In these sections the vacuum bag was easily removed from the radiator, and the panel surface was left with a glossy finish. This procedure was followed only when it was considered necessary to prevent the radiator fin from tearing because of concern over weakening the joint between the FEP Teflon radiator fin and the PFA Teflon transport tubing. However, subsequent visual inspections of the sections where LN_2 was applied revealed no areas where the tubing had separated from the fin material. The areas where the fin material had been torn were repaired by locally heating the material past the melting point so that the torn surfaces fused together. This produced a relatively neat joint which blends in with the rest of the radiator panel and is un-noticeable when viewed from a short distance.

Additional studies and element tests should be conducted to prevent this problem from recurring in the future. It is probable that the Kapton film could be sprayed with a light silicone coating which would prevent the molten Teflon from adhering to the vacuum bag.

The solar absorptivity of the radiator panel was measured at several locations with a Gier Dunkle optical reflectometer. All of the measurements were made in areas where the Kapton vacuum bag had been peeled away from the radiator leaving a diffuse surface appearance. The measured values ranged from $\alpha = .055$ to $\alpha = .078$. Measurements could not be made at interior sections of the panel where the glossy surface areas were obtained by removing the vacuum bag with LN_2. However, it is not expected that the

values would differ greatly from those of the diffuse areas.

The retraction springs for the prototype panel were purchased from Spring Engineers (Dallas) and sent to Schjeldahl, the inflation tube subcontractor. Schjeldahl bonded pockets along the inflation tubes to accommodate the retraction springs and delivered these to Vought as assemblies. The inflation tube assemblies were then attached to the edge of the radiator panel fin material in a fold of aluminized mylar material; the free edges of which were sown to the fin material.

5.0 CONCLUSIONS AND RECOMMENDATIONS

A number of conclusions have been reached as a result of the technology effort described in this report. Some of the more significant ones are itemized below:

- Soft tube flexible radiator technology is at a high readiness level and is now ready for engineering applications.
- The soft tube flexible radiator requires 40% less weight and 60% less stowage volume than an equivalent heat rejection rigid panel approach.
- The proper range of requirements for the soft tube flexible radiator is 1 to 12 kW of heat rejection for missions of 30 days or less in low earth orbit.
- Area control is required on the soft tube flexible to prevent flow instability and/or freezing because of the properties of the acceptable fluids.
- The hard tube flexible radiator has the promise of providing long life radiator which utilizes the lightweight fin design. Also, area control can be eliminated since fluid such as Refrigerant 21 can be utilized. More technology work is needed, however, to achieve the technology readiness needed for engineering application.

It is recommended that the soft tube flexible radiator be utilized for thermal control of future payloads for which its capabilities fit the requirements. A significant savings in weight, stowage volume and cost should result. It is further recommended that the hard tube flexible technology advancement effort be continued to take advantage of the lightweight fin approaches on future long life missions, such as Space Stations.

The combining of this lightweight fin technology with heat pipes to provide low weight heat pipe panels should be investigated.

6.0 REFERENCES

(1) Cox, R. L., "Development of an Inflatable Radiator System - Progress Report No. 4 - 22 November 1973 through 22 August 1974", Vought Report No. T213-RP-04.

(2) Cox, R. L.; Dietz, J. B.; and Leach, J. W., "Deployable Radiators for Waste Heat Dissipation from Shuttle Payloads", published in Raumfahrtforschung, Band 20, HEFT 5, September/October 1976, pp. 232-237.

(3) Hixon, C. W., "Development of a Prototype Flexible Radiator System - Final Report", Vought Report No. 2-30320/9R-52078, 1979.

(4) Hixon, C. W., "Design and Development of a Hard Tube Flexible Radiator System", Vought Report 2-30320/0R-52416, dated 25 April 1980.

(5) Hixon, C. W. and Oren, J. A., "Flexible Radiator Thermal Vacuum Test Report", Vought Report 2-32300/1R-03, dated 29 October 1982.

(6) Rittenhouse, J. B., "Meteoroids", Space Materials Handbook - Third Edition, July 1968.

APPENDIX A

DEPLOYABLE MAST DATA

ORIGINAL PAGE IS
OF POOR QUALITY

AEC-ABLE ENGINEERING COMPANY, INC.

P.O. BOX C GOLETA, CALIFORNIA 93116-0588

17 March 1982

Mr. John Oren, MS F-29
Vought Corporation
P. O. Box 225907
Dallas, Texas 75265

Dear Mr. Oren:

RE: Telephone Conversation this date

This note is to confirm the data given to you in our telephone conversation earlier today concerning the characteristics of an ABLE Automatically Deployable Boom. The characteristics are preliminary and should not be considered as limiting. Only minimal effort was made to minimize either weight or volume or to maximize stiffnesses or strengths. The requirements listed below were used in the sizing of this ABLE Boom.

1. Length = 29 feet
2. Tip Compression = 30 pounds
3. Panel Weight = 0.45 lb/ft^2
4. Panel Size = 80 x 348 inches
5. Minimum Frequency = 0.11 Hz
6. Tip Drum Weight = 26 pounds
7. Life = 800 cycles
8. Deployment/Retraction Rate = 3.6 ft/min
9. Constant-tension Panel
10. Shuttle compatible with Vernier Thrusters operating

The characteristics of the ABLE Boom which meet these requirements are based upon satisfying the 30-pound compressive-load requirement. Specific characteristics are as follows:

1. Boom Deployment Length = 29 feet
2. Boom Diameter = 9 inches
3. Stiffness:
   3.1 Bending, EI = 3.13×10^6 $lb\text{-}in^2$
   3.2 Shear, GA = 1.67×10^4 pounds
   3.3 Torsion, GJ = 3.39×10^5 $lb\text{-}in^2$

• 5790 THORNWOOD DRIVE • GOLETA, CALIFORNIA 93117 • 805/964-8707 •

4. Strength (Critical)
   4.1 Bending, M = 268 in-lb
   4.2 Shear, V = 12.6 pounds
   4.3 Torsion, T = 56.7 in-lb
   4.4 Axial, P = 63.8 pounds
5. Boom Weight = 6.7 pounds
6. Canister Weight = 14.6 pounds
7. Canister Height = 25 inches
8. Canister Diameter = 11 inches

The resulting natural frequencies are:

Bending Frequency = 0.175 Hz
Torsion Frequency = 0.507 Hz

The steady-state rotational accelerations induced by the Vernier Thrusters cause the following loading on the boom:

1. Shear = 0.045 pound
2. Moment = 15.7 in-lb

As you can see, there are very large strength margins over reactions to Vernier-Thruster-induced loads in the discussed design.

For four flight units, budgetary pricing is , and the program length would be approximately 18 to 24 months, depending upon contractual requirements. In response to your later telephone request, a single flight unit will cost about , and a single ground test unit without flight-rated electronics will cost about .

I trust these data are useful to you. If I can be of any further assistance, please call.

Sincerely yours,

Max D. Benton
President

MDB:jb
Encls: ABLE Automatically Deployable
Boom Brochure and Flyer
Dual-Drive Data Sheet

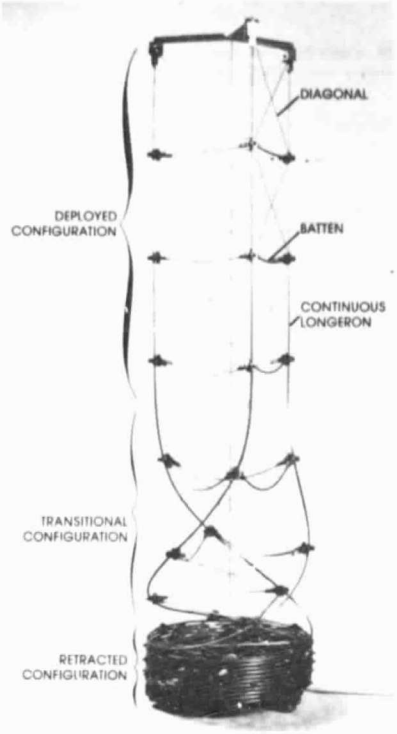

FIGURE 1
Continuous-Longeron Boom

INTRODUCTION

AEC-ABLE ENGINEERING COMPANY, INC. (AEC-ABLE) specializes in the design and manufacture of a variety of deployable lattice booms for ground, sea, air and space applications. These standard and custom-designed booms meet a broad range of structural and operational requirements. They have been made in diameters ranging from 4 to 40 inches and in lengths over 100 feet. These booms can be deployed either manually, automatically or semiautomatically with high reliability and long life. When retracted, they are only a small fraction of their deployed length which, when combined with their lightweight, makes them highly portable.

This brochure describes and gives design information on two types of ABLE booms that are **automatically** deployed and retracted. These automated systems are especially useful in space and other hostile environments which demand stiff, strong and dimensionally stable booms that are highly portable and remotely deployable.

Typical applications for automatically deployable ABLE boom systems are to deploy and support solar-cell arrays, magnetometers, hydrophones, spectrometers, antennas, interferometers or gravity-gradient masses. Their lightweight and compact stowage volume provide the portability needed for those applications. ABLE booms are also, potentially, a very useful element for remote manipulator systems in space, undersea and other unfriendly environments. Electrical conductors can be permanently attached to any of the several types of ABLE booms without impairing their capability for repeated deployment and retractions. Because of their low susceptibility to thermal distortions (see later section), ABLE booms are especially useful for applications requiring high dimensional stability in the solar radiation environment of space.

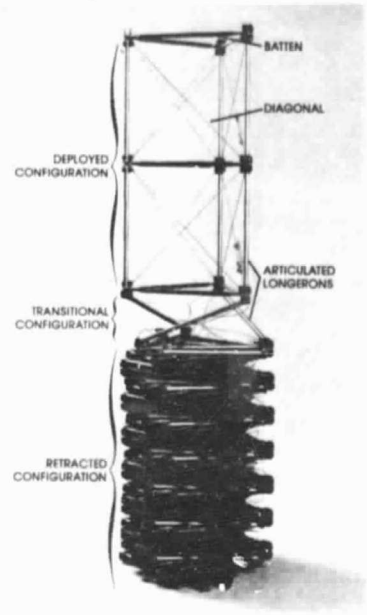

FIGURE 2
Articulated-Longeron Boom

AUTOMATIC ABLE BOOMS

There are two basically different types of ABLE booms. One is the "Continuous-Longeron Boom" shown in **Figure 1**. The continuous-longerons are elastically coiled when the boom is retracted. The second type is the "Articulated-Longeron Boom" shown in **Figure 2**. The corner detail of the articulated-longeron boom, with its extensible diagonal which permits longeron hinging for retraction, is shown in **Figure 3**.

Both of these types of ABLE booms are lightweight, open lattice structures that retract into very compact cylindrical stowage volumes. The height of the stowage volume is typically 2% of the deployed boom length.

A motorized canister can be used to automatically deploy, support and retract either of these two types of booms to their partial or full lengths. **Figure 4** shows a motorized canister that was made for a 14.4-inch diameter, 105-foot long, continuous-longeron ABLE boom. The continuous-longeron boom can also self-deploy by virtue of its strain energy in its retracted configuration. Therefore, its deployment mechanism can also consist simply of a stowage container and a payout lanyard to control its deployment rate. This "lanyard" type of deployment does not apply to the articulated boom because it cannot self-deploy.

Both types of ABLE booms and their deployment mechanisms are described here along with preliminary engineering design data. Data on thermal distortions of these booms in an outer space environment are presented in a later section of this brochure.

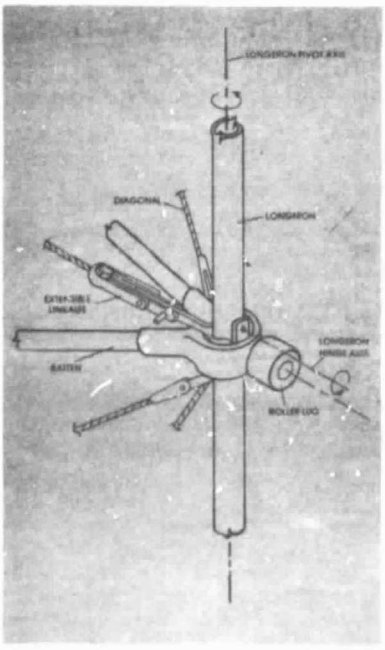

FIGURE 3
Articulated-Longeron Hinge with Cam-operated, Extensible Diagonal

CONTINUOUS-LONGERON ABLE BOOMS

The continuous-longeron boom is used for applications which require high dimensional stability and/or a high ratio of bending stiffness to weight. However, the stowage envelope for any particular application must be sufficiently large that the continuous longerons of the resulting boom design can be elastically coiled. The coilable boom is deployed by a canister, such as is shown in **Figure 4**, when the application requires that the boom develop its full strength and stiffness at any stage of its deployment, or when the deployed portion must not rotate about the boom axis during deployment. It may be deployed by use of only a control lanyard if the application does not require the boom to have its full strength, stiffness or dimensional stability until after it is deployed to its full length. Both types of deployment mechanisms are discussed later.

Figure 1 shows the principal parts of this boom and its retraction geometry. The longerons are continuous over the boom length and are connected to the batten frames by pivot fittings. Six relatively inextensible diagonals provide shearing strength and stiffness to each bay. When the boom is twisted about its axis, tension is increased in three of the six diagonals in each bay. This causes the batten members to buckle and shorten. As twisting proceeds, the longerons rotate about their pivots and assume a helical configuration. When fully retracted, the longerons are coiled in flat helices while the batten frames stack on one another. The distortions of the boom members are always elastic. Therefore, the boom can withstand many cycles of deployment and retraction.

The following formulas are for the more common properties of these coilable booms. They apply to booms with longerons that are solid and circular in cross section. Other cross sections may be used but the formulas must be modified accordingly. Note also that the following formulas are presented in terms of the allowable working strain ϵ of the longeron material because it is a critical material parameter for the coilable boom.

Bending Stiffness: $EI = 1.5\pi E R^4 \epsilon^2$

where: ϵ = maximum bending strain of longerons when completely coiled ($\epsilon = d/2R = F/E$)
F = coiling stress of longerons
d = longeron diameter
E = Young's modulus of longeron material
R = boom radius

ORIGINAL PAGE IS OF POOR QUALITY

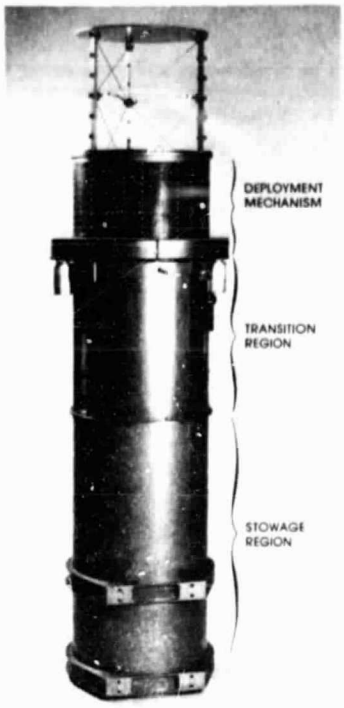

FIGURE 4
Motorized canister for automatic deployment of booms

Shearing Stiffness: $GA = 3EA_d \sin\phi \cos^2\phi$

where EA_d = extensional stiffness of one diagonal member when pretensioned to its service load
ϕ = angle between a diagonal and a batten member; typically ϕ is about 36°

Torsional Stiffness: $GJ = 0.5GAR^2$

Bending Strength: $M_{CR} = 7.44ER^3\epsilon^4$

Note that Euler buckling of a compressed longeron limits the bending strength and that the above formula is for bending in a direction which compresses one longeron and equally tensions the other two, and for a bay length of 1.25 R. Actual bay lengths may be as low as 1.0 R.

Shearing Strength: $V_{CR} = 1.84ER^2\epsilon^4$

Torsional Strength: $T_{CR} = 1.59ER^3\epsilon^4$

Euler buckling of battens limits V_{CR} and T_{CR}, and in the above formulas a typical batten design is assumed: batten diameter is 0.8 times the longeron diameter.

Boom Weight: $W_B = 9\pi\rho R^2\epsilon^2 L$

where ρ = density of longeron material
and L = boom length

Retracted Height: $H_B = \frac{3}{\pi} L(\epsilon + 0.005)$

ORIGINAL PAGE IS
OF POOR QUALITY

These formulas show that longeron material properties E and ϵ and the allowable boom radius R determine the performance that can be achieved with coilable ABLE booms. Principally, because of their high working strain, S-glass/epoxy rods with axially oriented fibers are very suitable for the longerons and battens. However, other materials can be used.

Figure 5 shows the bending stiffness, bending strength and weight versus the radius for coilable ABLE booms having solid, circular S-glass/epoxy longerons for which

$E = 7.5 \times 10^6$ psi
$\epsilon = 0.015$
$\rho = 0.075$ pci
Bay length = 1.25 R

The value of ϵ used here is a typical working strain for straight, unidirectional S-glass/epoxy rods and has resulted in highly reliable booms. Precurving the longerons during their manufacturing process can effectively increase the allowable working strain ϵ to 0.030.

By using longerons of non-circular cross section and by varying the bay length-to-radius ratio, the boom properties can be varied significantly. Therefore, the above formulas and data should be used only for preliminary design purposes.

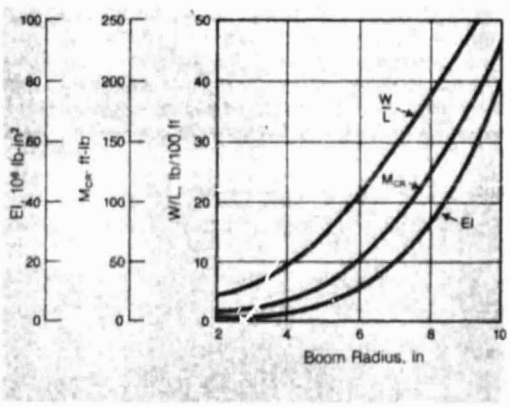

FIGURE 5
Mechanical Properties and Weights Versus Radii for S-glass/Epoxy, Continuous-Longeron ABLE Booms

ARTICULATED-LONGERON ABLE BOOMS

These systems should be used for applications which require booms of large bending stiffness or strength but for which the boom diameter is restricted; i.e., a coilable-longeron boom of a prescribed diameter may have severely limited bending stiffness and strength (as discussed earlier).

The articulated-longeron boom and its canister is shown in **Figure 2** along with a detail of its corners in **Figure 3**. The longeron, batten and diagonal members indicated in **Figure 2** comprise the principal structural components of the boom. Typically, the longerons are segments of metallic or composite material tubing which are articulated at the batten frames with universal hinge fittings. Six diagonal members, typically cables, provide shearing stiffness and strength for each bay of the boom (a bay is the boom portion between adjacent batten frames). Three of the six diagonals incorporate linkages which extend when unlatched, similar to the one shown in **Figure 3**. This combination of extensible diagonals and hinged longerons permits adjacent batten frames to be rotated about the boom axis, thus collapsing the bay into the compact, retracted configuration shown in **Figure 2**. Retraction and deployment of each bay proceeds independently of the extent to which adjacent bays are deployed. Any number of bays can be interconnected to provide a boom of a desired length.

For a prescribed boom diameter and longeron material, cross-sectional dimensions can be selected to provide the necessary bending stiffness or strength. Because the longerons of this type of boom are articulated, their materials and cross-sectional dimensions are not restricted by requirements for elastic coiling. However, to insure compact retraction, the distance between their hinge points must be no greater than 0.75 times the boom diameter.

Following are formulas for the more common properties of the articulated-longeron booms:

Bending Stiffness: $EI = 1.5C_1EA_\ell R^2$

where E = Young's modulus of longeron material
A_ℓ = cross-sectional area of one longeron
R = boom radius measured from boom axis to longeron centerline
C_1 = a reduction factor to account for flexibilities of articulating joints; typically $C_1 = 0.75$

Shear stiffness GA and torsional stiffness GJ are as previously defined for the continuous longeron booms.

Bending Strength (minimum): $M_{CR} = 1.5P_{CR}R$

where: P_{CR} = minimum strength of one longeron, whether that minimum is for Euler buckling between hinge pins, for bearing strength of joint, or for other limitations

This minimum bending strength is for one longeron loaded in its weakest direction (tension or compression), and the other two longerons are each oppositely loaded to one-half the load of the critical longeron.

Shearing Strength: $V_{CR} = \sqrt{3}T_d \cos \phi$

where T_d = tensile strength of one diagonal

Torsional Strength: $M_T = 1.5RT_d \cos \phi$

Note that the formulas for V_{CR} and M_T are based on the assumption that diagonal strengths (rather than batten, longeron or joint strengths) are critical for pure shear or torsional loadings.

Boom Weight: $W_B = 3C_2\rho A_V L$

where ρ = density of longeron material
A_V = longeron cross-sectional area
L = boom length

and C_2 = an empirical coefficient, typically C_2 = 2.5 to 3.0 for articulated booms

Retracted Height of Boom: $H_B = 0.75 \frac{Ld}{R}$

where d = longeron thickness in circumferential direction

ORIGINAL PAGE IS
OF POOR QUALITY

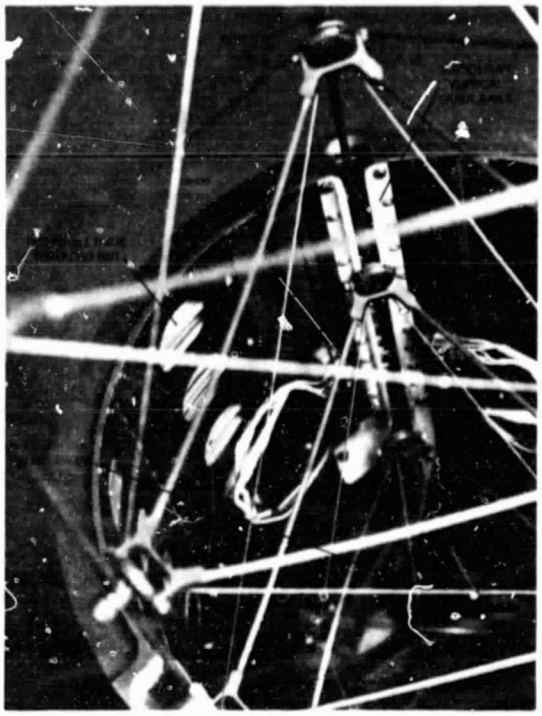

FIGURE 6
Deployment Mechanism for Continuous-or Articulated-Longeron ABLE Booms

As noted earlier, automatic deployment of this type of boom is accomplished by a deployment canister, such as is shown in **Figures 4 and 6**. The principal differences between the articulated-longeron-boom canister and the one for continuous-longeron booms are in the transitional section. That is, the transition section contains cams which automatically latch and unlatch the diagonal linkages when the articulated boom deploys and retracts. Also, the transition region in the canister is somewhat shorter for the articulated boom. However, the height and weight of a canister for an articulated boom may still be estimated by the formulas presented earlier for the continuous-longeron booms.

CANISTER DEPLOYMENT MECHANISM

Figures 4 and 6 are of a canister for deploying either a continuous- or articulated-longeron ABLE boom. The retracted part of the boom stows in the stowage region indicated in **Figure 4**. Rails in the transition region guide the longerons through their transitional configurations. The deployment mechanism consists of a large, power-rotated, three-threaded nut and three pairs of stationary, vertical guide rails. **Figure 6** is a closeup into the top of the canister in which some of those parts of the deployment mechanism are visible. Round roller lugs which protrude from the boom at each batten corner are engaged between the stationary guides and the threads of the nut to deploy and support the boom. When the nut is rotated by a drive motor, the boom is forced to deploy from or retract into the canister. The deployed part of the boom does not rotate in this mechanism part of the canister. Since one level of roller lugs is always engaged by the canister, the deployed portion of the boom is always supported. Therefore, the boom can be deployed to any fraction of its length and used there.

To accommodate the rotation of the stored portion of the boom, the bottom is mounted on a rotatable plate at the bottom of the canister.

The height of a canister can be estimated by the formula

$$H_{CAN} = H_B + 3R$$

where H_B is the boom's retracted height given by the previous formula and 3R is the combined height of the transition and deployment-mechanism sections of the canister.

The canister weight can be approximated by the empirical formula

$$W_{CAN} = 0.04\epsilon LR + 0.5R^2$$

where the weight is in pounds and the dimensions L (boom length) and R (boom radius) are in inches.

As can be seen from the preceding formula, the rotating-nut part of the canister becomes very heavy for booms of large radius. A lighter-weight deployment mechanism, incorporating three synchronously driven lead screws instead of the three-threaded nut, is recommended for larger-diameter canisters. The lead screws are mounted 120° apart atop the transition region of the canister, and their threads engage the boom lugs in much the same manner as do the threads of the three-threaded nut. The boom is thus forced to deploy or retract as the lead screws are synchronously rotated. The heights of canisters with lead screws is about the same as those with three-threaded nuts. However, no empirical formula has been developed for their weight.

LANYARD DEPLOYMENT MECHANISMS

When this type of mechanism is used, the boom self-deploys (as described previously) at a rate controlled by the payout rate of a restraining lanyard. This lanyard extends through the center of the boom along its axis. **Figure 7** shows this type of deployment mechanism, with the boom partially deployed. The transition region of the boom, the region between its retracted and deployed parts, propagates upward as the lanyard is paid out. The retracted part rotates as deployment proceeds. Since roller lugs are not used in the lanyard system, boom weights and outside diameters are slightly less than those for canister-deployed versions. Note that the transition region has reduced bending stiffness. Therefore, some operations are prohibited when the boom is partially deployed.

The lanyard is usually a metallic or fibrous tape and is wound on a reel. Lanyard payout rate is controlled, typically, by a viscous damper or an electric motor. When an electric motor is used, the boom can be retracted by reeling in the lanyard. The boom is twisted to initiate retraction by means of a bridle incorporated in the outboard end of the lanyard.

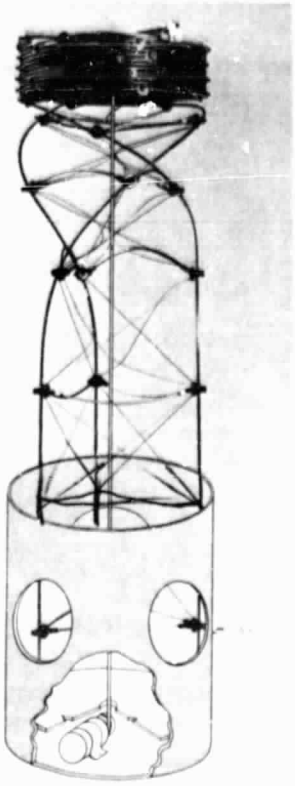

FIGURE 7
Lanyard Deployed
Continuous-Longeron Boom

When the longerons are solid circular rods, the nominal self-deployment force P developed by the coilable ABLE boom is

$$P = 1.178E\epsilon^4R^2$$

Because the lanyard mechanism and stowage container design can vary widely, depending on the application's specific requirements, their weights are not standardized. However, the lanyard mechanism and containers generally weigh much less than the canisters described previously, and the stowage volume is smaller in both length and diameter.

THERMAL DISTORTIONS OF ABLE BOOMS

Because all types of ABLE booms can be made so that they undergo very little thermal twisting or bending in the environment of solar radiation, ABLE booms are especially useful for space applications that require high dimensional stability. To meet some requirements, ABLE booms are fabricated with a uniform rate of pretwist over their length. The pretwist is used primarily to preclude thermal twisting, as explained later, but it also precludes the excessive thermal bending that would occur if one longeron shadowed another. Thermal distortions of ABLE booms are also minimized by careful selection of materials.

If sun rays are parallel with one set of diagonals of an initially straight lattice boom, then that set of diagonals would have a significantly lower temperature than the intersecting set which are nearly perpendicular to the rays. Shear distortions would result in the panels surrounding those intersecting diagonals, and those distortions would lead to both shearing and twisting of the overall boom. The rate of thermal twisting β' for a boom segment has been determined* to be

$$\beta' = \frac{aT_oF}{3R \sin\phi \cos\phi}$$

where
- a = coefficient of linear expansion for the diagonal material
- T_o = diagonal temperature when oriented perpendicular to sun rays
- F = a factor dependent on the orientation of the boom relative to the sun rays
- R = boom radius
- ϕ = angle between diagonals and battens

The factor F varies cyclically with the sun's azimuth angle (angular position of radial components of sun rays). The period of F is 120° and the integral of F over the period is zero. Therefore, to nullify thermal twisting, some lattice booms are manufactured with pretwist over their length equal to an integer multiple of 120°. The result is a greatly reduced net thermal twist between the base and tip of the boom. For instance, for booms with fiberglass-rod diagonals, **Figure 8** shows the maximum possible thermal twist β_L versus length-to-radius ratio and various pretwists. **Figure 8** illustrates that β_L is very large when no pretwist is used, and that β_L, though small for pretwisted booms, does increase as L/R increases. Note that boom bending stiffness and strength are not significantly reduced by pretwists resulting in longeron helix angles as large as 10°.

The data in **Figure 8** excludes an additional source of thermal twisting that is possible for pretwisted booms. If there is a difference between the average thermal strains of the longerons and diagonals, then an additional uniform twisting or untwisting $\Delta\beta_L$ occurs

$$\Delta\beta_L = \frac{2}{3}\left(\frac{\ell}{R}\right)^2(\epsilon_d - \epsilon_l)\beta_0$$

where
- ℓ = bay length
- R = boom radius
- ϵ_d = diagonal thermal strain
- ϵ_l = longeron thermal strain
- β_0 = initial pretwist of total boom length

ORIGINAL PAGE IS
OF POOR QUALITY

This effect is seen to be absent if $\beta_0 = 0$. The effect is generally quite small when longerons and diagonals are made of materials (e.g. fiberglass rods) with low coefficients of thermal expansion, and with surface properties which do not permit excessive heating. As an example, consider an ABLE boom with fiberglass longerons and diagonals ($a = 1.75 \times 10^{-6}$/°R), with an average temperature difference of 300° R between those members, and with a pretwist of 240° and $\ell/R = 1.25$. Then $\Delta\beta_L = 0.131°$.

Formulations also have been made for predicting thermal shearing distortions of ABLE booms, but they have not been integrated and otherwise evaluated to provide general parametric data. However, as a single-point example, the thermal-shear deflection of the tip of a 62-foot-long cantilevered boom with 120° pretwist and fiberglass diagonals was calculated to be about 0.2 inches. It is noted that shear deflections are independent of both radius and longeron thermal strains.

Also undeveloped, are parametric data for thermal bending due to mutual shadowing among the parts of ABLE booms. However, consider the boom in the previous example. Assume its radius is 4 inches and its fiberglass longeron, batten and diagonal diameters are respectively 0.120, 0.100 and 0.032 inches. The tip deflection due to thermal bending is calculated to be 1.20 inches and the corresponding tip slope is 0.095°.

All the thermal distortions in the above examples could be reduced even further by using, for instance, carbon/epoxy longerons and diagonals for which $a < 0.5 \times 10^{-6}$/°R.

The above formulae and trends for thermal distortions apply to both articulated- and continuous-longeron ABLE booms. Either type can be uniformly pretwisted by simply making all intersecting diagonals of the same unequal lengths.

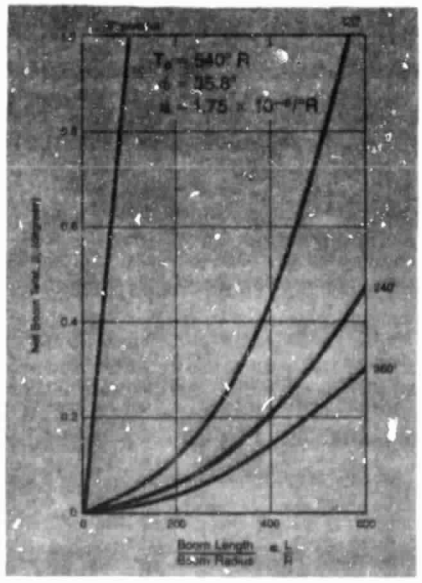

FIGURE 8
Net Thermal Twist Between Ends of ABLE Booms with Fiberglass Diagonals; Worst Sun Orientation and Various Amounts of Pretwist

*IBM Corporation: Development of a Microwave Interferometer Position Locator. NASA CR-112188, August 1973.